

**VIRAL AND HOST FACTOR INTERACTIONS IN THE REGULATION OF JC  
VIRUS REACTIVATION**

---

A Dissertation  
Submitted to  
The Temple University Graduate Board

---

In Partial Fulfillment  
of the Requirements for the Degree  
Doctor of Philosophy

---

By Michael J. Craigie  
May 2018

Examining Committee Members:

Ilker Kudret Sariyer, D.V.M, Ph.D., Thesis Advisor, Department of Neuroscience

Tracy Fischer, Ph.D., Committee Chair, Department of Neuroscience

Jennifer Gordon, Ph.D., Department of Neuroscience

Kamel Khalili, Ph.D., Department of Neuroscience

Michael Nonnemacher Ph.D., External Examiner, Drexel University College of Medicine

©

Copyright

2017

by

Michael J Craigie

All Rights Reserved

## **ABSTRACT**

**Title:** Viral and Host Factor Interactions in the Regulation of JC Virus Reactivation

**Candidate's Name:** Michael J Craigie

**Degree:** Doctor of Philosophy

Lewis Katz School of Medicine at Temple University, 2017

Advisor: Ilker Kudret Sariyer, D.V.M., Ph.D.

JC virus (JCV) is a human neurotropic polyomavirus and the etiologic agent of progressive multifocal leukoencephalopathy (PML), a demyelinating disease of the white matter. PML is primarily observed in immunocompromised patients, including patients with acquired immunodeficiency syndrome (AIDS) and those prescribed immunomodulatory therapies. During JCV infection, the virus encodes multiple viral proteins including T-antigen and agnoprotein. Originally, we demonstrated that T-antigen expression rescued serine/arginine rich splicing factor 1 (SRSF1)-mediated transcriptional suppression of JCV for both early and late promoter orientations. We demonstrated that T-antigen expression suppressed SRSF1 expression in glial cells through inhibition of SRSF1 transcription. We have recently shown that agnoprotein is secreted from transfected cells into the extracellular matrix, where it is internalized by neighboring uninfected astrocytes or microglia. The internalization of agnoprotein was found to impact astrocyte's cytokine profile, with treatment of astrocytes with media containing agnoprotein resulting in a significant reduction in granulocyte-macrophage colony-stimulating factor (GM-CSF) secretion. Subsequent reporter gene analysis demonstrated that agnoprotein can suppress GM-CSF transcription, implicating a possible mechanism for the reduction of GM-CSF secretion. Likewise, the treatment of a human monocyte cell line, U-937, with agnoprotein

resulted in decreased differentiation, dysregulated surface marker expression, and decreased phagocytic ability. Similarly, treatment of peripheral blood mononuclear cells with agnoprotein decreased cellular migration through an *in vitro* blood brain barrier model. These findings have suggested that extracellular agnoprotein modulates aspects of the immune response to JCV, primarily through suppression of GM-CSF secretion and a subsequent dysregulation on monocyte/macrophage function.

## ACKNOWLEDGEMENTS

I could have never made it through this program without my family, my father John, my mother Pamela, and my sister Jena. They were always there to provide moral support to continue with my studies and to patiently listen to my explanations of what I was doing in lab, even if they had very little understanding of anything I said.

I'd like to thank Ramona Bella. Without her, I'm not sure how far I could have progressed within this program. When I had a question about an experiment or needed an extra set of hands to help, she was always there to lend expertise and suggestions. She has proven to be irreplaceable in the completion of my doctorate.

My mentor and friend, Ilker Kudret Sariyer, has supported me throughout these 4 years, and some days I don't understand how he could have put up with me. He consistently taught me various strategies and techniques, some I quickly accepted and others I would tirelessly argue about, but in the end, everything that I was taught proved to be extremely valuable. I was very lucky to have Dr. Sariyer as my doctorate advisor.

The members of my advisory committee were also irreplaceable in this journey. Dr. Khalili, Dr. Fischer, and Dr. Gordon offered advice and strategies throughout my time here, allowing me to obtain the amount of data that I am presenting here. It is with their guidance that I could complete this program.

And to the other members of my graduate program and the neuroscience department that helped me during my time here.

# TABLE OF CONTENTS

	<u>Page</u>
ABSTRACT .....	iii
ACKNOWLEDGEMENTS .....	v
LIST OF TABLES .....	ix
LIST OF FIGURES .....	x
LIST OF ABBREVIATIONS.....	xiii
CHAPTER	
1. INTRODUCTION .....	1
1.1. Polyomaviruses and JCV .....	1
1.2. SRSF1.....	21
1.3. Progressive Multifocal Leukoencephalopathy .....	25
1.4. Hypothesis and Proposed Aims.....	36
2. MATERIALS AND METHODS.....	40
2.1. Cell Culture .....	40
2.2. Primary Monocyte Isolation and Culture .....	42
2.3. Plasmid Constructs .....	43
2.4. MBP-Recombinant Agnoprotein Production .....	45
2.5. Western Blot Assay.....	47
2.6. Luciferase Reporter Assay .....	49
2.7. Chromatin Immunoprecipitation (ChIP) Assay .....	50

2.8. Enzyme-Linked Immunosorbent Assay (ELISA) .....	52
2.9. Immunocytochemistry .....	53
2.10. Immunohistochemistry .....	55
2.11. Cytokine/Chemokine Array .....	57
2.12. MTT Assay .....	58
2.13. Monocyte Differentiation Assay .....	59
2.14. Phagocytosis Assay .....	60
2.15. Blood-Brain Barrier Model .....	61
3. MOLECULAR INTERPLAY BETWEEN T-ANTIGEN AND SPLICING FACTOR, ARGININE/SERINE-RICH 1 (SRSF1) CONTROLS JC VIRUS GENE EXPRESSION IN GLIAL CELLS .....	64
3.1. Introduction .....	64
3.2. Results .....	65
3.2.1. SRSF1 Mediated Suppression of JCV Early and Late Gene Transcription is Rescued by Large T Antigen .....	65
3.2.2. Large T Antigen Suppresses SRSF1 Expression in Glial Cells.....	68
3.2.3. Large T Antigen Suppresses SRSF1 Transcription in Glial Cells.....	70
3.2.4. Large T Antigen Associates with the SRSF1 Promoter to Inhibit Transcription .....	72
3.3. Discussion .....	74
4. MODULATION OF THE NEUROIMMUNE REGULATION OF JC VIRUS BY INTRACELLULAR AND EXTRACELLULAR AGNOPROTEIN .....	77
4.1. Introduction .....	77

4.2. Results .....	80
4.2.1. Agnoprotein is Released from Transfected Cells .....	80
4.2.2. Extracellular Agnoprotein is Internalized by Glial Cells.....	82
4.2.3. Intracellular Agnoprotein Inhibits GM-CSF Release by Astrocytes ...	84
4.2.4. Extracellular Agnoprotein and Recombinant Agnoprotein have no Impact on Primary Cell Viability.....	86
4.2.5. Agnoprotein Inhibits GM-CSF Transcription.....	90
4.2.6. GM-CSF Suppresses JCV Early and Late Gene Transcription .....	92
4.2.7. Agnoprotein Suppresses U937 Differentiation.....	96
4.2.8. Agnoprotein does not Impact U937 Cellular Viability.....	99
4.2.9. Agnoprotein Dysregulates U937 Surface Marker Expression.....	101
4.2.10. Extracellular Agnoprotein Suppresses Phagocytosis.....	103
4.2.11. Extracellular Agnoprotein Decreases Monocyte Migration across a Blood-Brain Barrier Model in Response to Astrocyte Activation.....	106
4.2.12. Immunohistochemical Analysis of PML Lesions for Agnoprotein, VP- 1, and GM-CSF .....	112
4.3. Discussion .....	118
5. CONCLUSIONS AND FUTURE DIRECTIONS.....	124
5.1. Conclusion.....	124
5.2. Future Directions.....	127
6. SCIENTIFIC PRODUCTS AND AWARDS .....	133
REFERENCES .....	135

## LIST OF TABLES

<u>Table</u>	<u>Page</u>
1. Pathologic States Associated with Progressive Multifocal Leukoencephalopathy prior to the AIDS epidemic.....	27
2. Antibodies Used for Western Blot, Immunocytochemistry, and Immunohistochemistry .....	48-49

## LIST OF FIGURES

<u>Figure</u>	<u>Page</u>
1. JC Virus Genome .....	3
2. JC Virus Initial Infection Route .....	5
3. Increase in Serotonin Receptor Expression Surrounding PML Lesions .....	9
4. JCV Cellular Entry and Nuclear Translocation.....	10
5. JCV Co-localization with Promyelocytic Leukemia Bodies.....	14
6. T-Antigen is Necessary for Functional JCV Replication.....	15
7. SV40 Viral Replication .....	17
8. Cellular Functions of SRSF1.....	22
9. SRSF1 Suppresses JCV Early and Late Gene Transcription .....	23
10. SRSF1 Expression is Required for Soluble Immune-Factor Mediated JCV Transcriptional Suppression .....	25
11. PML Brain MRI Showing Lesion Sites .....	26
12. Histopathological Features of PML .....	32
13. PML Lesion Histology .....	33
14. JCV Granule Cell Neuronopathy Histology.....	34
15. JCV Encephalopathy Histology .....	35
16. Agnoprotein is released from JCV-Infected Glial Cells .....	38
17. Blood-Brain Barrier Model .....	61
18. SRSF1-mediated Suppression of JCV-Early and –Late Gene Transcription is Rescued by T-antigen.....	66
19. T-Antigen Suppresses SRSF1 Expression in Glial Cells .....	69

20. T-Antigen Suppresses SRSF1 Transcription in Glial Cells .....	72
21. T-Antigen Suppresses SRSF1 Transcription via Interactions with the SRSF1 -1000 to +47 Base Pair Promoter Region .....	74
22. Agnoprotein is released from Transfected Cells .....	82
23. Agnoprotein is Internalized by Glial Cells .....	83
24. Internalized Agnoprotein shows Cytoplasmic and Perinuclear Localization .....	84
25. GM-CSF Release is Suppressed by Agnoprotein Internalization .....	86
26. Recombinant Agnoprotein from the Bacterial MBP-Expression System .....	89
27. Extracellular Agnoprotein has no Impact on Glial Cell Viability .....	90
28. Intracellular and Extracellular Agnoprotein Inhibit GM-CSF Transcription .....	92
29. GM-CSF Suppresses JCV-Early and –Late Gene Transcription .....	94
30. Extracellular Agnoprotein Suppresses U937 Differentiation .....	96
31. Quantification of U937 Differentiation in the Presence of Agnoprotein .....	98
32. Agnoprotein has no Impact on U937 Viability .....	100
33. Agnoprotein Dysregulates U937 Surface Marker Expression .....	102
34. Agnoprotein Inhibits Myeloid-Derived Cells Phagocytic Ability .....	105
35. Blood-Brain Barrier Model .....	107
36. Serum Induces PBMC Migration across the BBB Model .....	108
37. Agnoprotein Decreases Monocyte Migration across the BBB Model .....	110
38. GM-CSF Histology in Normal Frontal Cortex Sections .....	112
39. Agnoprotein, GM-CSF, VP-1, and H&E Histology for PML Brain MHBB #547 Lesion Sites A and B .....	115

40. Agnoprotein, GM-CSF, VP-1, and H&E Histology for PML Brain MHBB #547	
Lesion Site A .....	116
41. Agnoprotein, GM-CSF, VP-1, and H&E Histology for PML Brain MHBB #547	
Lesion Site B .....	117
42. Molecular Interplay between T-Antigen and SRSF1 in Regulation of JCV	
Transcription and Gene Splicing .....	125
43. Role of Extracellular and Intracellular Agnoprotein in the Neuroimmune Response	
to JCV .....	127
44. Impact of M-CSF and GM-CSF on Macrophage Phenotypes .....	130

## LIST OF ABBREVIATIONS

<u>Abbreviation</u>	<u>Full Name</u>
1. 5HT <sub>2A</sub> R .....	5-hydroxytryptamine receptor 2A
2. AIDS .....	Acquired Immunodeficiency Syndrome
3. AP .....	Alkaline Phosphatase
4. AP-1 .....	Activator Protein 1
5. APCs .....	Antigen Presenting Cells
6. ATCC .....	American Type Culture Collection
7. BBB.....	Blood-Brain Barrier
8. BSA.....	Bovine Serum Albumin
9. Cas.....	CRISPR-associated System
10. CCL2.....	Chemokine (C-C motif) Ligand 2
11. ChIP Assay.....	Chromatin Immunoprecipitation Assay
12. CM .....	Conditioned Media
13. CM-agno .....	Agnoprotein Conditioned Media
14. CNAC .....	Comprehensive NeuroAIDS Center
15. CNS.....	Central Nervous System
16. CRISPR.....	Clustered Regularly Interspaced Short Palindromic Repeats
17. CSF .....	Cerebral Spinal Fluid
18. CSF-1 .....	Colony Stimulating Factor 1
19. DAB .....	3,3'Diaminobenzidine
20. DAPI.....	4',6-diamidino-2-phenylindole
21. ddPCR.....	Digital Droplet PCR
22. DMEM .....	Dulbecco's Modified Eagle Media
23. DMEM/F12.....	Dulbecco's Modified Eagle Media / Nutrient Mixture F-12
24. ELISA .....	Enzyme Linked Immunosorbent Assay
25. FBS .....	Fetal Bovine Serum
26. GM-CSF.....	Granulocyte Macrophage Colony Stimulating Factor
27. HAD .....	HIV-Associated Dementia
28. HBSS.....	Hank's Balanced Salt Solution

29. HCMV.....	Human Cytomegalovirus
30. HEK293 .....	Human Endothelial Kidney Cell Line
31. HIV .....	Human Immunodeficiency Virus
32. HIVE.....	HIV Encephalopathy
33. HRP.....	Horseradish Peroxidase
34. ICAM1 .....	Intracellular Adhesion Molecule 1
35. ICC.....	Immunocytochemistry
36. IFN- $\gamma$ .....	Interferon-gamma
37. IgG .....	Immunoglobulin G
38. IHC.....	Immunohistochemistry
39. IPTG.....	Isopropyl $\beta$ -D-1-thiogalactopyranoside
40. JCV .....	JC Virus
41. JCVE.....	JC Virus Encephalopathy
42. JCVGCN.....	JC Virus Granule Cell Neuronopathy
43. JCVM.....	JC Virus Meningitis
44. LAR.....	Luciferase Assay Reagent
45. LB .....	Luria-Bertani Broth
46. LFA1 .....	Lymphocyte Function-Associated Antigen 1
47. LPS.....	<i>Escherichia coli</i> O26:B6 Lipopolysaccharides
48. Mad-1 .....	JCV Madison-1 Variant
49. Mad-4.....	JCV Madison-4 Variant
50. MBP .....	Maltose Binding Protein
51. MCP-1.....	Monocyte Chemoattractant Protein
52. M-CSF.....	Macrophage Colony Stimulating Factor
53. MHBB.....	Manhattan HIV Brain Bank
54. miRNA.....	microRNA
55. mRNA.....	messenger RNA
56. MTT .....	3-(4,5-Dimethylthiazol-2-yl)-2,5-Diphenyltetrazolium Bromide
57. NCCR.....	Non-Coding Control Region
58. ND10.....	Nuclear Domain 10 Bodies
59. NF-1 .....	Nuclear Factor-1

60. NMS	Normal Mouse Serum
61. PBMCs	Peripheral Blood Mononuclear Cells
62. PBS	Phosphate Buffered Solution
63. PBST	Phosphate Buffered Solution with Tween
64. PCNA	Proliferating Cell Nuclear Antigen
65. PHFA	Primary Human Fetal Astrocytes
66. PHFBE	Primary Human Fetal Brain Endothelial Cells
67. PHFM	Primary Human Fetal Microglia
68. PMA	Phorbol 12-Myristate 13-Acetate
69. PML	Progressive Multifocal Leukoencephalopathy
70. PML-IRIS	PML-Immune Reconstitution Inflammatory Syndrome
71. pRb	Retinoblastoma Protein
72. rAgno	Recombinant Agnoprotein
73. RBC	Red Blood Cell
74. RPMI	Roswell Park Memorial Institute
75. SDS-PAGE	Sodium Dodecyl Sulfate Polyacrylamide Gel Electrophoresis
76. shRNA	Short Hairpin RNA
77. siRNA	Small Interfering RNA
78. SLE	Systemic Lupus Erythematosus
79. SRSF1	Serine/Arginine Rich Splicing Factor 1
80. SV40	Simian Virus 40
81. TMB	3,3',5,5'-Tetramethylbenzidine
82. VCAM	Vascular Cell Adhesion Protein 1
83. VLA-4	Very Late Antigen 4
84. vMIA	Viral Mitochondrial Inhibitor of Apoptosis

# CHAPTER 1

## INTRODUCTION

### 1.1. Polyomaviruses and JCV

Polyomaviruses are a family of viruses first reported in 1953 by Ludwik Gross. Gross discovered that inoculating newborn mice with extracts from a mouse leukemia tumor was sufficient to induce tumor formation, resulting in the transforming agent classification as a “parotid agent”, named for the salivary gland (the parotid gland) in which tumor formation was typically induced (Gross, 1953). At the time, these agents were not classified as viral particles, however, research was continued by Stewart, Eddy, and Borgese, resulting in the characterization of the “parotid agent” as a tumor virus denoted the murine polyomavirus (Stewart *et al*, 1958). Following initial characterization, Sweet and Hilleman described a similar agent found in African green monkey kidney cells, named simian virus 40 (SV40) (Sweet and Hilleman, 1960). Sharing similarities with the initial murine polyomavirus, SV40 possesses transforming capabilities and is oncogenic in mice and other rodent species (Eddy *et al*, 1962).

Since the initial identification of murine polyomavirus and SV40, many other polyomaviruses have been identified in a variety of vertebrate hosts, including humans (Krumbholz *et al*, 2009). There are currently 76 identified polyomaviruses within four assigned and one unassigned genera (Polyomaviridae Study Group of the International Committee on Taxonomy of Viruses, 2016). The human polyomavirus JC virus is a member of the betapolyomavirus genus.

Polyomaviruses generally exhibit high species specificity and can infect only a narrow range of cells. In terms of cellular and species tropism, the proposed driving mechanism is the dependence on host and cell specific transcriptional factors required to initiate viral gene transcription since polyomaviruses depend entirely on host factors for transcription initiation (Ravichandran *et al*, 2006).

All polyomaviruses possess a circular double stranded DNA genome contained within an icosahedral viral capsid. Like other polyomaviruses, JC virus is a non-enveloped double stranded DNA virus with a circular genome of approximately 5,100 base pairs, varying slightly between strain variants (Figure 1) (Ferenczy *et al*, 2012; Frisque *et al*, 1984). Neurotropic JCV variants isolated from PML-patients generally possess a variant genome compared to the archetype strain, containing mutations primarily within the non-coding control region (NCCR) which contains the viral origin of replication and physically separates the early and late-coding regions. When JCV is shed in the urine of healthy patients, the virus contains the archetype linear non-coding control region, however viral particles found in the CSF of PML patients contain rearranged NCCRs, suggesting that mutations and rearrangements within the NCCR are essential to viral lytic infection (Gosert *et al*, 2010). Mutations within the NCCR are highly variable, but generally confer increased early gene expression and viral replication, resulting in greater infectivity and lytic disease progression (Gosert *et al*, 2010). The early coding region is transcribed prior to DNA replication and encodes the T-antigen proteins; Large T-antigen, small t-antigen, and three T'-splice variants. The T'-splice

variants are encoded following alternative splicing of the early coding region. The late coding region is transcribed simultaneously with DNA replication and encodes the viral capsid proteins (VP1, VP2, and VP3) as well as the regulatory agnoprotein.

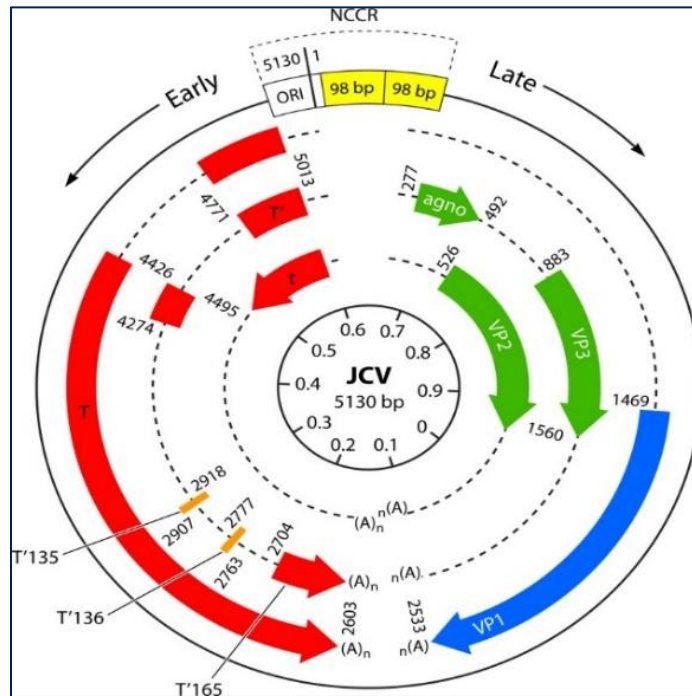


**Figure 1: JC Virus Genome.** The Mad-1 JCV genome is 5,130 base pairs and contains the genes for 9 viral proteins. The early region, oriented in the counter-clockwise direction, contains the genes for large T-antigen, small t antigen, and the T' splice variants (T'135, T'136, T'165). The late region, oriented in the clockwise direction, contains the genes for the capsid proteins (VP1, VP2, and VP3) and agnoprotein. The non-coding control region (NCCR) contains the origin of replication. (Reproduced with permission from Ferenczy *et al*, 2012 and the American Society for Microbiology)

During JCV infection viral proteins interact with both host and other viral factors, including cellular proteins and host DNA, during the infectious and replication cycles. The T-antigen proteins, including large T antigen, small t antigen, and the T' splice variants, all possess multiple functional domains to support their roles in viral gene transcription and viral replication (Tyagarajan *et al*, 2006). The most significant function of the T-antigens is shifting the host cell from G<sub>0</sub> into S phase

to induce cellular and viral replication (Dubbs *et al*, 1978). To initiate DNA replication, T-antigen interacts with two tumor-suppressors, retinoblastoma protein (pRb) and the transcription factor p53, which results in inactivation of the tumor suppressor proteins and subsequent bypass of cell cycle regulation, resulting in DNA replication due to induction of cellular proliferation (Ahuja *et al*, 2005; Campisi, 2003; Cobrinik, 2005; Sherr *et al*, 2002; Tyagarajan *et al*, 2006). From the late region genes, the virus produces four proteins, including three capsid proteins (VP1, VP2, and VP3), and the regulatory agnoprotein. The viral capsid proteins are primarily involved in cellular entry, with VP1 binding to negatively charged sialic-acid receptors on the cellular surface inducing viral particle endocytosis and entry into the cell (Dugan *et al*, 2008; Liu *et al*, 1998). The regulatory agnoprotein is a multifaceted protein with multiple functions throughout the viral life cycle. Studies have elucidated an essential role of agnoprotein during JCV infection, with an agnoprotein-negative JCV mutant strain losing infective capacity, resulting in no detectable viral protein expression (Okada *et al*, 2001; Sariyer *et al*, 2011). Likewise, agnoprotein has been proposed to function as a viroporin, a protein which modifies the permeability of the cellular plasma membrane, allowing for the release of viral particles following productive infection (Suzuki *et al*, 2010). Agnoprotein has also been implicated in modifying cellular pathways, including interactions with transcriptional activators and repressors as a method for regulating gene activation and to influence the activation of various DNA repair pathways (Darbinyan *et al*, 2004; Khalili *et al*, 2005; Safak *et al*, 2001).

JCV is a very ubiquitous virus, infecting upwards of 75% of the human population, although serotype positive rates varying greatly among different subpopulations (Bofill-Mas *et al*, 2000; Knowles *et al*, 2003; Major *et al*, 1998). Most JCV infections remain asymptomatic, with viral shedding in the urine and the presence of anti-JCV antibodies serving as evidence of viral infection (Berger *et al*, 2013a).

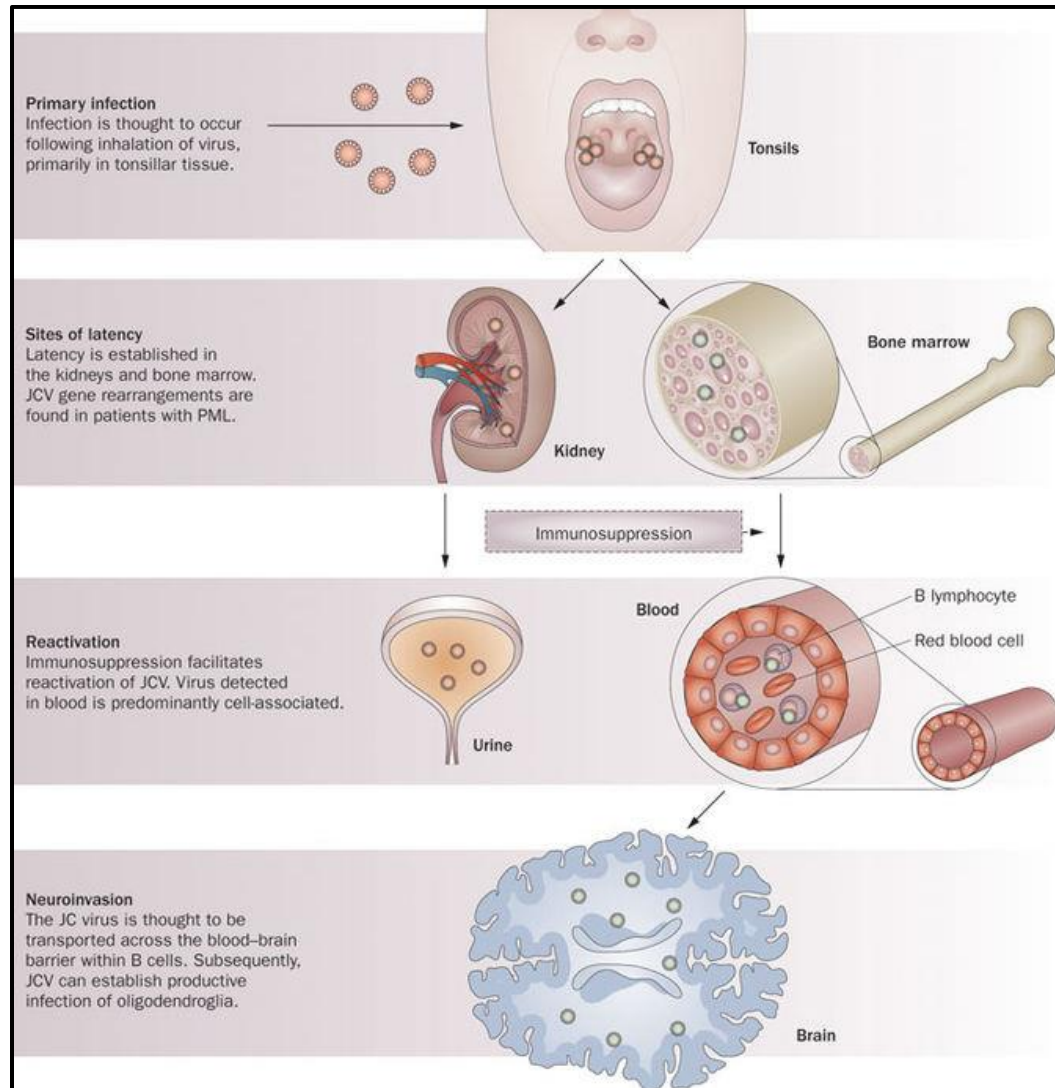


**Figure 2: JC Virus Initial Infection Route.** JC virus enters the body through the oral route, either through inhalation of viral particles or ingestion of virally contaminated water. After initiation viral entry, the virus spreads throughout the periphery and establishes latent sites of infection, including the kidney epithelial cells and hematopoietic progenitors within the bone marrow, resulting in periodic shedding of the virus within the urine. Within these sites, the virus undergoes genetic rearrangements, which allow for the development of PML during states of immunosuppression. (Reproduced with permission from Brew *et al*, 2010 and the Nature Publishing Group).

Currently, the mechanism of the initial JCV infection is not completely understood, however, multiple proposed models exist. The most commonly accepted model suggests that JCV enters the body through either respiratory-inhalation or oral-ingestion of virally-contaminated food or water (Berger *et al*, 2006; Brew *et al*, 2010; Calbrese *et al*, 2015) (Figure 2). This model arose due to data showing JCV infection within tonsillar stromal cells and hematopoietic progenitor cells, suggesting that the primary route of infection is either orally or through the immune cells of the upper respiratory system (Monaco *et al*, 1996 and Monaco *et al*, 1998).

Following initiation infection, the virus is trafficked throughout the body to peripheral sites by infected lymphocytes, including the bone marrow, lymph nodes and kidneys, allowing for the development of latently infected reservoirs (Tan *et al*, 2010). In the immunocompetent population, these sites remain latent indefinitely, however, changes in immune function may result in viral reactivation and eventual productive infection (Tan *et al*, 2010). The prevalent hypothesis suggests that suppression of immune function allows the virus to reactivate at latent peripheral sites, primarily within infected hematopoietic progenitors of the bone marrow, resulting in the development of latently infected mature B-lymphocytes. The infected lymphocytes facilitate the release of active viral particles, which eventually reach the central nervous system (CNS), resulting in oligodendrocyte infection and PML progression. One hypothesis explaining viral entry into the CNS is the “Trojan-horse” hypothesis, stating that latently infected B-cells cross over the blood-brain barrier (BBB), resulting in viral shedding from the infected B-cells and

infection of oligodendrocytes and astrocytes within the central nervous system (Monaco *et al*, 1996). This hypothesis is supported by studies in human immunodeficiency virus (HIV)-positive patients diagnosed with PML, in which chemokine (C-C motif) ligand 2 (CCL2) / monocyte chemoattractant protein (MCP-1) is upregulated, increasing the permeability of the BBB and ultimately increasing lymphocyte migration into the CNS, thus potentially inducing the migration of latently infected B-cells (Weiss *et al*, 1999). It is important to note that an alternative hypothesis posits that the brain itself may serve as a site of viral latency as JCV DNA but not viral proteins, has been found in the CNS of healthy patients (Degener *et al*, 1997).

JCV is characterized by a significantly restricted host cell range due to various factors. The primary mechanism enforcing host specificity is that T-antigen proteins interact solely with human DNA polymerase, inhibiting viral replication in other species. Within humans, JCV infection is restricted to oligodendrocytes, astrocytes, kidney epithelial cells, tonsillar stromal cells, and bone marrow-derived lineages (Monaco *et al*, 1996; Houff *et al*, 1988; Major *et al*, 1992; Tornatore *et al*, 1992; Monaco *et al*, 1998; Major *et al*, 1990; Atwood *et al*, 1992). The primary mechanism preventing cellular infection of JCV in non-permissive cells is inefficient viral binding to the cellular surface receptors due to faulty interactions between viral capsid proteins and host receptors preventing cellular entry and potential infection (Chen *et al*, 2002). However, JCV viral entry does not correlate with productive viral replication, and in a majority of permissive cell types, JCV

establishes either latency or a low-level persistent infection, primarily due to inefficient viral replication in non-glial cells (Monaco *et al*, 1996; Monaco *et al*, 1998; Suzuki *et al*, 2001; Wei *et al*, 2000). The glial-tropism of JCV is mediated by many factors, including the presence of glial-specific transcription and replication factors, including Tst-1 (Tuberculin Skin Test Reactivity, Absence of), nuclear factor 1 (NF-1), and Sp1 (Specificity Protein 1), which are restricted to glial cells (Feigenbaum *et al*, 1987; Henson *et al*, 1992; Lynch *et al*, 1991; Nakshatri, *et al*, 1990; Wegner *et al*, 1993; Tada *et al*, 1989). Additionally, the JCV viral promoter shows increased activity in glial cells as opposed to non-glial cells, suggesting another mechanism driving the glial-tropism (Feigenbaum *et al*, 1992; Kenney *et al*, 1984; Khalili *et al*, 1988).

The cellular entry of viral particles into host cells requires the interaction of sialic-acid containing receptors on the cell surface with the VP1 capsid protein (Dugan *et al*, 2008). The importance of sialic acids during cellular entry was elucidated by stripping permissive glial cells of both  $\alpha(2,3-)$  and  $\alpha(2,6-)$  sialic acid linkages and subsequently exposing the cells to viral particles, which showed that removal of sialic acids prevented JCV cellular entry (Dugan *et al*, 2008). However, when either  $\alpha(2,3-)$  or  $\alpha(2,6-)$  sialic acid linkages were restored individually, the cells regained their permissive nature, suggesting that both linkage types can be used by JCV to infect glial cells (Dugan *et al*, 2008).

Additionally, JCV has been shown to interact with the serotonin receptor, 5-hydroxytryptamine receptor 2A (5HT<sub>2A</sub>R), for cellular entry into glial cells (Elphick *et al*, 2004). To assess if the serotonin receptor was sufficient for viral uptake, non-permissive HeLa and the human endothelial kidney (HEK293) cell line were transfected with plasmids encoding the serotonin receptor, after which they were exposed to JCV viral particles. Transfected cells were readily infected by JCV whereas non-transfected cells remained non-permissive to infection (Elphick *et al*, 2004; Maginnis *et al*, 2010). Furthermore, histological samples from PML patients reveal significant increase in serotonin receptor expression in and around sites of lesions (Haley *et al*, 2015) (Figure 3). Baum *et al* showed that both chlorpromazine and clozapine, two antipsychotics which act as serotonin receptor antagonists, possess strong antiviral activity against JCV (Baum *et al*, 2003). These data have led to the hypothesis that the serotonin receptor may play a role in the glial tropism of JCV.

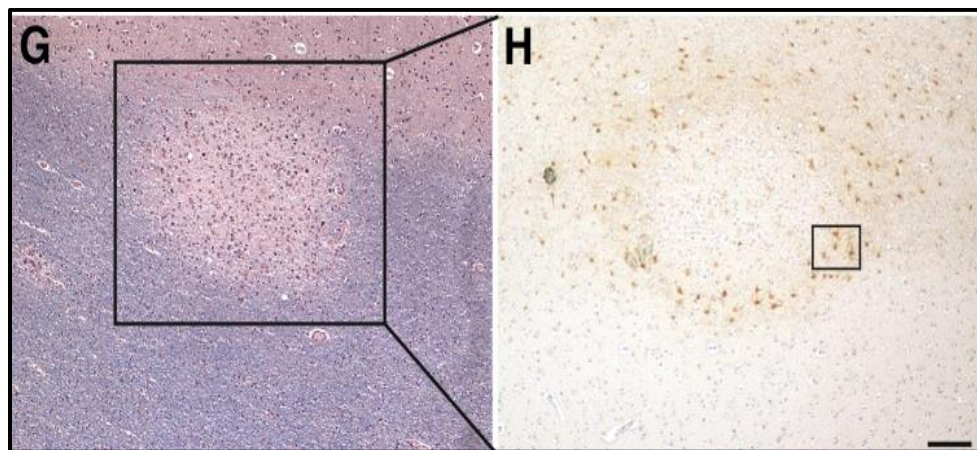


**Figure 3: Increase in Serotonin Receptor Expression Surrounding PML Lesions.** Serial sections of demyelinated lesions within PML brain samples were analyzed for serotonin receptor expression with immunohistochemistry. Panel G shows sections stained with Luxol fast blue, which stains myelin. Non-stained regions, denoted by the square, show demyelinated sites corresponding to PML

lesions. Panel H shows sections stained for the serotonin receptor, showing increased expression of the receptor around the lesion site yet not in adjacent regions. (Reproduced with permission from Haley *et al*, 2015 and the American Society for Investigative Pathology).

JCV genome nuclear translocation occurs through clathrin-dependent endocytosis (Ferenczy *et al*, 2012; Pho *et al*, 2000) (Figure 4). After viral binding to a permissive receptor, JCV is endocytosed in a clathrin-dependent manner and trafficked from clathrin-coated pits to Rab5-positive early endosomes (Querbes *et al*, 2004). The JCV-containing early endosome colocalizes with cholera toxin B in caveolin-1-positive late endosomes (Engel *et al*, 2011; Querbes *et al*, 2006). After entering the late endosomes, JCV is trafficked to the endoplasmic reticulum where it colocalizes with calregulin (Querbes *et al*, 2006).

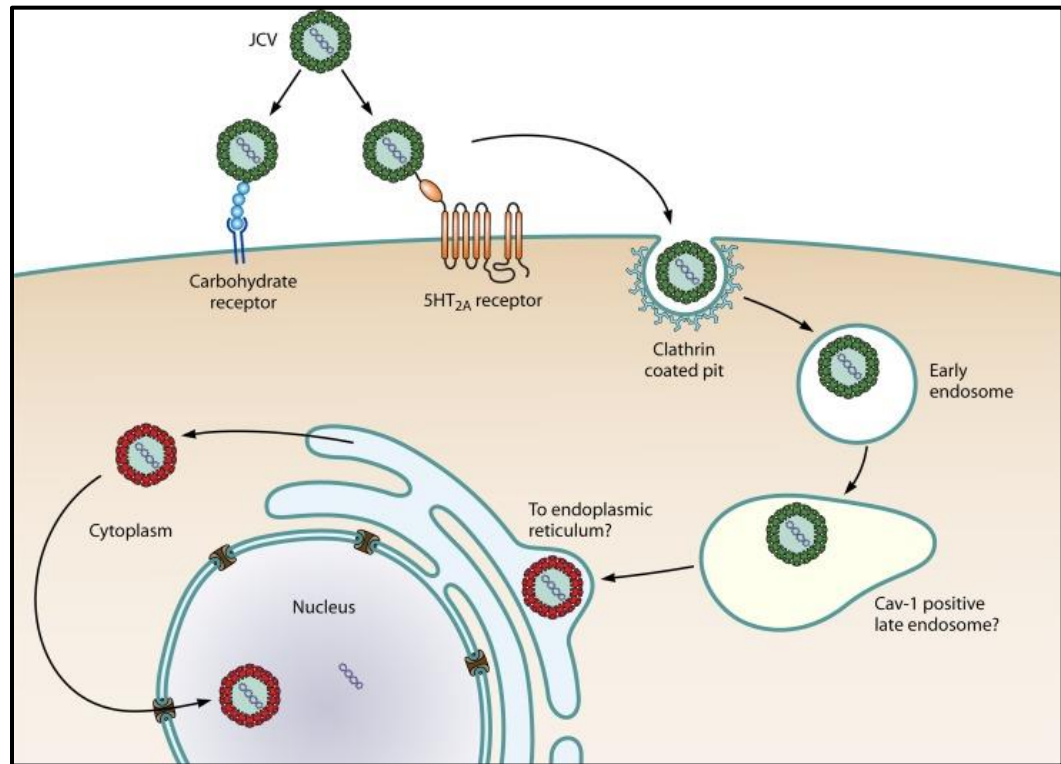


**Figure 4: JCV Cellular Entry and Nuclear Translocation.** Viral particles initiate viral entry by binding to either sialic-acid containing carbohydrate receptors or the serotonin (5HT<sub>2A</sub>) receptor, after which the virus is endocytosed, resulting in the formation of a clathrin coated pit. The virus is

*then trafficked to an early endosome and subsequently co-localized with late endosomes. JCV is then hypothesized to be trafficked to the endoplasmic reticulum and subsequently the cytoplasm, resulting in the exposure of nuclear localization signals and eventual nuclear translocation of the viral genome (Reproduced with permission from Ferenczy et al, 2012 and the American Society for Microbiology).*

The importance of endoplasmic reticulum trafficking for JCV is unknown, however it is critical to the infectious process of other polyomaviruses. Since SV40 and JCV share many characteristics, it is hypothesized that the overall infectious process is similar between the viruses. During SV40 infection, viral trafficking to the endoplasmic reticulum results in capsid disassembly, allowing for virion exposure and cytoplasmic translocation (Schelhaas *et al*, 2007). In the cytoplasm, the capsid is further decomposed through exposure to low intracellular calcium concentrations, which results in the exposure of viral nuclear localization signals and subsequent nuclear translocation of the JCV genome, initiating viral transcription (Ishii *et al*, 1996; Kasamatsu *et al*, 1998; Nakanishi *et al*, 1996; Yamada *et al*, 1993).

Within the nucleus, the viral genome serves as the template for host RNA polymerase II transcriptional machinery (Tada *et al*, 1989). Initial early gene transcription occurs without the presence of viral proteins and entirely utilizes host proteins, which is hypothesized to account for JCV cellular tropism at the transcriptional level (Raj *et al*, 1995). Initiation of early gene transcription occurs following NCCR interactions with host transcription factors, and as previously noted, the NCCR region is highly variable in PML-inducing JCV neurotropic variants and can vary between sites of persistence and productive infection, even in isolates obtained from the same patient (Gosert *et al*, 2010; Martin *et al*, 1985,

Martin *et al*, 1991; Marzocchetti *et al*, 2008; Tan *et al*, 2009; Tan *et al*, 2010). The JCV NCCR contains numerous transcriptional factor binding sites, including sites for Oct-6 (Octamer-Binding Transcription Factor 6), Tst-1, Pur- $\alpha$  (Purine Rich Element Binding Protein A), NF-1, and Spi-B, among others (Amemiya *et al*, 1992; Chen *et al*, 1997; Kerr *et al*, 1994; Marshall *et al*, 2010, Shivakumar *et al*, 1994; Tada *et al*, 1992; Wegner *et al*, 1993). One major difference among JCV variants is that the Madison-1 (Mad-1) variant NCCR contains two 98-bp tandem repeats whereas the Madison-4 (Mad-4) variant NCCR contains a deletion in the second tandem repeat, resulting in the deletion of the late-proximal TATA box (Marshall *et al*, 2012).

JCV early gene transcription initiates following host transcriptional factor binding and interactions with the viral NCCR. Unlike many human DNA viruses, such as adenoviruses, JCV does not bring along any viral transcriptional activating proteins. For example, the adenoviral capsid proteins facilitate viral gene expression and viral replication, whereas JCV relies completely on host factor availability and binding (Schreiner *et al*, 2012). One host factor that mediates JCV transcription is NF-1, which binds to a site adjacent of the JCV promoter TATA box, thereby regulating JCV early gene transcription through mediation of RNA polymerase machinery binding to the promoter region (Shivakumar *et al*, 1994; Tamura *et al*, 1988). NF-1 is hypothesized to contribute to the glial tropism of JCV infection, since it is highly expressed in glial cells with limited or lacking expression in non-glial cells (Sumner *et al*, 1996). To test this hypothesis, CD34+

precursor KG-1 cells, which are susceptible to JCV infection were differentiated with phorbol 12-myristate 13-acetate (PMA) treatment to decrease NF-1 expression resulting in a subsequent loss of susceptibility to JCV infection (Monaco *et al*, 2001). However, differentiated cells transfected with an expression plasmid for NF-1 class D regained permissiveness to JCV infection, suggesting that NF-1 class D has a regulatory role on JCV infection, although if this regulation was due to early gene transcription or another mechanism was not identified (Monaco *et al*, 2001).

Additionally, the activator protein 1 (AP-1) family of transcription factors interacts with JCV to regulate early gene transcription and viral replication. Factors c-Jun and c-Fos, both AP-1 family members, interact with T-antigen to suppress T-antigen mediated activation of early gene transcription and viral replication (Kim *et al*, 2003). By binding to T-antigen, c-Jun suppresses the binding of T antigen to the JCV early promoter region to suppress viral transcription and replication (Kim *et al*, 2003).

After T-antigen expression, JCV shifts from early to late gene transcription simultaneously with the initiation of viral replication. The shift from early to late gene transcription is mediated by YB-1, pur- $\alpha$ , and T-antigen. Following nuclear translocation of the viral genome, pur- $\alpha$  binds to the viral lytic control element to facilitate and induce early gene transcription and T-antigen expression (Chen *et al*, 1995). T-antigen then accumulates within the nucleus, resulting in T-antigen binding to the transcription factor YB-1 to form a complexed structure. The T-

antigen: YB-1 complex binds to the lytic control element with a stronger affinity than pur- $\alpha$ , resulting in pur- $\alpha$  displacement and the initiation of JCV late gene transcription (Chen *et al*, 1995; Kerr *et al*, 1994; Safak *et al*, 1999; Safak *et al*, 1999).

After T-antigen expression, JCV DNA replication is initiated within permissive cells. JCV DNA replication is a very slow process, even within permissive glial cells. DNA replication is first detected at 3 to 5 days post-infection and remains detectable for several weeks (Feigenbaum *et al*, 1987; Khalili *et al*, 1987; Major *et al*, 1985). Many factors participate in viral DNA replication, including T-antigen and host DNA polymerase.

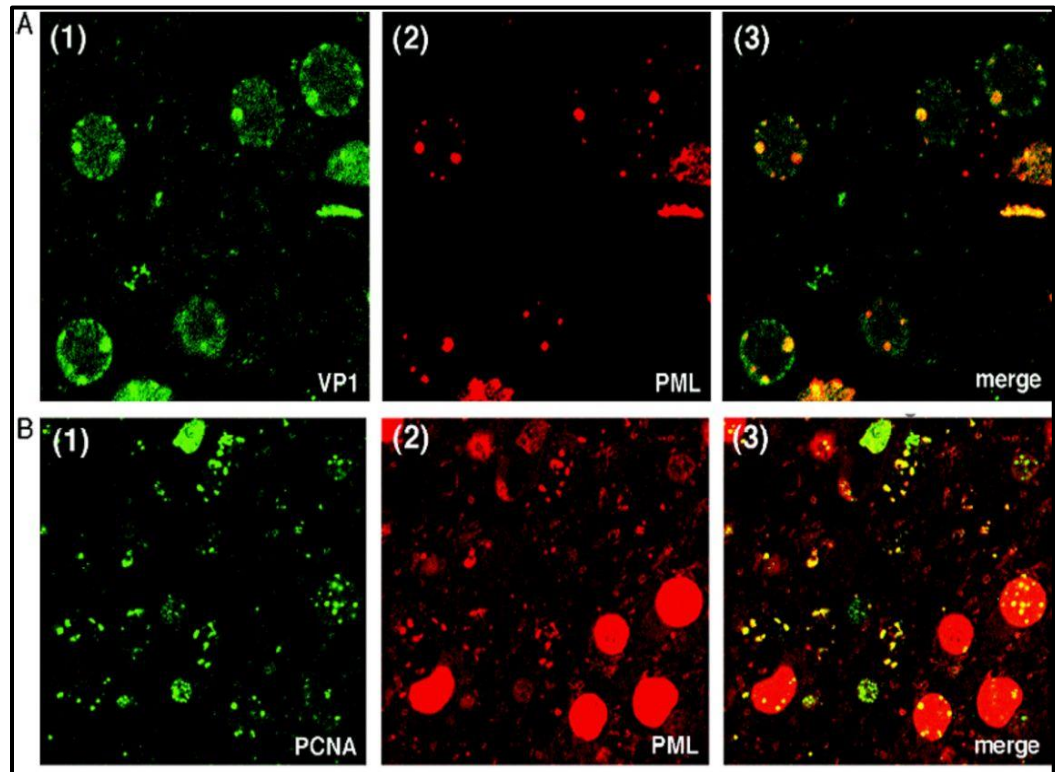


**Figure 5: JCV Co-localization with Promyelocytic Leukemia Bodies.** Serial sections of PML lesions. Panel 1 shows sections stained for JCV capsid protein VP1 and promyelocytic leukemia bodies. Merged images show that VP1 co-localization with the promyelocytic leukemia bodies.

Panel 2 shows parallel sections stained for proliferating cell nuclear antigen and promyelocytic leukemia bodies. Merged images show that PML is highly expressed in proliferating cells. These data combined suggest that JCV co-localizes with promyelocytic leukemia bodies in proliferating cells. (Reproduced with permission from Shishido-Hara *et al*, 2008 and Oxford University Press).

JCV DNA replication occurs within the nucleus at nuclear domain 10 (ND10) bodies, which are nuclear loci characterized by the accumulation of promyelocytic leukemia proteins, Daxx, Sp100, and other cellular factors (Gasparovic *et al*, 2009; Negorev *et al*, 2001). During JCV infection, the viral genome localizes at ND10 bodies, which is hypothesized to promote viral replication due to the localization of many transcriptional activating factors at these bodies, including proliferating cell nuclear antigen (PCNA), which interacts with DNA polymerase for functional replication (Shishido-Hara *et al*, 2008) (Figure 5).

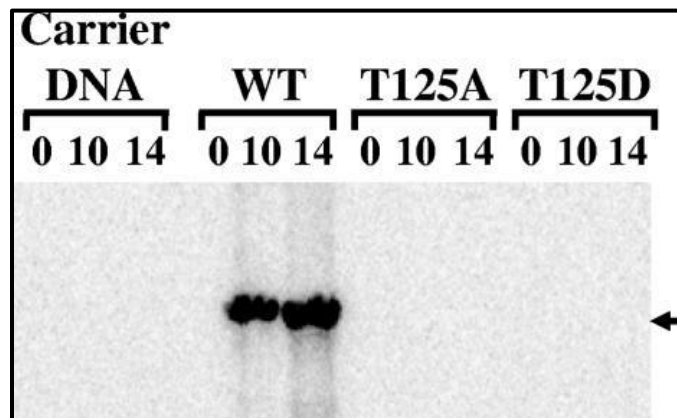


**Figure 6: T-Antigen is Necessary for Functional JCV Replication.** The DNA replication of JC virus was assessed for the wild type strain and two strains with mutations within the T-antigen coding region denoted T125A and T125D, corresponding to the amino acid mutation. At 0-, 10-, and 14-days post-JCV genome transfection, low-molecular weight DNA was collected and analyzed for replicated DNA. Strains with mutations in T-antigen, producing a non-functional protein, demonstrated no viral replication (Reproduced with permission from Tyagarajan *et al*, 2006 and the American Society for Microbiology).

JCV large T-antigen is the primary viral driver of replication and functional lytic infection. JCV T-antigen mutant strains have inefficient viral replication and

infection does not result in cellular lysis (Tyagarajan *et al*, 2006) (Figure 6). To initiate viral replication, T-antigen binds to the viral origin of replication at the GAGGC pentanucleotide sequence, resulting in formation of a tertiary structure that mediates efficient viral replication (Amirhaeri *et al*, 1988; Frisque *et al*, 1983; Major *et al*, 1992). Likewise, T-antigen functions drives the host cell from G<sub>0</sub> to S phase to induce viral replication through interactions with both pRb and p53 (Bollag *et al*, 2000; Del Valle *et al*, 2001; Orba *et al*, 2009; Tavis *et al*, 1994; White *et al*, 2006).

Although the mechanism of DNA replication for JCV is not completely understood, it is proposed to be analogous to SV40 DNA replication. During SV40 DNA replication, T-antigen forms a double hexamer structure and functions as a helicase while forming a complex with topoisomerase I, DNA polymerase  $\alpha$ , and replication protein A to promote viral replication (Bullock *et al*, 1991; Fairman *et al*, 1988; Nesper *et al*, 1997) (Figure 7). After T-antigen binds to the viral origin of replication, it unwinds the genomic duplex and forms the pre-priming complex with replication protein A. This complex undergoes replication beginning with the 5' end of the leading strand, which is interrupted after PCNA binds to the strand and displaces the polymerase complex. T-antigen interacts with DNA polymerase  $\delta$ , PCNA, and replication factor C during the elongation aspect of replication (Lee *et al*, 1990; Tsurimoto *et al*, 1990; Weinberg *et al*, 1990). After replication is complete, the SV40 genome exists as two interlinked circles, however,

topoisomerase I and topoisomerase II function to cleave and religate the genomes separately (Nesper *et al*, 1997).

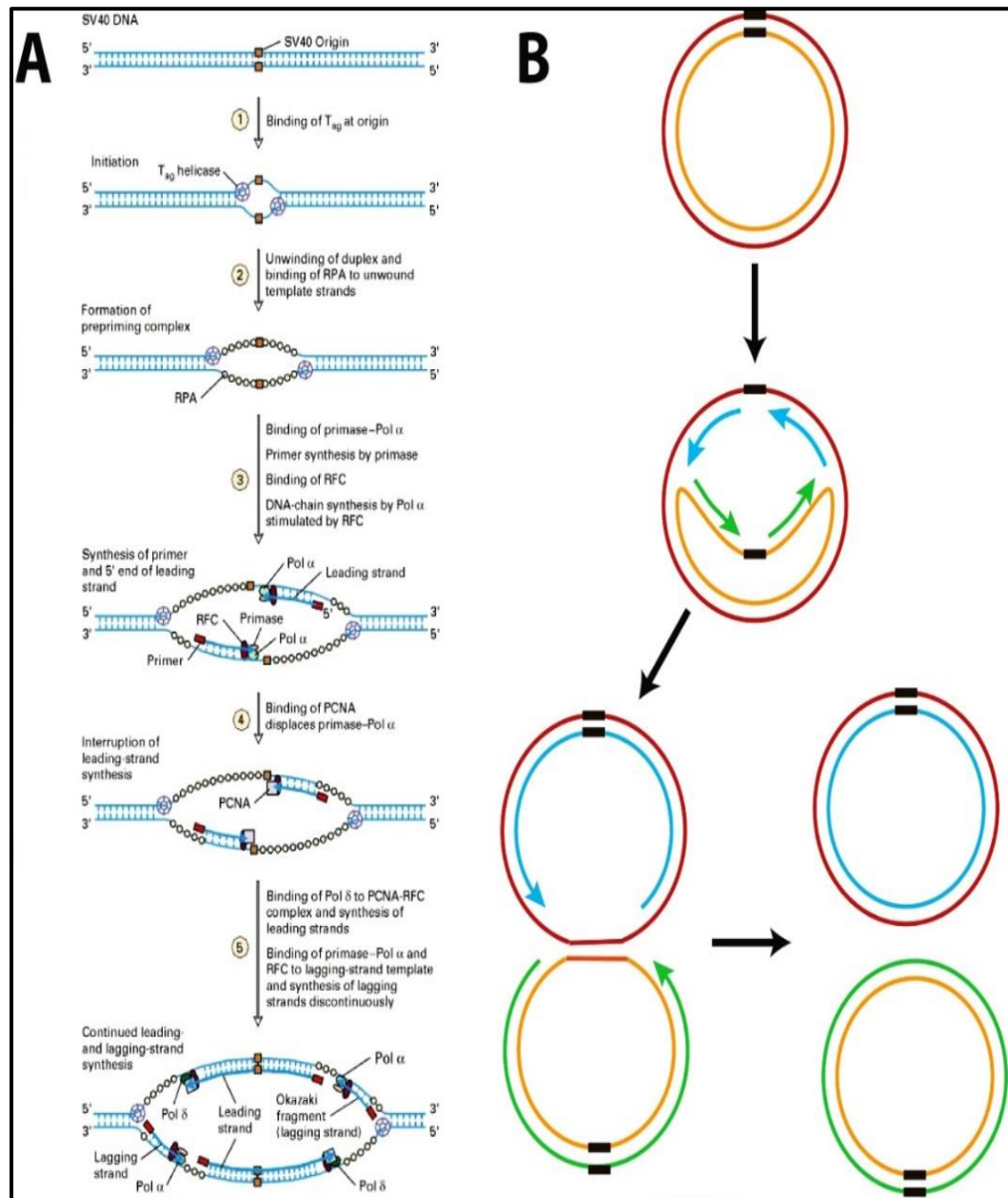


**Figure 7: SV40 Viral Replication.** SV40 viral replication initiates with T-antigen binding to the SV40 origin of replication, resulting in unwinding of the double-stranded DNA through T-antigen helicase activity. DNA polymerase  $\alpha$  binds to the primed complex, which results in the synthesis of viral DNA. (Reproduced figure obtained from National Institutes of Health and is in the public domain. Source: *Molecular Cell Biology*, 4th edition, Lodish H, Berk A, Zipursky SL, et al. New York: W. H. Freeman; 2000).

The immune system is the body's primary defense against JCV reactivation and productive infection. In terms of JCV, it appears that a compromised adaptive immune system is the primary risk factor for productive infection (Gheuens *et al*, 2010). Briefly, the adaptive immune system responds to viral infections through the function of antigen presenting cells (APCs), CD4+ and CD8+ T-cells. After an APC recognizes a pathogen, it presents the foreign antigen to CD4+ T-cells, which become activated after this priming. CD4+ T-cell activation induces the activation of CD8+ T-cells in addition to promoting the differentiation and maturation of B-cells in the periphery. Activated CD8+ T-cells serve to eliminate virally infected cells. (Reuwer *et al*, 2017). Clearly CD4+ cells play a major role in controlling JCV infection, as a majority of PML patients have comorbidities affecting CD4+ counts, including HIV and CD4+ lymphocytopenia, among others (Casado *et al*, 2014; Haider *et al*, 2000; Puri *et al*, 2010; Weber F. *et al*, 2001; Weber T. *et al*, 2001). Additionally, CD8+ cell function appears to control JCV infection as well, with favorable PML prognosis associated with anti-JCV CD8+ activity (Khanna *et al*, 2009a; Koralnik *et al*, 2002; Monaco and Major, 2015). While the cellular-mediated aspect of adaptive immunity plays a major role in control of JCV infection, the role of B-cells and the humoral aspect of adaptive immunity is less clear (Ferenczy *et al*, 2012; Koralnik 2002; Koralnik *et al*, 2002; Reuwer *et al*, 2017). When assessing at risk populations, a high antibody index in the JCV DxSelect™ test correlates with an increased risk of PML development (Lee *et al*, 2013). Interestingly, 63 of 64 patient samples collected 6-180 months prior to PML diagnosis in natalizumab-treated patients tested JCV antibody positive (Lee *et al*,

2013). The only sample that tested negative was a sample taken 15 months prior to PML development, however a sample collected from the same patient 2 months prior to PML development was antibody positive (Lee *et al*, 2013). Validation assays showed a 50-60% serotype positive rate among all control groups, consistent with published literature (Kean *et al*, 2009; Knowles *et al*, 2003; Lee *et al*, 2013; Stolt *et al*, 2003). However, some studies suggest that the presence of neutralizing immunoglobulin G (IgG) antibodies to JCV variants correlates with PML survival. In the study by Ray *et al*, 6 AIDS+ PML patients were assessed for the presence of neutralizing antibodies to wild-type JCV and neurotropic variant strains of JCV. All six patients possessed neutralizing antibodies to the wild-type strain, however, no patient initially possessed neutralizing antibodies to the neurotropic variants. Of the six total patients, only three survived, and interestingly, each surviving patient developed high titers of neutralizing antibodies to their specific JCV neurotropic variant strain, whereas the non-survivors did not develop a significant neutralizing antibody titer (Ray *et al*, 2015). This data suggests that neutralizing antibodies may play a role in JCV regulation, however, further studies are required to elucidate their complete role. The primary complication with assessing the role of antibodies during JCV infection is the lack of comprehensive literature. When assessing PML development in patients with primary antibody deficiencies, there are a limited number of case reports (Gorelik *et al*, 2010; Plavina *et al*, 2014). Examples of PML development co-morbid with selective humoral immunodeficiency, as opposed to non-selective disorders such as lymphomas that affect both humoral and cellular-mediated immunity, include a 4-year-old child with congenital

hypogammaglobulinemia, a 37-year old man with X-linked agammaglobulinemia, and a patient with Franklin disease and hypogammaglobulinemia (Bezrondik *et al*, 1998; Tasca *et al*, 2009; Teramoto *et al*, 2003). Hypogammaglobulinemia is a condition characterized by a reduction in serum immunoglobulin levels, due to underlying immune system defects or secondary immunodeficient states. X-linked agammaglobulinemia, called Bruton syndrome, is a primary humoral immunity deficiency syndrome resulting from mutations within the Bruton tyrosine kinase gene, which is required for B-cell development and maturation. Patients with Bruton syndrome do not develop mature B-cells and produce no immunoglobulins. Franklin disease, also called gamma heavy chain disease, is a rare B-cell lymphoplasma cell proliferative disorder characterized by abnormal heavy chain immunoglobulin production, resulting in structural abnormalities due to truncated heavy chain proteins that cannot form disulfide bonds with the light chains of the antibody complex, forming non-functional antibodies. The important note is that these cases are show that PML can develop in patients with humoral immunodeficiency with normal cellular immunity, although development of PML with functioning cellular immunity is extremely rare. Likewise, it is important to note that the cellular functions of B-cells and the presence of antibodies are intertwined, and the B-cell deficiency may be the risk factor for PML development as opposed to the hypogammaglobulinemia (Reuwer *et al*, 2017)

One of the primary mechanisms of immune-mediated viral suppression is the release of cytokines and chemokines by a wide variety of cell types, including

leukocytes. To assess the role of soluble immune factors on JCV infection, JCV-infected glial cells were treated with conditioned media from uninduced or induced peripheral blood mononuclear cells (PBMCs). Treatment of infected cells with conditioned media from induced PBMCs significantly suppressed expression of T-antigen and inhibited viral replication (De Simone *et al*, 2015). To determine the exact factor responsible for viral suppression, multiple candidate cytokines were assessed for antiviral activity. Of the cytokines assessed, including interleukins, interferons, and other factors, only interferon gamma (IFN- $\gamma$ ) possessed significant antiviral effects (De Simone *et al*, 2015).

## **1.2. SRSF1 and JCV**

While the immune system is viewed as the primary mechanism for controlling JCV infection, other non-immunological factors play a major role in JCV regulation and inhibition of viral reactivation. One example is the alternative splicing factor serine/arginine-rich splicing factor 1 (SRSF1), which is involved in the alternative splicing of human pre-messenger RNA (mRNA), non-sense mediated mRNA decay, micro RNA (miRNA) processing, and other necessary cellular functions (Das *et al*, 2014) (Figure 8).

While playing a constitutive role in the host cell, SRSF1 also possess antiviral capabilities through impacting viral splicing and transcription in infected cells. Originally, SRSF1 was identified as a regulator of SV40 infection in which SRSF1 was impacts early gene splicing to increase small t-antigen splicing and decrease large T-antigen early gene splicing (Ge *et al*, 1990).

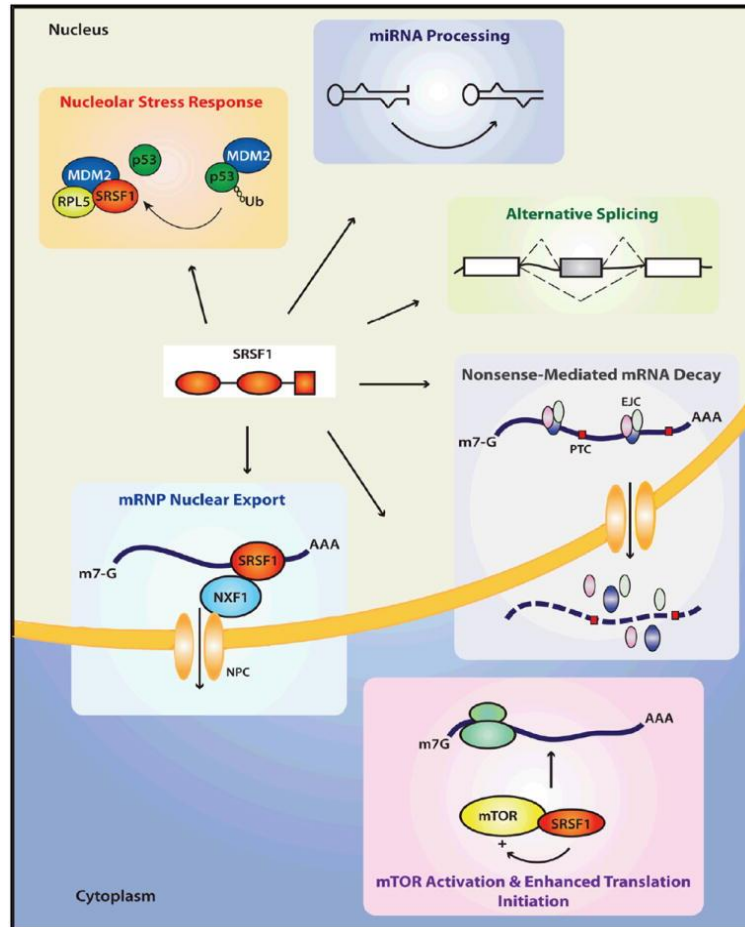


**Figure 8: Cellular Functions of SRSF1.** The alternative splicing factor SRSF1 has multiple functions within the host cell, including miRNA processing, mTor activation, non-sense mRNA degradation, and alternative splicing. (Reproduced with permission from Das et al, 2014 and the American Association for Cancer Research).

During the JCV infectious cycle, SRSF1 functions as a negative regulator through various mechanisms of viral suppression. SRSF1 primarily suppresses viral transcription and replication in glial cells through interactions with the JCV promoter DNA sequence (Sariyer and Khalili, 2011) (Figure 9). When primary human fetal astrocytes were treated with short hairpin RNA (shRNA) against SRSF1, resulting in SRSF1 gene silencing, and subsequently infected with JCV, there was a significant increase in viral protein production, suggesting that JCV replication is suppressed by SRSF1 expression (Sariyer and Khalili, 2011). SRSF1

also impacts the protein expression of all JCV proteins, most likely due to transcriptional suppression, and this inhibits the transforming properties of the T-antigens (Uleri *et al*, 2011).

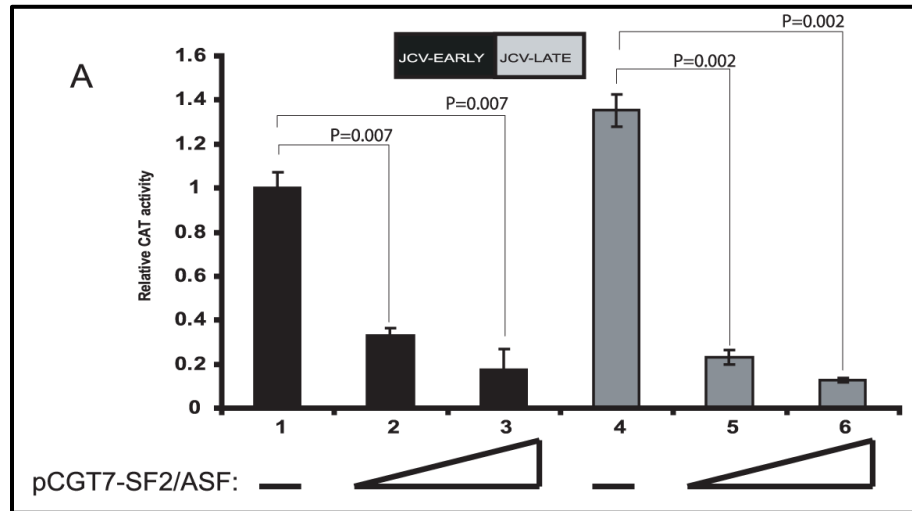


**Figure 9: SRSF1 Suppresses JCV Early and Late Gene Transcription.** PHFA were transfected with luciferase reporter constructs for JCV-early (black bars) or JCV late (grey bars) alone or with increasing concentrations of an SRSF1 expression plasmid. SRSF1 expression resulted in a significant decrease of both JCV early and late gene transcription. (Reproduced with permission from Sariyer and Khalili, 2011 and Open Access PLoS Journal Group).

While SRSF1 possesses a strong negative regulatory impact of JCV, viral proteins are hypothesized to possess the capability to rescue this suppressive mechanism. This thesis assessed if T-antigen expression in cells was sufficient to rescue transcriptional suppression mediated by the expression of SRSF1. A potential interaction between viral proteins and host cellular factors would represent a novel finding into the mechanisms underlying the reactivation of JCV from a latent state to a productive infection.

As previously mentioned, one of the major questions remaining for JCV is what factors are required for viral reactivation to occur. Two of the primary negative regulators of JCV are SRSF1 and the immune system. With the primary risk factor of PML development being immunosuppression, it is possible that the immune system regulates SRSF1 expression. If the immune system regulates SRSF1 expression, it would explain how JCV can reactivate even in glial cells where SRSF1 is most highly expressed. Recent studies elucidated the role of soluble immune factors in controlling SRSF1 expression, potentially serving as an antiviral mechanism. When astrocytes were treated with conditioned media from induced PBMCs there was a significant increase in SRSF1 expression, suggesting that immune activation serves to increase the expression of SRSF1, potentially as an antiviral mechanism (Sariyer R *et al*, 2016). When further assessed, treatment with conditioned media induced SRSF1 transcription, however, whether this mechanism was a direct interaction with the cytokines or indirect induction due to immune signaling pathway cascades remains unclear. Interestingly, data suggests that SRSF1 is the primary driver of cytokine mediated JCV transcriptional suppression. When SRSF1 expression was knocked down in cells using silencing RNA (siRNA), PBMC conditioned media treatment did not suppresses JCV transcription (Sariyer R *et al*, 2016) (Figure 10). Taken together, these data suggest that SRSF1 expression is partially controlled by immune soluble factors and that this control plays a major role in preventing JCV reactivation.

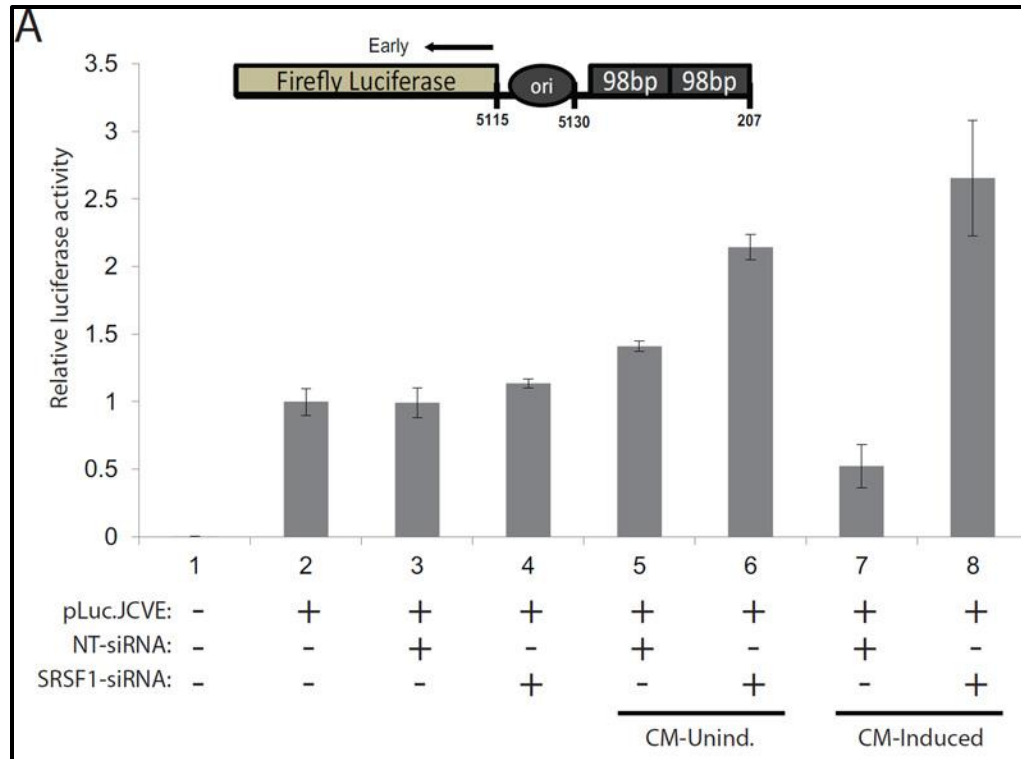


**Figure 10: SRSF1 Expression is Required for Soluble Immune-Factor Mediated JCV Transcriptional Suppression.** PHFA were transfected with a luciferase reporter construct for JCV-early alone or with SRSF1-siRNA to knock down SRSF1 expression or control NT-siRNA. SRSF1-siRNA treatment inhibited soluble immune factor mediated JCV transcriptional suppression. (Reproduced with permission from Sariyer R et al, 2016 and Springer).

### 1.3. Progressive Multifocal Leukoencephalopathy

Progressive multifocal leukoencephalopathy is a neurological disease which presents with widespread, or multifocal, demyelination of both gray and white matter (Al-Tawfiq *et al*, 2015; Astrom *et al*, 1958; Gheuens *et al*, 2010; Wüthrich *et al*, 2009) (Figure 11). PML is the result of latent JCV reactivation and productive infection, which generally occurs during comorbid immunomodulatory conditions. During the course PML, multiple pathological changes occur which affect both glial cells and the surrounding neuronal axons. The primary cells presenting with JCV infection are oligodendrocytes, while astrocytes have also been shown to support productive infection (Kondo *et al*, 2014; Richardson-Burns *et al*, 2002).

After infection, both glial cell populations express viral proteins, resulting in oligodendrocyte swelling and lysis and the presentation of a “bizarre” astrocyte phenotype, with cellular lysis resulting in the focal destruction of myelin protein (Brooks *et al*, 1984; Cavanaugh *et al*, 1959; Piña-Oviedo *et al*, 2007; Wharton Jr *et al*, 2016). Due to destruction of myelin, there is widespread axonal dysfunction and a loss of neuronal cell bodies due to cellular insults on demyelinated axons due to lysis of infected cells, with the neuronal loss being a permanent outcome of PML in most cases (Roux *et al*, 2011; Wüthrich *et al*, 2009).

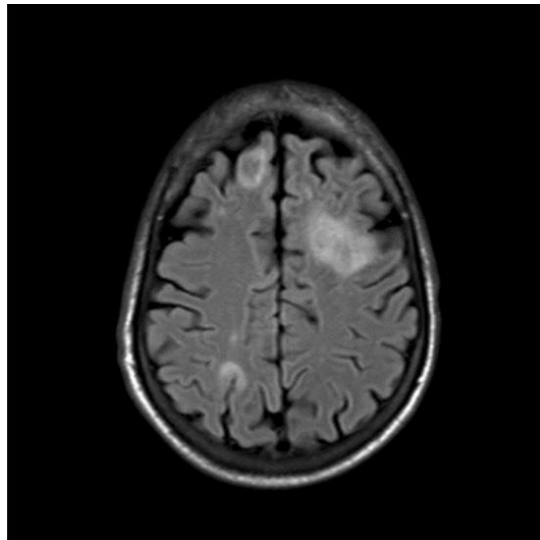


**Figure 11: PML Brain MRI Showing Lesion Sites.** Brain MRI images of a 55-year-old man diagnosed with nodular lymphocyte predominant Hodgkin’s lymphoma. After diagnosis, patient underwent R-CHOP chemotherapy. After 5 cycles of chemotherapy, the patient was admitted with seizure activity, resulting in a CT and subsequent MRI of the brain. Imaging showed multifocal cortical and subcortical lesion sites (light areas). (Reproduced with permission from Al-Tawfiq *et al*, 2015 and Elsevier).

While JCV latent infection is common throughout the population, development of PML remained rare until the AIDS epidemic and the widespread use of immunomodulatory antibody therapies. Initially, PML rarely developed and was only found in patients with underlying oncological conditions impacting immune function, including leukemias and lymphomas (Astrom *et al*, 1958; Richardson Jr.;

1961) (Table 1). While potential cases of PML exist dating back to the 1930s, the first recorded case of PML was in 1958, in which a patient suffering from chronic lymphocytic leukemia and Hodgkin’s lymphoma presented with pathologies similar to PML, including the development of white matter lesions throughout the CNS (Astrom *et al*, 1958; Bateman *et al*, 1945; Christensen *et al*, 1955; Hallervorden *et al*, 1930; Richardson *et al*, 1961, Winkleman *et al*, 1941).

**Table 1: Pathologic States Associated with Progressive Multifocal Leukoencephalopathy prior to the AIDS epidemic.** Summary of 22 patients who developed PML between 1930 and 1961 and the comorbid pathological state. (Reproduced with permission from Richardson Jr *et al*, 1961, Copyright Massachusetts Medical Society).

<b>TABLE 1. Pathologic States Associated with Progressive Multifocal Leukoencephalopathy.</b>	
DISEASE	NO. OF CASES
Hodgkin’s disease	6
Chronic lymphatic leukemia	4
Lymphosarcoma	3
Chronic myelogenous leukemia	2
Sarcoidosis	2
Carcinomatosis	2
Miliary tuberculosis	1
Coronary heart disease	1
Unknown (old age)	1
Total	22

PML became a prevalent condition following the HIV epidemic, as between 3-5% of AIDS patients develop PML during HIV infection (Khanna *et al*, 2009b). As JCV is normally maintained in a latent state by the immune system, it follows that risk for PML development occurs during immune suppression or immunomodulation. There are two primary groups of at-risk populations when analyzing PML patients, which are AIDS patients and patients undergoing immunomodulatory pharmacological therapies. The cohort with the highest risk of

developing PML remains AIDS patients, as PML occurs at a rate significantly higher in this cohort than in cohorts with other causes of immunosuppression (Bienaime *et al*, 2006; Focosi *et al*, 2010; Taoufik *et al*, 1998; Verma *et al*, 2004; Zheng *et al*, 2009).

As a disease, AIDS has a widespread negative impact on the immune system and immunological function, as it presents with chronic immunosuppression, impacts cytokine release, shifts the body towards a more “pro-viral” cytokine profile, and increases the permeability of the BBB to increase infiltration of infected cells into the brain (Houff *et al*, 2008). Studies have suggested that HIV and JCV interact in a synergistic manner, resulting in PML occurrence in these patients. Both HIV and JCV remain latent in CD34+ progenitor cells and mature B-cells following the differentiation of the pro-B cells into B-cells, and can reactivate within the mature differentiated cells (Monaco *et al*, 1996; Houff *et al*, 2008; Monaco *et al*, 1998; Carter *et al*, 2010). Likewise, HIV Tat protein has been shown to interact with JCV by increasing JCV early and late gene transcription and increasing JCV propagation in Tat-expressing cells (Chowdhury *et al*, 1993; Chowdhury *et al*, 1990; Chowdhury *et al*, 1992; Nukuzuma *et al*, 2010; Stettner *et al*, 2009; Tada *et al*, 1990). *In vitro* studies have demonstrated that Tat is secreted from infected cells and internalized by oligodendrocytes leading to the hypothesis that uptake of extracellular Tat by oligodendrocytes could be one of the initial mechanisms for JCV reactivation in AIDS patients (Ensoli *et al*, 1993; Daniel *et al*, 2004; Taylor *et al*, 1992; Enam *et al*, 2004). Infection with HIV also significantly increases the

permeability of the BBB and increases peripheral lymphocyte migration into the brain, both of which may result in increased trafficking of JCV-latently infected lymphocytes into the brain and eventual viral reactivation and PML development, primarily through Tat protein-mediated increased expression of CCL2/MCP-1 (Puri *et al*, 2010; Ault *et al*, 1997; Berger *et al*, 2001; Petito *et al*, 1992). Data suggests some semblance of a relationship between JCV and HIV in which HIV changes the host conditions significantly to allow for JCV reactivation, however, the exact mechanisms of this relationship need to be determined.

With the advent of monoclonal antibodies and other immunomodulatory therapies to treat a wide-range of diseases, it is not surprising that PML development is associated with some of these pharmacological agents. Typically, these therapies are used to treat autoimmune diseases, such as multiple sclerosis or rheumatoid arthritis, or lymphoproliferative diseases, such as lymphomas or leukemias. However, these therapies carry a substantial risk for the development of PML due to changes in the immune system function of these patients.

An immunomodulatory therapy that carries a high risk for PML development is natalizumab, a humanized monoclonal antibody used to treat relapsing multiple sclerosis (MS). Natalizumab functions by binding to the  $\alpha 4$  chain of very late antigen-4 (VLA-4), which mediates cell migration and infiltration into the CNS by binding to the vascular cell adhesion molecule (VCAM), allowing leukocytes to bind to the endothelial cells of blood vessels for extravasation out of circulation to

sites of inflammation (Engelhardt, 2008; Engelhardt and Kappos, 2008; Rice *et al*, 2005). The hallmark of MS is chronic leukocytic infiltration into the brain, which is potently suppressed by natalizumab. Another effect of natalizumab treatment is impact on the B-cell population, functioning to increase CD34+ progenitor cells in the blood and bone marrow, increasing circulating pre-B and B cells in the periphery, and increasing the expression of factors involved in the differentiation of B cells from progenitor cells (Jing *et al*, 2010; Krumbholz *et al*, 2008; Lindberg *et al*, 2008). Importantly, one factor upregulated by natalizumab treatment is Spi-B, a factor involved in promoting the differentiation of B cells which has also been found to increase JCV transcription, thus functioning as a potential mechanism for increased PML risk following natalizumab therapy (Marshall *et al*, 2010). Currently, it has been approximated that 3.85 per 1,000 patients undergoing therapy with natalizumab will develop PML, however, the true incidence remains to be determined (Ferenczy *et al*, 2012).

There are many other immunomodulatory therapies that significantly increase the risk of developing PML over the course of the therapy. Rituximab is a humanized monoclonal antibody that targets CD20 that is used to treat hematological cancers, such as non-Hodgkin's lymphoma, and autoimmune diseases, such as rheumatoid arthritis. Treatment with rituximab results in the destruction of peripheral B cells, since binding of the antibody to CD20 results in NK-cell mediated killing of B-cells, as well as inducing apoptosis in targeted cells (Rudnicka *et al*, 2013). Destruction of peripheral B-cells functions to remove malignant or auto-reactive B-

cells, resulting increased differentiation of pre-B cells in the bone marrow. Since JCV is suggested to infect hematopoietic progenitors in the bone marrow, this treatment may serve to increase the population of JCV positive B-cells in the body (Major 2010; Reff *et al*, 1994; McLaughlin *et al*, 1998).

Efalizumab is a humanized monoclonal antibody that targets CD11b and was used to treat psoriasis. Treatment with efalizumab functioned by disrupting leukocyte function-associated antigen type 1 (LFA-1) binding to intercellular adhesion molecular 1 (ICAM-1), which served to prevent the migration of T lymphocytes to sites of inflammation (Lebwohl *et al*, 2003). However, in 2009, efalizumab was withdrawn from the market by Genentech, Inc. due to the occurrence of PML following treatment, which was found in 1 in 500 patients treated with the drug.

From these at-risk cohorts, it appears that the mechanism behind the increased risk of PML following immunomodulatory therapy is multifaceted, with the overarching theme being a significant decrease in immune surveillance as well as the differentiation of progenitor cells into terminally differentiated lymphocytes, potentially serving as a mechanism for dissemination of latent JCV into the CNS. As immunomodulatory antibodies are being used now more than ever to treat a wide range of diseases, there is the potential that a potential side effect of the drug will be PML development. Antibody therapies that result in PML development will continue to elucidate mechanism of JCV control by the immune system.

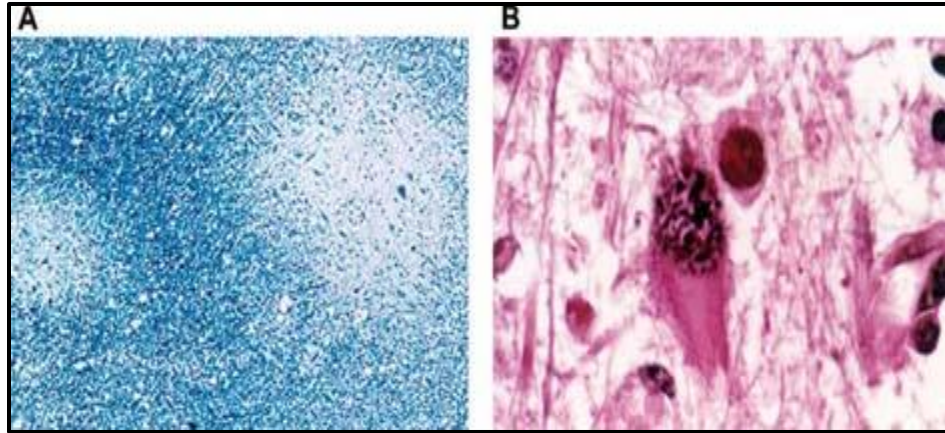


**Figure 12: Histopathological Features of PML.** Panel A shows frontal lobe sections of a PML patient stained with Luxol fast blue, showing large focal areas of widespread demyelination. Panel B shows enlarged oligodendrocytes presenting with inclusion body containing nuclei, the hallmark of productive JCV infection as well as a characteristic “Bizarre astrocyte” with increased chromatin presence and lobulated nuclei. (Reproduced with permission from Sweet *et al*, 2002 and John Wiley and Sons Publishers.).

The primary pathological feature of PML is multifocal demyelination as opposed to monofocal demyelination due to the widespread dissemination of the viral particles within the CNS, suggesting multiple infection origin sites (Berger *et al*, 2013b). Demyelination results in the formation of PML lesions of various size, with the minimal size being roughly 1 mm in diameter upwards to centimeter-sized diameters. In terms of histopathological features, the primary feature is infected oligodendrocytes characterized by the presence of viral inclusion bodies in the nuclei of infected cells, the loss of chromatin structure due to viral replication, and abnormally large nuclei due to the presence of viral particles (Al-Tawfiq *et al*, 2015; Shishido-Hara, 2010; Sweet *et al*. 2002) (Figures 12 and 13). Likewise, infected astrocytes present with a “bizarre astrocyte” phenotype, which generally encompasses lobular hyperchromatic nuclei (Figures 12 and 13). In terms of lymphocytic infiltration, PML lesions are generally devoid of the presence of leukocytes, however, some patients have significant inflammatory cell infiltrates,

generally a symptom of reconstitution of the immune system and improved long-term prognosis (Kepes *et al*, 1975; Richardson Jr *et al*, 1983)

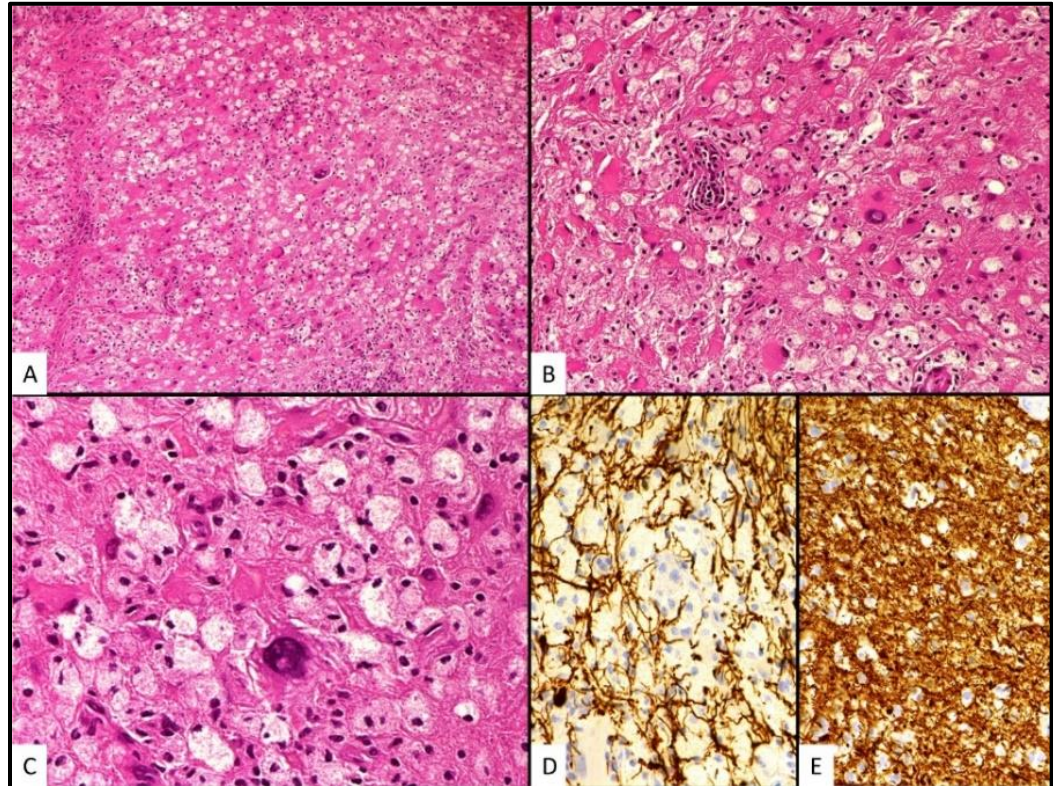


**Figure 13: PML Lesion Histology.** Brain biopsy of a 55-year-old man diagnosed with nodular lymphocyte predominant Hodgkin's lymphoma and PML. Panels A-C show lesion sites with oligodendrocytes containing viral inclusion bodies and decreased chromatin presence at different magnifications (A: 10x, B: 20x, C: 40x). Panel D shows widespread myelin loss with axonal preservation. Panel E shows a normal brain region for myelin comparisons. (Reproduced with permission from Al-Tawfiq *et al*, 2015 and Elsevier).

In addition to PML, JCV is the etiologic agent of three other diseases; JCV granule cell neuronopathy (JCVGCN), JCV encephalopathy (JCVE) and JCV meningitis (JCV M). JCVGCN is characterized by JCV productive infection restricted to granule cell neurons within the cerebellum. Granule cell neuronal productive infection results in cerebellar atrophy in the absence of white matter lesions, suggesting that the JCV variant is not infecting oligodendrocytes as expected during

JCV reactivation (Koralnik *et al*, 2005). The first reported case of JCVGCN was found in a 43-year old woman presenting with neurological deficits 15 months after HIV-seropositivity, including slurred speech, unsteady gait, dizziness, weakness, and vision deficits (Koralnik *et al*, 2005). MRI analysis revealed cerebellar atrophy without accompanying white matter abnormalities. This patient was the first patient where JCV productive infection of granule cell neurons was shown (Figure 14).

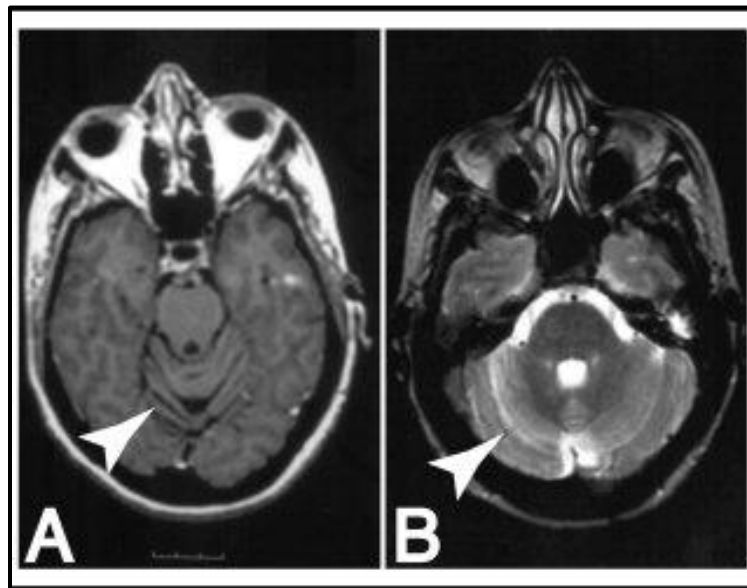


**Figure 14: JCV Granule Cell Neuronopathy Histology.** MRI of a 43-year-old woman diagnosed with HIV. After 15 months, the patient presented with motor deficits and imaging studies were completed. Panel A shows cerebellar atrophy at the arrow head. Panel B shows no white matter abnormality within the brain. (Reproduced with permission from Koralnik *et al*, 2005 and John Wiley and Sons Publisher Group).

JCVE is characterized by JCV productive infection of cortical pyramidal neurons (Dang *et al*, 2012; Wüthrich *et al*, 2009). Cortical pyramidal neuronal productive infection results in diffuse cortical lesions in the absence of white matter lesions and necrosis at the gray matter-white matter junctions (Wüthrich *et al*, 2009). The first reported case of JCVE was found in a 74-year old woman presenting with progressive aphasia and cognitive deficits five months after completing radiation

and chemotherapy for non-small-cell lung cancer. MRI analysis revealed multifocal cortical lesions found in the temporal, parietal, and frontal cortexes (Figure 15). This patient was the first patient where JCV productive infection of cortical pyramidal neurons was shown.

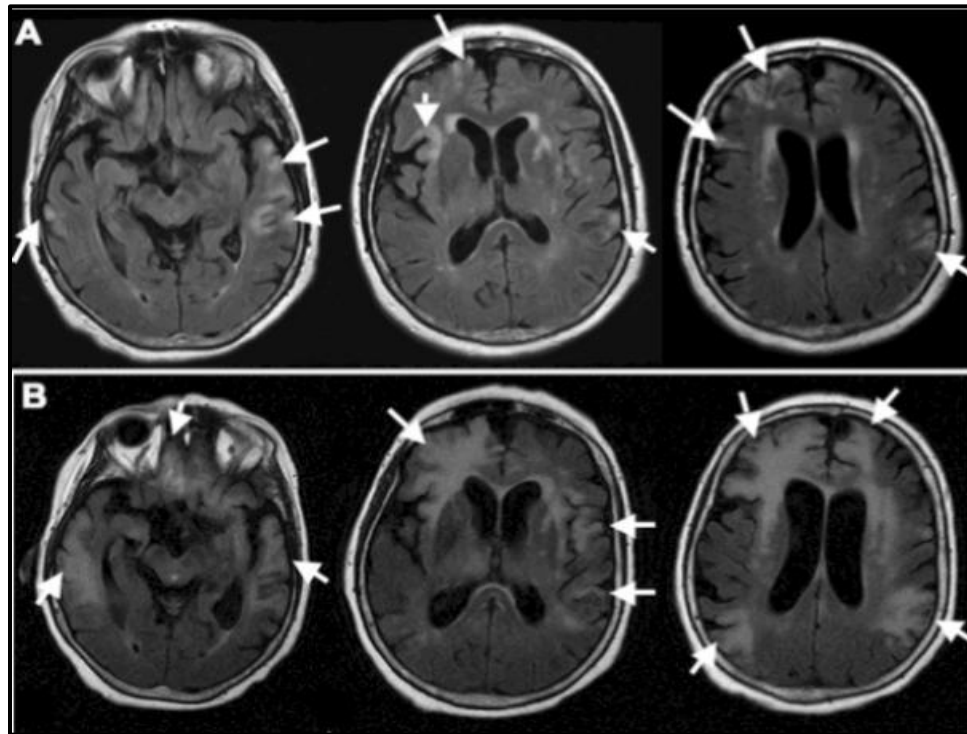


**Figure 15: JCV Encephalopathy Histology.** MRI of a 74-year-old woman diagnosed with non-small-cell-lung cancer. Five months after completing chemotherapy, the patient presented with neurological deficits and progressive aphasia and imaging studies were completed. Panel A shows lesion sites in both cerebral hemispheres at the arrow heads. Panel B shows imaging 3 months after the initial images, in which additional cortical areas have developed lesion sites and there is necrosis at the gray matter-white matter junctions (Reproduced with permission from Wüthrich *et al*, 2009 and John Wiley and Sons Publisher Group).

The first reported case of JCVM was found in a 38-year old woman previously diagnosed with systemic lupus erythematosus (SLE) presenting with sudden onset of altered consciousness, fever, and headache (Viallard *et al*, 2005). The patient had meningeal syndrome with neck stiffness and double vision, but did not have focal neurological deficit. Previous reports have detected JCV DNA in the CSF of

meningitis patients without immunosuppression or factors that would result in meningitis, leading to the hypothesis that JCV may be the etiologic agent (Behzad- Behbahani *et al*, 2004). This presented case demonstrates that JCV infection is an etiologic agent that must be considered during the onset of meningitis.

#### **1.4. Hypothesis and Proposed Aims**

Presently, the factors resulting in PML reactivation remain unknown. Wholly, the immune system functions to prevent JCV reactivation, with extremely limited cases of PML in patients with no immunosuppression at the time of PML development (Crossley *et al*, 2016; Sethi *et al*, 2012). Additionally, research has elucidated that many cellular factors function to prevent or inhibit JCV reactivation without entirely relying on immune system function. Our laboratory has focused on the role of SRSF1, a host alternative splicing factor, which has been shown to negatively regulate JCV transcription and replication. Outside research has focused on the role of cellular transcription factors, such as YB-1 and c-Jun, in the regulation of JCV transcription and replication. Based on this research, it would be prudent to postulate that there are many other host factors that regulate JCV reactivation through various steps within the viral life cycle. However, with a majority of the research focusing on either host factor impact on the virus or viral protein interactions with the virus during infection, a niche of JCV research has arisen focusing on how viral factors interact and modulate host factor and immune system regulation of JCV. Following immunosuppression, we hypothesize that interactions between JCV regulatory proteins and the neuroimmune signaling between

peripheral immune cells and glia in response to JCV infection regulates JCV gene expression and viral replication in glial cells. To investigate this proposed hypothesis, we present two specific aims, encompassing the experiments required to discern the validity of the hypothesis.

Specific aim #1 focuses on viral protein interactions with host factors, primarily with the strong JCV-negative regulator SRSF1. Throughout Chapter #3 of this thesis, we will present experiments completed to assess the molecular interplay between T-antigen and SRSF1 in the control of JC virus gene expression in glial cells. This specific aim was conceived by preliminary data characterizing SRSF1 as a strong negative regulator of JCV transcription and replication within glial cells (Sariyer and Khalili, 2011) (Figure 9). We investigated the role of JCV regulatory proteins, T-antigen and agnoprotein, in regulation of SRSF1-mediated viral transcriptional suppression. Our results suggest that T-antigen rescues JCV transcriptional suppression by suppressing SRSF1 transcription and subsequent protein expression through a possible interaction with the SRSF1 promoter region. These results reveal a novel viral mechanism for bypassing host negative regulation.

Specific aim #2 focuses on viral protein interactions with the immune system, primarily via agnoprotein release by infected glial cells. Throughout Chapter #4 of this thesis, we will present experiments completed to assess how extracellular agnoprotein mediates the immune response to JC virus infection. This specific aim

was conceived by preliminary data proposing that agnoprotein is released from infected glial cells (Otlu *et al*, 2014) (Figure 16).

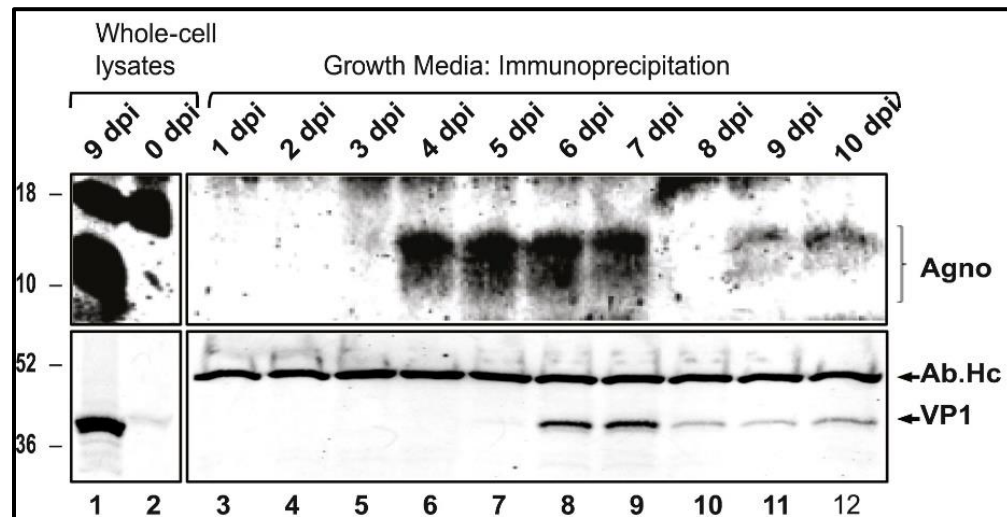


**Figure 16: Agnoprotein is released from JCV Infected Glial Cells.** SVG-A cells were infected with JCV Mad-1 and growth media was collected and 24-hour intervals following infection, up to day 10. At day 9, whole-cell lysates were collected as well. Collected growth media underwent immunoprecipitation for agnoprotein and VP-1 with whole cell extracts serving as controls for protein expression. Immunoprecipitation showed that agnoprotein is present within the media following cellular infection. (Reproduced with permission from Otlu *et al*, 2014 and Elsevier).

Our data suggests that agnoprotein is released from cells and internalized by non-infected astrocytes and microglia, resulting in agnoprotein-mediated GM-CSF transcriptional suppression and subsequent reduction of GM-CSF release. Additionally, our data suggests that extracellular agnoprotein mediates monocytes and macrophage function by impacting differentiation, surface marker expression, phagocytosis, and migration to sites of neuroinflammation. These results reveal a novel immunomodulatory function of agnoprotein and suggest a possible mechanism partly involved in the limited inflammation observed at PML lesions.

The totality of these experiments can be found within this thesis, in which the culmination of the experiments has supported the validity of the proposed

hypothesis. Inevitably, as has been the case since time immemorial, further research is required to completely elucidate the mechanisms resulting in viral reactivation. Here, we have presented the discovery of novel functions of JCV viral proteins, thereby furthering the development of a complete model for JCV reactivation.

## CHAPTER 2

### MATERIALS AND METHODS

#### 2.1. Cell Culture and Transfection

The **human oligodendrogloma cell line, TC620**, was obtained from American Type Culture Collection (ATCC) and used to mimic oligodendrocytes, the primary cell type infected by JCV. TC620 cells were grown in Dulbecco's Modified Eagle Medium (DMEM) supplemented with 10% heat-inactivated fetal bovine serum (FBS) and penicillin/streptomycin (100 µg/mL). Cells were maintained at 37° C in a humidified incubator with 5% CO<sub>2</sub>.

The **human glioblastoma cell line, T98G**, was obtained from ATCC and used to mimic astrocytes, which are hypothesized to be impacted by JCV reactivation and PML. T98G cells were grown in DMEM supplemented with 10% heat-inactivated FBS and penicillin/streptomycin (100 µg/mL). Cells were maintained at 37° C in a humidified incubator with 5% CO<sub>2</sub>.

The **human monocyte cell line, U937**, was obtained from ATCC and used to mimic monocytes, one of the major immune cells that is hypothesized to be impacted by JCV and PML. U937 cells were grown in Roswell Park Memorial Institute (RPMI) 1640 media supplemented with 10% heat-inactivated FBS and penicillin/streptomycin (100 µg/mL). Cells were maintained at 37° C in a humidified incubator with 5% CO<sub>2</sub>.

**Primary human fetal astrocytes (PHFA)** were obtained from a fetal donor brain provided by the Comprehensive NeuroAIDS Core (CNAC) facility at the Lewis Katz School of Medicine of Temple University. PHFA were used to mimic primary

astrocytes throughout the aforementioned experiments. PHFA were cultured in Dulbecco's Modified Eagle's Medium/Nutrient Mixture F-12 (DMEM/F12) supplemented with 10% heat-inactivated FBS, penicillin/streptomycin (100 µg/mL), GlutaMax (100 µg/mL), and insulin (100 µg/mL). Cells were maintained at 37° C in a humidified incubator with 5% CO<sub>2</sub>.

**Primary human fetal brain endothelial cells (PHFBE)** were obtained from a fetal donor brain provided by the CNAC facility at the Lewis Katz School of Medicine of Temple University. PHFBE were used to mimic endothelial cells of the blood-brain barrier throughout monocyte migration assays. PHFBE were cultured in Clonetics Endothelial Cell Basal Medium-2 supplemented with FBS, hydrocortisone, human fibroblast growth factor, vascular endothelial growth factor, R3-IGF, recombinant insulin-like growth factor, ascorbic acid, human epidermal growth factor, GA-1000, and heparin. Cells were maintained at 37° C in a humidified incubator with 5% CO<sub>2</sub>.

**Primary human fetal microglia (PHFM)** were obtained from a fetal donor brain provided by the CNAC facility at the Lewis Katz School of Medicine of Temple University. PHFM were used in part of the phagocytosis assay. PHFM were cultured in DMEM/F12 supplemented with 15% heat-inactivated FBS, gentamycin (50 µg/mL), L-glutamine (100 µg/mL), fungizone (50 µg/mL), insulin (100 µg/mL), D-biotin (10 ng/mL) and NI supplement (Sigma #N6530). Cells were maintained at 37° C in a humidified incubator with 5% CO<sub>2</sub>.

## 2.2. Primary Monocyte Isolation and Culture

Primary human monocytes were isolated from whole blood provided by Biological Specialty Corporation (Colmar, PA) using the StemCell Technologies EasySep™ Human Buffy Coat CD14 positive selection kit. The blood was diluted 1:1 in EasySep™ Buffer and centrifuged at 200g for 30 minutes at room temperature with acceleration and breaking set to the lowest setting to prevent red blood cell lysis and disruption of the leukocyte band. After centrifugation, the concentrate leukocyte band was transferred to a 14-mL polystyrene round-bottom tube for monocyte isolation. To remove remaining red blood cells, an equal volume of EasySep™ red blood cell (RBC) lysis buffer was added and the solution was mixed. For an example isolation, 4.5 mL of buffy coat was combined with 4.5 mL of RBC lysis buffer, resulting in 9 mL of diluted sample. To the diluted sample, 450 µL of CD14 positive selection cocktail containing anti-CD14 clone BA-9 antibody (50 µL antibody cocktail per mL sample) was added and the solution was incubated at room temperature for 15 minutes. The antibody cocktail contains a tetrameric antibody complex, with two antibody regions, one against CD14 to bind to the cell and one against dextran to bind to the magnetic nanoparticles. After incubation, 450 µL of EasySep™ whole blood magnetic nanoparticles (50 µL magnetic nanoparticles per mL sample) were added and mixed, followed by 10 minutes of incubation at room temperature. After incubation, 1 mL EasySep™ buffer was added to the sample to reach a final volume of 10 mL. The tube was then placed into a “Big Easy” EasySep™ magnet and incubated for 10 minutes at room temperature. After this incubation, the magnet was quickly inverted, and the

supernatant was emptied, after which the tube was removed from the magnet and 10 mL of EasySep™ buffer was added to the tube. The tube was placed into the magnet again and incubated for 5 minutes at room temperature. The magnet was again quickly inverted to remove the supernatant and another 5-minute incubation was performed after the addition of another 10 mL of EasySep™ buffer. After three total isolation steps (one 10-minute isolation and two 5-minute isolations), the tube was removed from the magnet and the cells were resuspended in RPMI 1640 media supplemented with 10% FBS.

Isolated primary human monocytes used to assess monocyte migration in a blood-brain barrier model. Primary human monocytes were grown in RPMI 1640 media supplemented with 10% heat-inactivated FBS and penicillin/streptomycin (100 µg/mL). Cells were maintained at 37° C in a humidified incubator with 5% CO<sub>2</sub>.

### **2.3. Plasmid Constructs**

The pcDNA3.1-T-Antigen expression vector construct was described previously (Craigie et al, 2015). Briefly, the T-antigen gene was PCR amplified and subcloned into the pcDNA3.1 (+) expression vector at the EcoRI restriction enzyme site.

The pcGT7-SRSF1 expression plasmid was kindly provided by Javier F. Cáceres (Medical Research Council Human Genetics Unit, Western General Hospital, Edinburgh, Scotland, United Kingdom) and was described previously (Cáceres *et al*, 1997). Briefly, SRSF1 cDNA was PCR amplified and subcloned into the pcGTHCF<sub>FL</sub>T7 expression vector at XbaI/BamHI restriction enzyme sites. The resulting vector expresses the NH<sub>2</sub>-terminal epitope tag of MASMTGGQQMG, the

first 11 amino acids of the bacteriophage T7 gene 10 capsid protein (Cáceres *et al*, 1997).

The pcGT7-agnoprotein expression plasmid was described previously (Otlu *et al*, 2014). Briefly, the JCV agnoprotein coding sequence was PCR amplified and subcloned into the pcGTHCF<sub>FL</sub>T7 expression vector at XbaI/BamHI restriction enzyme sites. The resulting vector expresses the NH<sub>2</sub>-terminal epitope tag of MASMTGGQQMG, the first 11 amino acids of the bacteriophage T7 gene 10 capsid protein (Cáceres *et al*, 1997).

The luciferase reporter constructs pLuc.JCV-Early and pLuc.JCV-Late were described previously (Wollebo *et al*, 2011). Briefly, the full-length JCV Mad1 NCCR was PCR amplified and subcloned into the SmaI restriction enzyme site immediately upstream of the luciferase gene in the pGL3 luciferase reporter vector by blunt end cloning (Promega, Madison, Wisconsin, USA).

The pLuc.SRSF1 luciferase reporter construct was created by subcloning the PCR amplification of the SRSF1 promoter region from the -1000 to +49 region into the pGL3 luciferase reporter vector at the BamHI restriction enzyme site upstream of the luciferase gene.

The GM-CSF luciferase reporter construct, pLuc.GMCSF, was kindly provided by Peter Cockerill (College of Medical and Dental Science, Institute of Biomedical Research, University of Birmingham, UK) and was described previously (Cockerill *et al*, 1999). Briefly, the GM-CSF promoter was PCR amplified for the -627 to +28 region and subcloned into the pXPG luciferase reporter plasmid at the HindIII restriction enzyme site upstream of the luciferase gene.

To create the JCV bi-directional dual reporter plasmid, the full-length JCV Mad1 NCCR was PCR amplified and subcloned into the pSF-Renilla-Photinus vector (Sigma-Aldrich, OGS595) at the NotI/EcoRI restriction enzyme sites between the firefly luciferase and renilla luciferase genes.

#### **2.4. MBP Recombinant Agnoprotein Production**

*E. coli* maltose binding protein (MBP) fused with JCV agnoprotein fusion protein complexes were produced using DH5 $\alpha$  *E. coli* cells transformed with the pMAL-c5X-JCV-Agno-Full Length plasmid kindly provided by Dr. Sami Saribas and previously described (Saribas *et al*, 2011). The full length agnoprotein gene was inserted into the pMAL-c5x vector in the same translational reading frame as the maltose-binding protein gene (*malE*), resulting in the expression of MBP-agnoprotein fusion protein complexes. Transformed *E. coli* was grown overnight in 100 mL LB media supplemented with ampicillin (100  $\mu$ g/mL). After overnight growth, the culture was split and diluted 1:10 in a total volume of 500 mL of fresh LB media supplemented with ampicillin (100  $\mu$ g/mL) and glucose (2g/L) and was grown at 37° C for 2-3 hours until the optical density at 600 nm reached 0.5, corresponding to optimal confluency. MBP production was induced by incubation with 0.5 mM isopropyl  $\beta$ -D-1-thiogalactopyranoside (IPTG) for 3 hours at 37° C. Cultures were harvested by centrifugation at 10,000 RPM for 30 minutes using a Thermo Scientific F12-6X500 LEX rotor. Bacterial pellets were resuspended in 10 mL amylose column buffer (20 mM Tris-HCl pH 7.4, 200 mM NaCl, 1 mM EDTA). The mixture was incubated on ice for 30 minutes with lysozyme and

protease inhibitor cocktail to degrade the bacterial cell wall, after which lysis was completed through 40 pulses with a sonicator. The lysates were cleared by centrifugation at 15,000 RPM for 30 minutes using a Sorvall HB-6 rotor, after which the supernatants were collected for MBP processing. The cleared lysates were incubated overnight with 800  $\mu$ L of amylose fast flow resin beads, which bind to MBP, at 4° C overnight. The next day, beads were centrifuged at 3,000 RPM for 5 minutes using a Sorvall RT7 plus centrifuge to pellet the MBP-bound amylose resin beads. The supernatant was removed, and beads were washed three times in amylose column buffer to remove remaining unbound proteins. To ensure that efficient binding occurred, 5  $\mu$ g of beads were separated on a 10% SDS-PAGE gel and visualized with Coomassie blue staining. Once the presence of MBP was determined, the MBP-agnoprotein complexes were eluted from the beads by incubation with 10 mM maltose buffer overnight at 4° C at a 1  $\mu$ g/ $\mu$ L concentration. After overnight incubation, samples were centrifuged, and the supernatants were collected for cleavage of the fusion protein. Agnoprotein was cleaved from the fusion protein complex using Factor Xa protease (New England BioLabs #P8010S), which cleaves at the Ile-(Glu/Asp)-Gly-Arg cleavage site, present between the MBP and the fused agnoprotein protein (Eaton *et al*, 1986; Nagai *et al*, 1985; Quinlan *et al*, 1989). For cleavage, 50  $\mu$ g of MBP-agnoprotein were treated with 1  $\mu$ L of Factor Xa in 2 mM CaCl<sub>2</sub> buffer overnight at 23° C. Following cleavage, residual MBP was removed by incubation with amylose fast flow resin beads. Concentration of the final recombinant agnoprotein (rAgno) was determined

and protein quality and immunogenicity were assessed through Western blot using an anti-agnoprotein antibody.

## **2.5. Western Blot Assay**

Cells were harvested using trypsin incubation at different times based on experimental conditions. Detached cells were collected and centrifuged at 1,800 RPM in a Sorvall RT7 centrifuge for 5 minutes. Cellular pellets were resuspended in TNN lysis buffer (150 mM NaCl, 40 mM tris pH 7.4, 1% NP-40, 1 mM DTT, 1 mM EDTA) supplemented with protease inhibitors and rotated for 1 hour at 4° C to ensure efficient lysis. After lysis, samples were centrifuged at 14,000 RPM for 10 minutes at 4° C in a VWR centrifuge. Supernatants were collected, and protein concentration was determined using a Bradford assay with a Genesys 10S Vis spectrophotometer. Western blots were completed with 60 µg of protein extracts unless otherwise noted. Protein extracts were boiled at 95° C for 10 minutes to ensure efficient denaturing. Denatured samples were resolved through sodium dodecyl sulfate polyacrylamide gel electrophoresis (SDS-PAGE). For small proteins, such as agnoprotein, 18% acrylamide gels were used and for larger proteins, such as T-antigen, 10% acrylamide gels were used. After resolution, 18% gels were transferred to 0.2-micron nitrocellulose membranes at 250 mA for 30 minutes at 4° C and 10% gels were transferred to 0.45-micron nitrocellulose membranes at 60 mA overnight at 4° C, both transfers completed in transfer buffer (25 mM tris pH 7.4, 200 mM glycine, 20% methanol). After transfer, membranes were blocked with 10% non-fat dry milk in 1X phosphate-buffered saline (PBS) containing 1% Tween-20 (PBST) for 1 hour at room temperature. Membranes were

then incubated with primary antibodies diluted in 5% non-fat dry milk PBST overnight at 4° C, undergoing constant rocking. Membranes were washed three times with PBST and incubated for 1 hour at room temperature with 1:5000 secondary antibody diluted in PBST. Membranes were washed three times with PBST and visualized with the Odyssey CLx Imaging System (LI-COR). Primary antibodies and secondary antibodies used for Western Blotting are listed in Table 2.

**Table 2: Antibodies Used for Western Blot, Immunocytochemistry, and Immunohistochemistry. A representative table to the antibodies used in all experiments.**

<b>Target Epitope</b>	<b>Species</b>	<b>Experimental Usage</b>	<b>Manufacturer</b>
Agnoprotein (IgG) #7903	Rabbit polyclonal	Western Blot, ELISA, ICC, IHC	Lampire Biologics
Agnoprotein (serum) #7903	Rabbit polyclonal	Western Blot	Lampire Biologics
B-Tubulin	Mouse monoclonal	Western Blot	Li-Cor
GAPDH	Mouse monoclonal	Western Blot	Cell Signaling Technology
GM-CSF	Mouse monoclonal	Western Blot, IHC	R&D Systems
SRSF1	Rabbit polyclonal	Western Blot	Abcam
SV40 T-Antigen	Mouse monoclonal	Western Blot, IHC	EMD/Millipore
JCV VP1	Mouse Monoclonal	IHC	Dr. Robert Atwood, Brown University

Secondary - Anti- mouse 800	Goat anti- Mouse	Western Blot	Li-Cor
Secondary -Anti- rabbit 680	Goat anti- Rabbit	Western Blot	Li-Cor
Secondary - Biotinylated	Goat anti- Rabbit	IHC	Vector
Secondary - Biotinylated	Goat anti- Mouse	IHC	Vector
Secondary -Alkaline Phosphatase	Goat anti- Rabbit	IHC	Pierce
Secondary -Alkaline Phosphatase	Goat anti- Rabbit	IHC	Pierce

## 2.6. Luciferase Reporter Assay and Dual Reporter Assays

T98G were plated in 6-well tissue culture dishes and transiently transfected with a luciferase reporter plasmid. The luciferase reporter plasmids used assessed either the promoter activity of SRSF1 (-1000 to +49 base pair region) or the promoter activity of GM-CSF (-627 to +48 base pair region). At 48-hours post-transfection, cells were harvested with trypsin and actively lysed with Promega reporter lysis buffer. Lysed cells were centrifuged at 14,000 RPM for 10 minutes at 4° C in a VWR centrifuge. Supernatants were collected, and luciferase activity was assessed by combining 20 µL supernatant with 100 µL luciferase assay reagent (LAR II) provided by Promega and mixing. Luminescence activities were assessed using a Zylux Corporation Femtomaster FB12 luminometer and corrected for protein concentration.

TC620 were plated in 6-well tissue culture dishes and transiently transfected with the luciferase-renilla dual reporter plasmid, in which the luciferase protein is under control of the JCV late region promoter and the renilla protein is under control of the JCV early region promoter. At 48-hours post-transfection, cells were harvested with trypsin and actively lysed with Promega reporter lysis buffer. Lysed cells were centrifuged at 14,000 RPM for 10 minutes at 4° C in a VWR centrifuge. Supernatants were collected, and luciferase activity was assessed by combining 20 µL supernatant with 100 µL luciferase assay reagent (LAR) II provided by Promega and mixing, after which luciferase luminescence activity was read. Renilla activity was assessed by adding 100 µL Stop-and-Glo® buffer to the supernatant-LAR mixture and mixing, after which the renilla luminescence activity was read. Luminescence activities were read using a Zylux Corporation Femtomaster FB12 luminometer and corrected for protein concentration.

## **2.7. Chromatin Immunoprecipitation Assay**

A chromatin immunoprecipitation (ChIP) assay was used to assess possible interactions between JCV T-antigen and the SRSF1 promoter region as a mechanism for transcriptional suppression. T98G cells were plated in a 100-mm tissue culture dish and transfected with 10 µg of pcDNA3.1-T-antigen. At 48 hours post transfection, proteins and DNA were cross-linked with 1% formaldehyde (volume/volume). Following crosslinking, cells were harvested trypsin incubation. After trypsin, cells were collected and centrifuged at 1,800 RPM in a Sorvall RT7 centrifuge for 5 minutes. Pellets were resuspended in TNN lysis buffer (150 mM NaCl, 40 mM tris pH 7.4, 1% NP-40, 1 mM DTT, 1 mM EDTA) supplemented

with protease inhibitors and rotated for 1 hour at 4° C. Cell lysates were sonicated 40 times with a Cole-Parmer Instruments Ultrasonic Processor sonicator for efficient chromatin fragmentation. Fragmented lysates were incubated overnight with Protein G beads pre-bound with anti-Large-T-Antigen antibody for immunoprecipitation. Following immunoprecipitation, samples were centrifuged at 3000 RPM for 5 minutes in a Sorvall RT7 centrifuge and the pelleted Protein G-beads were washed twice with low salt wash buffer (0.1% SDS, 1% Triton X-100, 2 mM EDTA, 20 mM Tris-HCl pH 8.0, and 150 mM NaCl), twice with high salt wash buffer (0.1% SDS, 1% Triton X-100, 2 mM EDTA, 20 mM Tris-HCl pH 8.0, and 500 mM NaCl), once with lithium chloride wash buffer (0.25 M LiCl, 1% NP-40, 1% sodium deoxycholate, 1 mM EDTA, 10 mM Tris-HCl pH 8.0) and twice with TE buffer (10 mM Tris pH 8.0, 1 mM EDTA). Bound proteins were eluted from beads by incubation with ChIP elution buffer (1% SDS, 100 mM NaHCO<sub>3</sub>) and supernatants were collected after centrifugation. Bound DNA was purified by reversing protein-DNA cross-links through treatment with 5 M NaCl, after which the DNA was purified with phenol-chloroform extraction to remove any remaining proteins and precipitated with ethanol precipitation. Purified DNA fragments were analyzed with PCR analysis to amplify the SRSF1 promoter region using the following primers: SRSF1-Promoter-Forward (-1000 to +47): 5'ACCTTCCAAAGCTTTCCAGATTCAG-3' and SRSF1-Promoter-Reverse (+47 to +27): 5'-ACCTTCCACTCGAGGAAGGAAACAGC-3'. PCR amplification of the SRSF1 promoter region used the following conditions: 95° C

for 5 minutes, 35 cycles of 95° C for 30 seconds, 58° C for 40 seconds, 72° C for 65 seconds, and 72° C for 10 minutes.

## **2.8. Enzyme-Linked Immunosorbent Assay**

An enzyme-linked immunosorbent assay (ELISA) was used to assess extracellular agnoprotein concentration from the growth media of pcGT7-agnoprotein transfected TC620. TC620 cells were plated in 100-mm dishes and transiently transfected with 10 µg of pcGT7-agnoprotein or pcGT7-alone. At 48 hours following transfection, conditioned growth media (CM) was collected and centrifuged to remove cellular debris. A 96-well plate was coated overnight with 50 µL of sample and 150 µL ELISA coating buffer (0.05 M Sodium Carbonate-Bicarbonate, pH 9.6) at 4° C. After coating, wells were washed three times for five minutes each with washing buffer (50 mM Tris, 0.14 M NaCl, 0.05% Tween 20, pH 8.0) to remove any non-bound proteins. Wells were blocked with 200 µL assay buffer (50 mM Tris, 0.14 M NaCl) containing 10% bovine serum albumin (BSA) for 2 hours at room temperature. After blocking, samples were incubated overnight at 4° C with anti-agnoprotein IgG primary antibody diluted 1:800 in 200 µL assay buffer. Wells were washed three times for 5 minutes each with washing buffer, after which secondary antibody, anti-rabbit-horseradish peroxidase (HRP)-conjugated was added at a 1:1500 dilution in 200 µL assay buffer and incubated for two hours at room temperature. Wells were then washed three times for 5 minutes each to decrease potential background readings resulting from unbound HRP-conjugated secondary antibody.

To induce color change, wells were incubated with 100  $\mu$ L TMB (3,3',4,4'-tetramethylbenzidine) solution. TMB reacts with HRP to produce a blue colored solution. Incubation time was determined based on the observed color change, with typical incubation time ranging from 10 to 30 minutes. Incubation was stopped when the highest standard concentration samples reached a medium blue color. To stop the reaction, 100  $\mu$ L of stop solution (0.16 M sulfuric acid) was added, changing the color of the solution from blue to yellow. Absorbances were measured at 450 nm and recorded.

The concentration of the samples was determined based on a standard curve using MBP-agnoprotein as the standard. Standard concentrations of MBP-agnoprotein were 1000, 500, 250, 125, 62.5, 31.25, 15.625, and 0 ng/mL.

## **2.9. Immunocytochemistry**

To assess extracellular agnoprotein uptake in astrocytes and microglia, PHFA or PHFM were plated in two-well chamber slides with 500,000 cells per well and cultured until confluent, after which cells were treated with CM-control or CM-agnoprotein (CM-agno) for 48 hours. Extracellular agnoprotein presence was confirmed via ELISA and western blot. Cells were treated at 0 hours and 24-hour time points, with treatments consisting of 1 mL of fresh media and 1 mL of conditioned media. At 48 hours, cells were fixed with 1 mL ice-cold acetone and methanol (50:50 mixture) for 1 minute and washed five times with 1X PBS. Slides were blocked with 1 mL of 10% BSA in 1X PBS for 1 hour at room temperature. Slides were incubated overnight with rocking at 4° C with primary anti-agnoprotein IgG antibody diluted 1:300 (3.5  $\mu$ L in 1 mL) in 5% BSA in 1X PBS. After overnight

incubation, slides were washed five times with PBS to remove any unbound antibody and incubated with secondary antibody solution, 1:500 FITC-rabbit or 1:500-Rhodamine-rabbit, in 5% BSA in 1X PBS for 2 hours at room temperature with gentle rocking. After secondary antibody, slides were washed five times with 1X PBS and cover slips were mounted using Vectashield mounting medium containing 4,6-diamidino-2-phenylindole (DAPI) (Vector Laboratories) for DNA staining and nucleus localization.

Slides were visualized using a Leica Fluorescent microscope (Leica Biosystems Inc.) to visualize internalized agnoprotein and DAPI corresponding to cellular nuclei.

The impact of extracellular agnoprotein on monocyte/macrophage surface marker expression was assessed by treating differentiating monocytes with CM-control or CM-agno. U937 cells were plated in a two-well chamber slide (1,000,000 cells per well) and induced for differentiation with 100 ng/mL PMA treatments for 24 hours. Cells were treated with 1 mL CM-control or CM-agnoprotein in addition to 1 mL fresh RPMI 1640 media at 24 and 48 hours post-induction. At 72 hours, cells were fixed with 1 mL ice-cold acetone and methanol (50:50 mixture) for 1 minute and washed five times with 1X PBS. Slides were blocked with 1 mL of 10% BSA in 1X PBS for 1 hour at room temperature. Slides were incubated overnight with rocking at 4° C with primary anti-CD16, anti-CD68, or anti-CD71 antibody diluted 1:300 (3.5 µL in 1 mL) in 5% BSA in 1X PBS. After overnight incubation, slides were washed five times with 1X PBS to remove any unbound antibody and incubated with secondary antibody solution, 1:500-Rhodamine-mouse, in 5% BSA

in PBS for 2 hours at room temperature with gentle rocking. After secondary antibody, slides were washed five times with 1X PBS and cover slips were mounted using Vectashield mounting medium containing DAPI (Vector Laboratories).

## **2.10. Immunohistochemistry**

To confirm the *in vitro* data suggesting that extracellular agnoprotein impacts GM-CSF release, immunohistochemistries (IHCs) were completed on PML lesions obtained from AIDS-positive PML patients and normal brain frontal cortex control sections. AIDS-positive PML-positive samples were kindly provided by the Manhattan HIV Brain Bank (MHBB) headed by Susan Morgello, M.D., and normal brain frontal cortex sections were kindly provided by the CNAC facility at the Lewis Katz School of Medicine of Temple University headed by Kamel Khalili, Ph.D. Tissues were formalin fixed and paraffin-embedded prior to mounting as 5  $\mu\text{m}$  sections.

After obtaining sectioned and mounted parallel tissue sections, slides were incubated overnight at 60° C to soften the paraffin, after which paraffin was cleared by three 30-minute incubations in xylene. After de-paraffinization, tissue sections were hydrated with an alcohol series consisting of two three-minute incubations in 100% ethanol, two three-minute incubations in 90% ethanol, two three-minute incubations in 70% ethanol, and two three-minute incubations in distilled water. After the hydration series, sections underwent antigen retrieval with a 30-minute incubation in citrate buffer (10 mM citric acid, anhydrous, pH 6.0) at 95° C. After antigen retrieval, the process of development differed based on the chromogen used, either DAB (3,3'-diaminobenzidine) peroxidase or vector red.

When using DAB peroxidase, the endogenous peroxidases in the tissue were quenched through a 20-minute incubation in methanol containing 3% hydrogen peroxide. Sections were washed three times in 1X PBS. Sections were blocked with 1X PBS containing 5% normal horse serum for 2 hours at room temperature. After blocking, slides were rinsed with 1X PBS and incubated with anti-GM-CSF primary antibody diluted 1:25 in 1X PBS containing 0.1% BSA overnight at 4° C. Following overnight incubation, slides were washed three times in 1X PBS and incubated for 2 hours with secondary antibody (goat-anti-mouse-HRP) diluted at 1:200 in 1X PBS containing 0.1% BSA. Slides were washed three times in 1X PBS and incubated with avidin-biotin complex for 1 hour, after which sections were washed. Slides were then incubated with SIGMAFAST DAB (Millipore Sigma #D4293) solution for 5 minutes, after which slides were washed in tap water and counterstained.

When using Vector® red, tissue sections were not quenched with hydrogen peroxide in methanol for endogenous peroxidase activity since the signal is determined by alkaline phosphatase (AP) activity. Since there are low levels of AP in the brain, tissue sections were not blocked for endogenous AP activity. Tissue sections designated for Vector® red staining were blocked in 1X PBS containing 5% normal horse serum for 2 hours at room temperature. After blocking, slides were rinsed with 1X PBS and incubated with anti-GM-CSF primary antibody diluted 1:25 in 1X PBS containing 0.1% BSA overnight at 4° C. Following overnight incubation, slides were washed three times in 1X PBS and incubated for 2 hours with secondary antibody (goat-anti-mouse-AP) diluted at 1:200 in 1X PBS

containing 0.1% BSA. Slides were washed three times in 1X PBS and incubated with Vector® red alkaline phosphate substrate kit solution (Vector Laboratories Incorporated, #SK5100) for 30 minutes in the dark. After, sections were washed in alkaline phosphatase buffer (150 mM Tris, 0.1% Tween-20; pH 8.3) and counterstained.

Slides were counterstained through incubation in hematoxylin for 15 minutes followed by a 10-minute wash with running tap water. Tissue sections were then dehydrated with an alcohol series of two three-minute incubations in 70% ethanol, two-three minute incubations in 90% ethanol, and two-three minute incubations in 100% ethanol. Slides were then cleared with xylene with two 30-minute incubations and cover slips were mounted with Richard-Allan Scientific mounting solution (Fischer Scientific #4111). After mounting, cells were imaged using a Keyence BZ-X710 All-in-One Fluorescence Microscope (Keyence Corporation of America).

### **2.11. Cytokine/Chemokine Array**

PHFA were plated in 60 mm tissue-culture treated dishes and grown until confluence. After reaching confluency, cells were treated with CM-control or CM-agnoprotein for 24 hours. At 24 hours, conditioned media was aspirated and fresh DMEM:F12 media was added to the wells and incubated for 24 hours. After incubation, media was collected and centrifuged at 3000 RPM for 5 minutes in a Sorvall RT7 centrifuge to eliminate cellular debris. Cleared media was processed with a RayBiotech C-Series human cytokine antibody array C3. Briefly, the cytokine array membrane was placed into the RayBioTech provided tray and

blocked for 30 minutes at room temperature with the provided blocking buffer. After blocking, wells were aspirated and 1.5 mL of diluted growth media from treated cells (750  $\mu$ L growth media with 750  $\mu$ L blocking buffer) was added to each well and incubated for 4 hours at room temperature. Media was then aspirated from the wells and membranes were washed three times in Wash Buffer I and twice in Wash Buffer II, both provided by RayBioTech. After the washes, membranes were incubated with the provided biotinylated antibody cocktail for 2 hours at room temperature. Each membrane was washed as previously described. Membranes were then incubated for 2 hours at room temperature with the provided HRP-Streptavidin solution and washed again as previously described. Membranes were transferred onto a flat section of plastic wrap and covered with 500  $\mu$ L of the provided detection buffer mixture for two minutes at room temperature. After the incubation, membranes were immediately covered with another section of plastic wrap to form a “sandwich” structure. This structure was then transferred to a Fischer Biotech Autoradiography Cassette and covered with two pieces of autoradiography film (GeneMate) which underwent exposure for roughly 10 minutes. After exposure, the films were developed with a Kodak X-OMAT 2000A processor and cytokine intensities were analyzed using Adobe Photoshop CS5.

## **2.12. MTT Cell Proliferation Assay**

To measure cellular viability, an MTT colorimetric assay was used, which assesses NADPH-dependent cellular metabolism. The primary principle behind the mechanism involves the conversion of soluble MTT (3-(4,5-dimethylthiazol-2-yl)-2,5-diphenyltetrazolium bromide) into the insoluble formazan, which can be

solubilized by strong acids, resulting in a color change corresponding to the level of cellular metabolism (Liu *et al*, 1997; Mosmann *et al*, 1983).

Cells (T98G, TC620, PHFA, PHFM, and U937) were plated in a 6-well dish and treated with CM-control, CM-agnoprotein, MBP, or recombinant agnoprotein for 48 hours. At 48 hours, 200  $\mu$ L of MTT solution (5 mg/mL MTT in 1X PBS) was added into each well and incubated for 2 hours at 37° C. After 2 hours, media was collected and centrifuged to pellet any floating cells. Following centrifugation, 1 mL of MTT solvent (100 mL isopropanol, 0.1 % NP-40, 4 mM HCl) was added into each well and cellular pellets were resuspended in 1 mL of MTT solvent and added into their respective wells, resulting in a total of 2 mL of MTT solvent per well. The MTT solvent was collected and the absorbance at 570 and 630 nm (reference read) were determined using a ThermoScientific Genesys 10S Vis Spectrophotometer. The absorbance at 630 nm was subtracted from the absorbance at 570 nm to yield the experimental absorbance value.

### **2.13. Monocyte Differentiation Assay**

Monocyte attachment served as a model of differentiation following agnoprotein treatments of U937 cells to determine if agnoprotein suppresses monocyte differentiation into macrophages. Briefly, U937 cells were plated in a 6-well tissue culture dish and pulsed with 100 ng/mL PMA to induce differentiation and simultaneously treated with either CM-control CM-agnoprotein, MBP or recombinant agnoprotein. At 2 hours, PMA-containing media was removed and fresh media was added and cells were re-treated with the appropriate conditions.

At 24, 48, and 72 hours wells were washed with fresh media to remove unattached cells. At these time points, 5 representative phase contrast images were collected for each condition. Each image was analyzed and attached cells, which were characterized as differentiated macrophages, were quantified. The total number of cells for each condition were averaged and plotted onto a bar graph with standard deviations.

#### **2.14. Phagocytosis Assay**

Monocyte, macrophage, and microglia phagocytosis served as a model of the function of myeloid-derived cells following treatments with agnoprotein. For the phagocytosis assay, four cell types were used, U937 cells, U937-derived macrophages, human primary macrophages, and PHFM. U937 cells were plated in a 96-well plate and were pulsed with 100 ng/mL PMA to induce differentiation and treated with either CM-Control CM-agno, MBP or recombinant agnoprotein simultaneously. U937-derived macrophages were pre-derived from U937 cells plated in a 96-well plate that were pulsed with 100 ng/mL PMA for 2 hours to induce differentiation and sub-cultured for 3 days prior to agnoprotein treatments. Primary human macrophages were derived from primary human monocytes plated in a 96-well plate that were pulsed with 100 ng/mL PMA for 2 hours to induce differentiation and sub-cultured for 3 days prior to agnoprotein treatments. PHFM were plated in a 96-well plate and pulsed with 100 ng/mL PMA for activation and treated with either CM-Control CM-agno, MBP or recombinant agnoprotein simultaneously. All cell types contained a non-PMA treated control and a PMA-

only treated control for quantification purposes. Likewise, all conditions were completed in triplicate.

To assess phagocytosis, the ThermoScientific Vybrant™ Phagocytosis Assay Kit (ThermoScientific #V-6694) was used. At 48 hours after treatments, agnoprotein-containing media was aspirated from each well and 100 µL of fluorescein-labeled *Escherichia coli* K-12 bioparticles (1 mg/mL) resuspended in Hanks' balanced salt solution (HBSS) was added to each well. Cells were incubated with the *E. coli* particles for 2 hours at 37° C. After 2 hours, the wells were aspirated and treated with 100 µL of trypan blue for 1 minute, to quench extracellular fluorescence to prevent background readings from non-phagocytosed *E. coli* particles. Trypan blue was aspirated from each well and the fluorescence was measured for each well using 480 nm excitation and 520 nm emission spectra with a Fischer Scientific Multiskan FC microplate reader.

The effect of agnoprotein on phagocytosis was determined using PMA-only treated cells as the basal level of phagocytosis.

### **2.15. Blood-Brain Barrier Model**

Agnoprotein suppression of monocyte migration towards activated astrocytes was assessed using a blood-brain barrier model. The designed BBB model (Figure 17) utilizes a Corning Transwell™ permeable support for 6-well plates with a 3.0 µm polyester membrane (Corning #3452) to mimic the permeable BBB. This membrane allows for migration of monocytes from the top chamber into the bottom chamber following either astrocyte activation or the presence of migratory stimuli, such as GM-CSF.

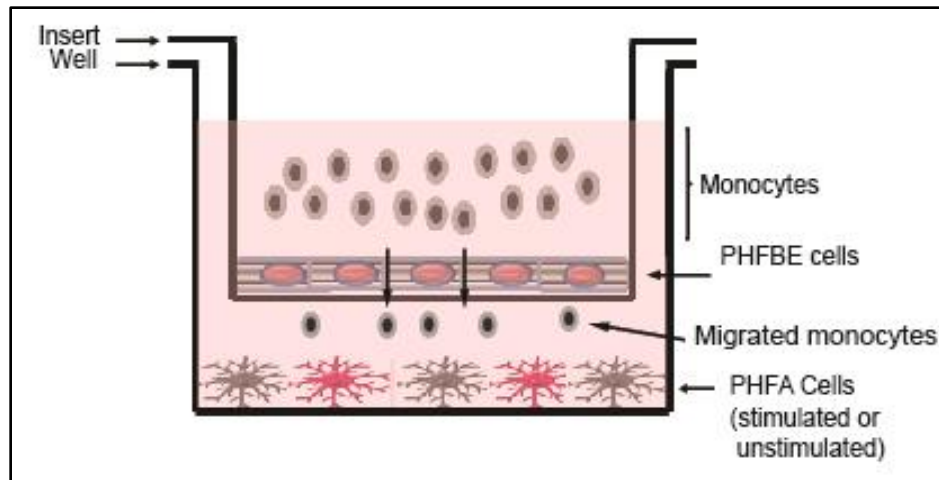


**Figure 17: Blood-Brain Barrier Model.** A schematic representation of the blood-brain barrier model used for PBMC and monocyte migration assays. PHFA were cultured in a 6-well tissue culture dish and co-incubated with a 3.0 µm Transwell permeable support confluent with PHFBE. PBMCs or monocytes were added into the Transwell insert and migration was assessed at various time points. Different experimental conditions altered treatments of PHFA, including treatments with recombinant agnoprotein or LPS.

Briefly, PHFA were seeded in a 6-well tissue culture dish and cultured for 48 hours. Simultaneously, primary human fetal brain endothelial cells (PHFBE) were seeded onto the Transwell permeable supports in a separate 6-well tissue culture dish and grown for 48 hours until developing a confluent layer mimicking the BBB. After 48 hours, PHFA media was replaced with a low serum version, which contained 3% FBS instead of the normal 10% FBS and the permeable supports were added into the PHFA-seeded wells, resulting in co-cultured wells containing PHFA and PHFBE. The use of low serum media was preempted by developmental studies showing that the serum within the media induces monocyte migration, presumably through low level activation of astrocytes, however the mechanism was not assessed. Do to this, low serum media was used to reduce the levels of background monocyte migration without significantly impacting cellular viability (Figure 36).

After 24 hours of co-culture of the PHFA and PHFBE, astrocytes were activated with 10 ng/mL *E. coli* 026:B6 lipopolysaccharides (LPS) (Sigma-Aldrich #L8274) for 24 hours. Previous studies have shown the use of LPS as an inducing agent for neuroinflammation (Gorina *et al*, 2011; Li *et al*, 2016; Tarassishin *et al*, 2014). Concurrent with LPS activation, PHFA were treated with recombinant agnoprotein at concentrations of 50, 100, and 200 ng/mL. At this time, 1 million PBMCs or 3 million primary human monocytes were added into the top chamber of the well. At 3-, 6-, and 24-hours post-activation, cellular migration through the endothelial cell layer was assessed with phase microscopy and cell counting using a hemocytometer. Since monocytes are non-adherent cells, migrated monocytes typically remained in suspension, allowing for counting migrated cells in the media. However, the process of monocyte migration and astrocyte activation both serve to induce monocyte differentiation into adherent macrophages, thus phase contrast images furthered the assessment of the total number of migrated cells. Experiments were completed in triplicate and the average monocyte migration was calculated.

## CHAPTER 3

### MOLECULAR INTERPLAY BETWEEN T-ANTIGEN AND SPLICING FACTOR, ARGININE/SERINE-RICH 1 (SRSF1) CONTROLS JC VIRUS GENE EXPRESSION IN GLIAL CELLS

#### 3.1. Introduction

One of the primary cellular factors involved in regulation of JC virus gene transcription and replication is the host splicing factor SRSF1. Multiple studies have shown that JCV is negatively regulated by SRSF1 at multiple levels of the viral life cycle (Sariyer *et al*, 2011; Sariyer, I.K. *et al*, 2016; Sariyer, R. *et al*, 2016, Uleri *et al*, 2011; Uleri *et al*, 2013) (Figure 9). The anti-JCV functions of SRSF1 initiate by association with the JCV promoter region, contained within the NCCR, thereby interfering with polymerase activity and ultimately suppressing viral transcription (Sariyer *et al*, 2011). Since time immemorial, there has existed a cat-and-mouse game between viruses and the host organisms that they infect, with the host developing antiviral mechanisms, from the bacterial clustered regularly interspaced short palindromic repeats (CRISPR) – CRISPR-associated system (Cas) system to the complex immune system in higher order species (Westra *et al*, 2012). While the host has evolved many antiviral mechanisms, viruses have evolved as well, developing strategies to bypass host defense mechanisms, primarily through utilization of viral regulatory proteins. It was hypothesized that JCV, in a similar mechanism as many other human viruses, can bypass host defense mechanisms, such as the suppressive functions of SRSF1, through the actions of the viral proteins, either through functions of the T-antigens or the regulatory

agnoprotein (Chin *et al*, 2001; Duschene *et al*, 2010; Goldmacher *et al*, 1999). Within this section, we present studies assessing the role of JCV regulatory proteins, Large T-antigen and agnoprotein, in rescuing SRSF1-mediated viral suppression of JCV transcription.

## **3.2. Results**

### **3.2.1. SRSF1-Mediated Suppression of JCV Early and Late Gene Transcription is Rescued by Large T-Antigen**

The ability of JCV proteins to bypass SRSF1 mediated negative regulation of early and late gene transcription was assessed through a luciferase reporter assay. PHFA were plated in a 6-well tissue culture plate with 100,000 cells per well and grown until confluency. After becoming confluent, cells were transiently transfected in triplicate with luciferase reporter constructs containing the JCV early or late promoter sequence (pLuc.JCV-Early or pLuc.JCV-Late) with varying combinations of the following expression plasmids: SRSF1 (pcGT7-SRSF1), T-antigen (pcDNA3.1-T-antigen), or agnoprotein (pcGT7-agnoprotein). Transfections of pLuc.JCV-Early or pLuc.JCV-Late used 2 µg of plasmid DNA, while expression plasmids were used at 3 µg per plasmid, with pcDNA3.1-empty vector used to normalize the total amount of transfected DNA to 8 µg per well. At 48 hours post-transfection, cells were harvested using trypsin and centrifuged, with the resulting cellular pellet resuspended in Promega reporter active lysis buffer and rotated for 1 hour at 4° C. After lysis, samples were centrifuged to pellet cellular debris. After centrifugation, 20 µL of the supernatant was added to 100 µL of

luciferase assay reagent (LAR). The luciferase activity was read using a luminometer and corrected for protein concentrations for each sample.

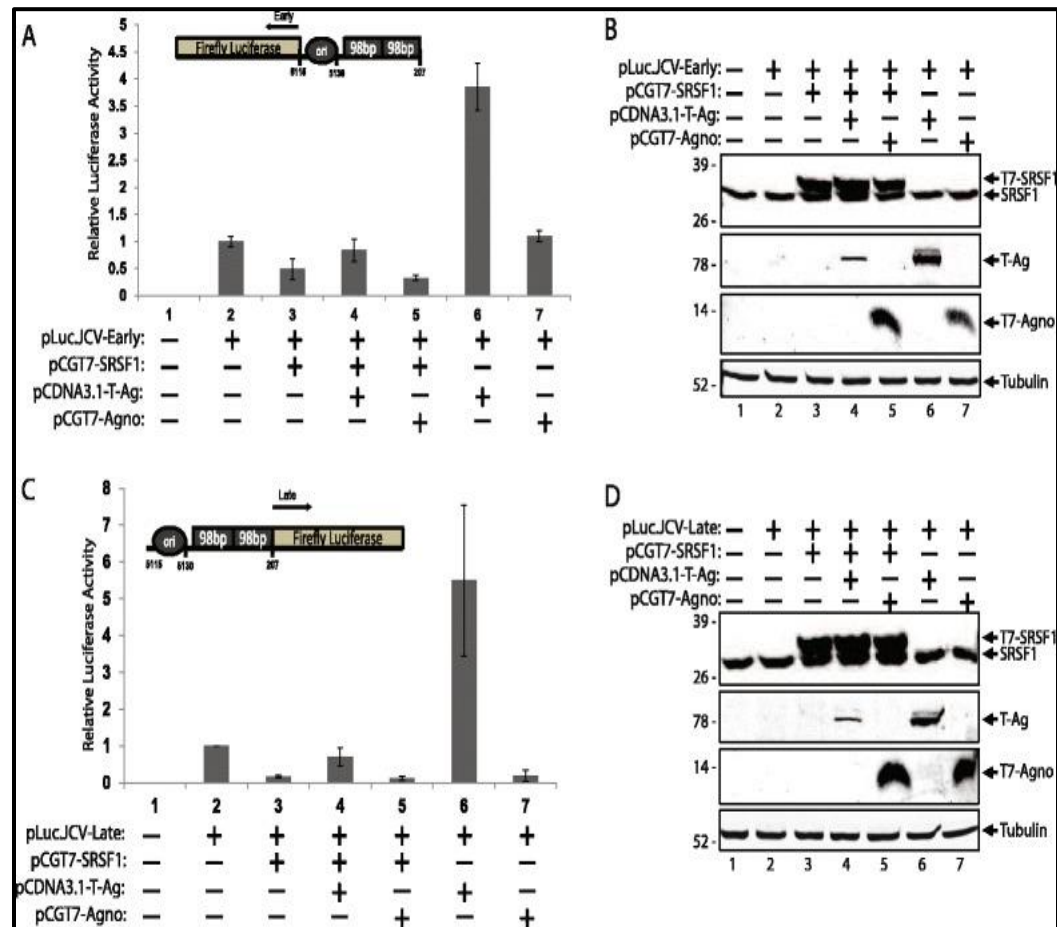


**Figure 18: SRSF1 mediated suppression of JCV-early and -late gene transcription is rescued by T-Antigen.** **A.** PHFA were transiently transfected with the pLuc.JCV-Early plasmid and the listed combinations of expression plasmids for SRSF1, T-antigen, or agnoprotein. At 48 hours, cells were harvested and lysates were analyzed by luciferase reporter assay. Luminescence was determined and corrected for protein concentrations. **B.** Western blot analysis of whole cell lysates was completed in parallel to the samples in panel A. **C.** PHFA were transiently transfected with the pLuc.JCV-Late plasmid and the listed combinations of expression plasmids for SRSF1, T-antigen, or agnoprotein. At 48 hours, cells were harvested and lysates were analyzed by luciferase reporter assay. Luminescence was determined and corrected for protein concentrations. **D.** Western blot analysis of whole cell lysates was completed in parallel to the samples in panel C. (Reproduced with permission from Craigie et al, 2015 and the Virology Journal under the Creative Commons Attribution 4.0 International License).

Untransfected cell lysates served as the negative control for luciferase activity (Figure 18A and 18C, Lane 1). The corrected luciferase activity was normalized to

the basal transcriptional activity, which was determined by transfection with pLuc.JCV-Early or pLuc.JCV-Late plasmid alone (Figure 18A and 18C, Lane 2). To reproduce SRSF1-mediated JCV transcriptional suppression of both early and late genes, SRSF1 was overexpressed, resulting in a 50% decrease in JCV early gene transcriptional activity and almost complete suppression of JCV late gene transcriptional activity (Figure 18A and 18C, Lane 3).

After determination of basal JCV transcription levels and reproducing SRSF1-mediated transcriptional suppression, the impact of JCV proteins T-antigen and agnoprotein on JCV gene transcription, primarily in regard to rescuing capabilities when co-expressed with SRSF1, was assessed. SRSF1-mediated transcriptional suppression of both JCV early and late regions was rescued by the expression of T-antigen, even when SRSF1 was over-expressed, suggesting that T-antigen drives viral transcription and rescues SRSF1-mediated transcriptional suppression (Figure 18A and 18C, Lane 3). However, no rescuing ability was observed with agnoprotein expression. Dual expression of agnoprotein and SRSF1 resulted in no deviation from SRSF1-mediated suppression, suggesting that agnoprotein does not drive JCV transcription or impact SRSF1-mediated transcriptional suppression (Figure 18A and 18C, Lane 4).

Additionally, the impact of T-antigen and agnoprotein alone on JCV early and late transcription was assessed. Expression of T-antigen resulted in a significant increase in both JCV early and late gene transcription (Figure 18A and 18C, Lane

5). When taken in combination with the rescuing capability of T-antigen when co-expressed with SRSF1, confirming that T-antigen induces JCV early and late gene transcription and may interact with SRSF1 to inhibit SRSF1-mediated transcriptional suppression. Expression of agnoprotein did not impact JCV early gene transcription whereas JCV late gene transcription was suppressed in the presence of agnoprotein (Figure 18A and 18C, Lane 6).

To ensure that changes in transcriptional activity were the result of SRSF1 overexpression or T-antigen and agnoprotein expression, western blot analysis of the whole cell protein lysates were completed in parallel to the luciferase assays from the same experimental set-up (Figure 18B and 18D). Overexpression of SRSF1 substantially decreased T-antigen expression, with SRSF1-overexpression having no impact on agnoprotein expression in co-transfected cells (Figure 18B and 18D, Lanes 4-8).

### **3.2.2. Large T-Antigen Suppresses SRSF1 Expression in Glial Cells**

Next, the mechanism of T-antigen induced rescue of SRSF1-mediated JCV transcriptional suppression was assessed. The initial hypothesis proposed that T-antigen alters SRSF1 expression to bypass SRSF1-mediated transcriptional suppression. To assess protein expression levels, PHFA and T98G cells were plated in a 6-well tissue culture dish and transfected with 0, 2, and 6  $\mu$ g of pcDNA3.1-T-Antigen, with total DNA normalized with pcDNA3.1-empty, resulting in an increasing amount of T-antigen expression within the cells. At 48 hours, cells were

trypsinized and whole cell extracts were collected and pelleted with centrifugation at 1,800 RPM for 5 minutes. Cellular pellets were lysed with TNN lysis buffer and rotated for 1 hour at 4° C, followed by centrifugation at 14,000 RPM for 10 minutes to pellet cellular debris, with the supernatant being collected for further analysis. The endogenous cellular expression of SRSF1 and the transfection efficiency of T-antigen expression was assessed via Western Blotting.

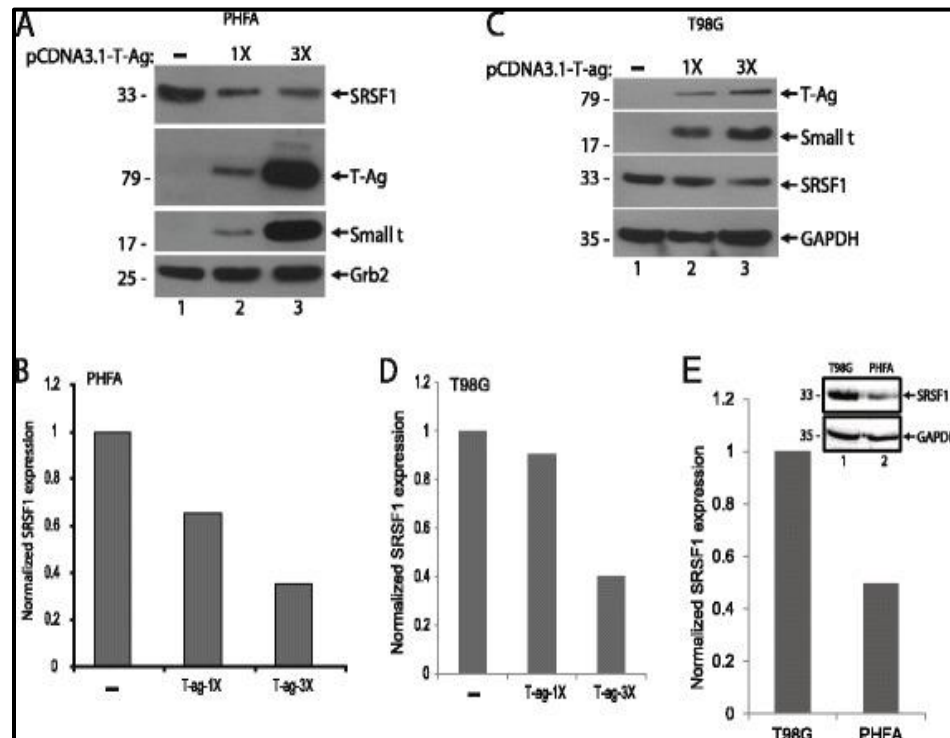


**Figure 19: T-Antigen Suppresses SRSF1 Expression in Glial Cells.** *A.* Western blot analysis for SRSF1 expression of PHFA transiently transfected with increasing concentrations of T-antigen. Grb2 served as the loading control. *B.* Quantification of SRSF1 expression levels from panel A following protein level correction. *C.* Western blot analysis for SRSF1 expression of T98G transiently transfected with increasing concentrations of T-antigen. GAPDH served as the loading control. *D.* Quantification of SRSF1 expression levels from panel C following protein level correction. *E.* Quantification of endogenous SRSF1 expression between T98G cells and PHFA following protein level correction. Western blot is shown as the insert with GAPDH serving as the loading control. (Reproduced with permission from Craigie et al, 2015 and the Virology Journal under the Creative Commons Attribution 4.0 International License).

SRSF1 expression in PHFA significantly decreased at 1x and 3x concentrations of T-antigen expression, quantified as a 60% decrease in SRSF1 expression over three

replicates (Figure 19A and 19B). A similar trend occurred in T98G-transfected cells, with increasing expression of T-antigen resulting in a 60% decrease of SRSF1-expression at the highest expression of T-antigen (Figure 19C, 19D). Protein levels were assessed by Western Blot for Grb2 in PHFA and GAPDH in T98G, showing that the decrease in SRSF1 expression was a direct result of T-antigen expression as opposed to differences in loaded protein amounts.

The endogenous level of SRSF1 in T98G and PHFA was assessed by Western Blotting. Over three replicates, the quantified expression of SRSF1 was found to be 50% less in PHFA as opposed to T98G cells. This result is confirmed by multiple studies suggesting that SRSF1 expression is increased in cancer cells as opposed to primary cells, such as PHFA (Anczukow *et al*, 2015).

### **3.2.3. Large T-Antigen Suppresses SRSF1 Transcription in Glial Cells**

With T-antigen suppressing SRSF1 expression, the mechanism behind this suppression in glial cells was investigated. T98G cells were plated in a 6-well tissue culture plate with 100,000 cells plated per well and were grown until confluency. After becoming confluent, cells were transiently transfected with luciferase reporter constructs containing the SRSF1 -1000 to +48 bp promoter region (pLuc.SRSF1-1000) with increasing concentrations of viral protein expression plasmids encoding either T-antigen (pcDNA3.1-T-antigen) or agnoprotein (pcGT7-agnoprotein). Transfections of pLuc.SRSF1-1000 used 2 µg of plasmid DNA, while expression plasmids were used at 2 or 4 µg per plasmid (for 1X and 2X concentrations), with pcDNA3.1-empty vector used to normalize the total amount of transfected DNA. At

48 hours post-transfection, cells were harvested with trypsin, collected, and centrifuged. The resulting cellular pellet was resuspended in Promega reporter active lysis buffer and rotated for 1 hour at 4° C. After lysis, samples were collected and centrifuged to remove cellular debris. After centrifugation, 20 µL of the supernatant was added to 100 µL of luciferase assay reagent. The luciferase activity was read using a luminometer and corrected for protein concentrations for each sample. Untransfected cell lysates served as the negative control for luciferase activity (Figure 20A, Lane 1). The corrected luciferase activity was normalized to the basal transcriptional activity, determined by transfecting cells with pLuc.SRSF1-1000 plasmid alone (Figure 20A, Lane 2). When T-antigen was expressed, SRSF1 promoter activity decreased in a dose dependent manner, with 1X T-antigen expression suppressing SRSF1 transcription by 40% and 2X T-antigen expression suppressing SRSF1 transcription by 60%. When agnoprotein was expressed, there was no discernable impact on SRSF1 transcription. Cells were also transfected with the green fluorescent protein expression vector pSELECT-GFP in 1x and 2x concentrations to assess transfection efficiencies. Fluorescent microscopy analysis of live cells showed a transfection dependent increase of GFP expression (Figure 20A, upper panel of bar graph). All conditions were completed in triplicate and the graphed values are the averages of the three replicates.

To ensure that deviations in transcriptional activity were the result of T-antigen and agnoprotein expression, western blot analysis of the whole cell protein lysates were completed in parallel to the luciferase assays from the same experimental set-up (Figure 20B). GAPDH served as the protein loading control.

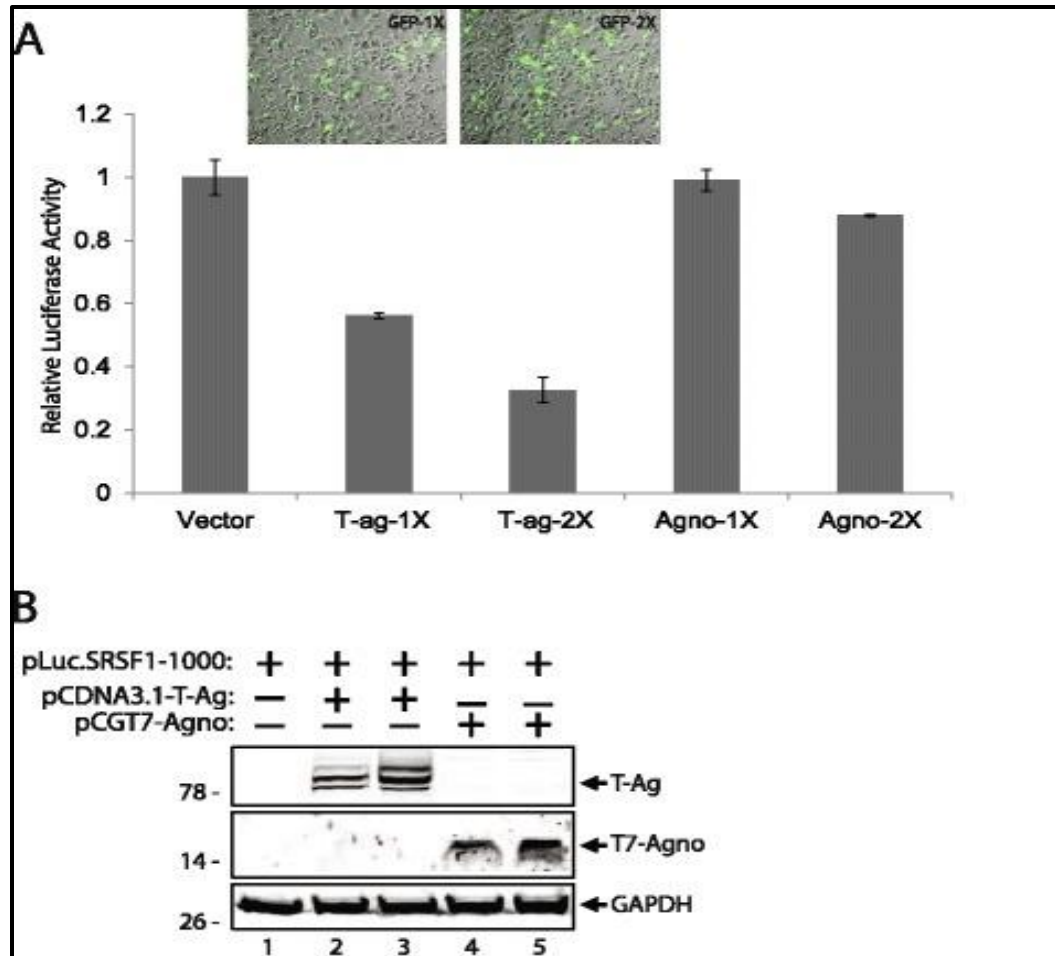


**Figure 20: T-Antigen Suppresses SRSF1 Transcription.** *A.* PHFA were transiently transfected with the pLuc.SRSF1 and increasing concentrations of T-antigen or agnoprotein expression plasmids. At 48 hours, cells were harvested and lysates were analyzed by luciferase reporter assay. Luminescence was determined and corrected for protein concentrations. *B.* Western blot analysis of whole cell lysates was completed in parallel to the samples in panel A. (Reproduced with permission from Craigie et al, 2015 and the Virology Journal under the Creative Commons Attribution 4.0 International License).

### 3.2.4. Large T-Antigen Associates with the SRSF1 Promoter to Inhibit Transcription

With data suggesting that T-antigen suppresses SRSF1 expression via suppression of SRSF1 transcription, we assessed the mechanism of T-antigen mediated transcriptional suppression. The primary hypothesis postulated that T-antigen, a well-documented DNA binding protein, interacts with the SRSF1 promoter region and suppresses RNA polymerase binding to the promoter to suppress SRSF1

transcription. To assess this hypothesis, a ChIP assay was used to probe potential protein-DNA interactions. T98G cells were plated in 100 mm dishes and grown until confluency, at which point they were transfected with 10  $\mu$ g of either pcDNA3.1-T-antigen or pcDNA3.1-empty as the negative control. At 48 hours, cells were treated with formaldehyde to cross-link existing protein-DNA complexes, allowing for pull-down and subsequent amplification of DNA fragments associated with target proteins. After cross-linking, cells were lysed using TNN buffer and the resulting lysis solution was sonicated to fragment chromatin to facilitate immunoprecipitation and PCR amplification. The lysates underwent overnight immunoprecipitation with Protein G beads pre-bound with anti-Large T antigen antibody. After immunoprecipitation, lysates were centrifuged to pellet the Protein G beads, which were washed in lysis buffer prior to protein elution. Bound proteins were eluted with ChIP elution buffer (1% SDS, 100 mM NaHCO<sub>3</sub>), after which the beads were pelleted and the protein-DNA complex containing supernatant was collected for further processing. After elution, samples were treated with 5M NaCl to reverse cross linking, followed by treatments with proteinase and RNase to remove protein and RNA fragments. The resulting DNA fragments were purified with phenol: chloroform extraction to remove impurities followed by ethanol precipitation. The DNA fragments underwent PCR amplification of the SRSF1 -1000 to +49 promoter region (PCR primers can be found in Materials and Methods, Section 2.7).

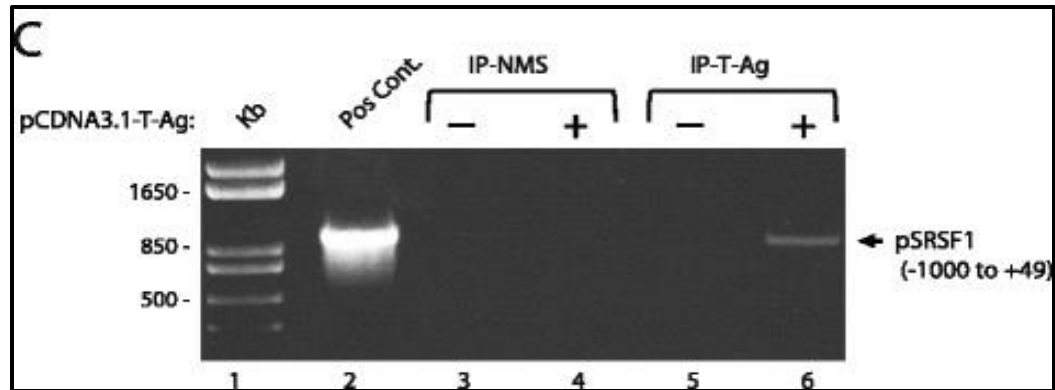


**Figure 21: T-Antigen Suppresses SRSF1 Transcription via Interactions with the Promoter Region.** T98G cells were transfected with T-antigen and DNA-protein complexes were cross-linked at 48 hours. The complexes were used for ChIP analysis. Purified DNA was amplified for the SRSF1 -1000 to +49 bp promoter region. In lane 2, the pLuc-SRSF1 plasmid served as the positive control following DNA amplification. In lanes 3 and 4, samples from cells transfected with control vector or pcDNA3.1-T-Ag underwent immunoprecipitation using normal mouse serum as controls prior to PCR amplification. In lanes 5 and 6, samples from cells transfected with control vector or pcDNA3.1-T-Ag underwent immunoprecipitation using anti-SV40-T-Antigen antibody prior to PCR amplification (Reproduced with permission from Craigie et al, 2015 and the Virology Journal under the Creative Commons Attribution 4.0 International License).

PCR amplification of the pLuc.SRSF1-1000 plasmid served as the positive control (Figure 21, Lane 2). Transfected cells were also subjected to immunoprecipitation with normal mouse serum (NMS) as a control, showing no background associated of the pSRSF1 with the protein-G beads (IP-NMS, Figure 21, Lanes 3 and 4). Untransfected cells showed no SRSF1 promoter amplification following immunoprecipitation, while T-antigen transfected cells showed amplification of the SRSF1 promoter following T-antigen immunoprecipitation, suggesting a possible interaction between T-antigen and the SRSF1 promoter (Figure 21, Lanes 5 and 6). However, this data does not discriminate between direct and indirect interactions, requiring further analysis to determine the mechanism.

### 3.3. Discussion

A major aspect of viral infections is the race between the host's ability to recognize the viral infection and either quarantine the virus or destroy the virus and the viral

ability to avoid detection or bypass the antiviral mechanisms. This race results in an interplay between host regulatory factors, including the immune system and antiviral proteins, and viral regulatory proteins. This interplay determines if the virus initiates productive viral infection or if the regulatory factors eliminate the virus. However, in terms of actual viral infection, the interplay is not so straightforward. When analyzing JCV infection, the virus bypasses some host mechanisms, preventing viral elimination and forming latent sites of low level infection, however, the virus is still regulated by other aspects of the host, which inhibits productive infection in a majority of the population.

With cellular factors exerting a negative pressure on viral transcription and replication, viruses have evolved to utilize their regulatory proteins to bypass host regulation. A seminal example of this is human cytomegalovirus (HCMV) infection and productive viral transcription and replication. After initial host and cellular entry, the immune system detects HCMV presence, resulting in induction of interferon gamma production and release. The activation of the interferon gamma signaling pathway results in the upregulation of other antiviral factors, including viperin, an iron-sulfur cluster-binding antiviral protein (Chin *et al*, 2001; Duschene *et al*, 2010; Shaveta *et al*, 2010). When HCMV initially infects a permissive cell type, the virus encodes a viral protein, viral mitochondrial inhibitor of apoptosis (vMIA), which interacts with viperin during the infectious process to traffic viperin to the mitochondria (Seo *et al*, 2011). Additionally, the virus induces viperin expression through an IFN-dependent pathway, resulting in the expression of

viperin, but notably resulting in redistribution of viperin from the endoplasmic reticulum to the Golgi apparatus and mitochondria (Chin *et al*, 2001; Seo *et al*, 2011). Redistribution of viperin results in disruption of cellular metabolism and enhancement of HCMV infectivity (Al-Barazi *et al*, 1996; Colberg-Poley *et al*, 2000; Goldmacher *et al*, 1999; Goldmacher *et al*, 2002; Seo *et al*, 2011).

JCV likewise expresses viral regulatory proteins, primarily T-antigen, that are required for productive viral infection. During JCV infection, assuming the virus bypasses immune regulation, SRSF1 serves as a major cellular antiviral factor. Prior to this study, SRSF1 was identified as a strong negative regulator of JCV through suppression of viral transcription and replication, thereby suppressing the expression of viral genes (Sariyer and Khalili, 2011; Uleri *et al*, 2011; Uleri *et al*, 2013). The aim of this chapter focused on assessing the interplay between SRSF1 and JCV viral proteins. The results presented within show that T-antigen rescues SRSF1-mediated JCV transcriptional suppression of both the early and late regions. T-antigen expression was found to suppress the expression of SRSF1 by suppressing SRSF1 transcription, resulting in viral transcriptional rescue. With T-antigen possessing DNA binding capabilities, the ability of T-antigen to interact with the SRSF1 promoter was investigated as a method of transcriptional suppression. The results showed that T-antigen possibly interacts with the SRSF1 promoter region, potentially serving as a mechanism to suppress SRSF1 transcription and subsequent expression within cells.

## CHAPTER 4

### MODULATION OF THE NEUROIMMUNE REGULATION OF JC VIRUS BY INTRACELLULAR AND EXTRACELLULAR AGNOPROTEIN

#### 4.1. Introduction

After initial JCV infection, the virus disseminates to peripheral sites where it forms long term latent infections, including the kidneys, tonsillar stromal cells, hematopoietic progenitor cells within the bone marrow, and potentially the brain (Dubois *et al*, 1997; Monaco *et al*, 1996; Monaco *et al*, 1998; Tan *et al*, 2010). Typically, JCV remains latent while the immune system functions normally, however, the virus can reactivate following the onset of immunosuppression, resulting in the development of PML. During PML, JCV primarily infects oligodendrocytes, resulting in cellular lysis and multifocal demyelination throughout the brain with widespread tissue damage (Houff *et al*, 1988).

The physiological changes required for JCV reactivation are not completely elucidated. Analysis of PML patient similarities reveals almost all patients had immunosuppression simultaneously to PML development, yet the aspects of immunosuppression are not the same. Some patients present with a reduced T-cell population, some patients have suppression of T-cell function, while other patients have increased B-cell proliferation.

The clinical presentation of JCV is well understood, with the clinical hallmark of PML lesions being the general lack of lymphocytic infiltration, with histological

analysis of PML lesions showing a lack of leukocytes. However, some patients have significant inflammatory cell infiltrates, generally a symptom of PML combined with immune reconstitution inflammatory syndrome (PML-IRIS) (Kepes *et al*, 1975; Richardson Jr *et al*, 1983). The lack of widespread inflammation appears to contradict what would be expected as the clinical outcome of widespread lytic infection throughout the brain. Current literature reveals limited information of the immunobiology of JCV reactivation within the CNS, particularly glial cells, and the roles of various viral and host factors in JCV regulation. As PML occurs primarily within immunosuppressed patients, it is proposed that the molecular interplay between JCV proteins and the neuroimmune signaling pathways controls JCV reactivation and productive infection resulting in PML development.

While assessing potential mechanisms of limited inflammation, one possible functional target group are the JCV regulatory proteins, primarily agnoprotein. Within the late coding region, JCV contains the gene for agnoprotein, a small regulatory protein that is produced simultaneously with viral replication (Frisque *et al*, 1984). During viral infection, agnoprotein localizes to the cytoplasm and perinuclear regions of the cells, both *in vitro* and within histological analysis of PML lesions (Del Valle *et al*, 2002; Okada *et al*, 2001; Okada *et al*, 2002). The functions of agnoprotein are multifaceted, with one study suggesting that agnoprotein functions as a viroporin which increases plasma membrane permeability to increase infectivity and release of viral particles due to data showing that agnoprotein deletion mutants have suppressed viral release and

propagation and the viral particles that are released are defective in viral DNA contents (Sariyer *et al*, 2011; Suzuki *et al*, 2010). Agnoprotein also interacts with other viral proteins, particularly T-antigen, to enhance the T-antigen DNA binding activity to the viral origin of replication (Saribas *et al*, 2012). Yet, agnoprotein may also possess an extracellular role, as it has been shown to be released from infected glial cells during the viral life cycle (Otlu *et al*, 2014).

One possible role for secreted agnoprotein is to serve as an immunomodulatory protein, to either facilitate the viral infection of uninfected cells by priming the cells for a pro-viral environment or by functioning to mask viral infection, preventing the immune system from recognizing the viral infection and mounting a sufficient antiviral response. Within this section, we investigated the role of extracellular agnoprotein in modulation of the host-immune response to the JCV infection cycle within the CNS.

## **4.2. Results**

### **4.2.1. Agnoprotein is Released from Transfected Cells**

To assess the immunomodulatory role of agnoprotein, agnoprotein release from cells was determined as a potential mechanism to modulate immune signaling pathways in uninfected cells. As JCV predominantly infects oligodendrocytes, our model utilized TC620 cells, an oligodendroglioma cell line. TC620 cells were cultured in a 100 mm-dish at a concentration of 500,000 cells per well and transiently transfected with 10 µg of pcGT7-Agnoprotein or pcGT7-empty vector

for control. At 48 hours, conditioned media was collected, and cells were trypsinized, collected and pelleted with centrifugation. After pelleting, cellular pellets were lysed with TNN lysis buffer and rotated for 1 hour at 4° C, followed by centrifugation to remove cellular debris, with the supernatant being collected for further analysis. To assess the presence of extracellular agnoprotein, conditioned media underwent immunoprecipitation. The conditioned media was precleared with Protein G beads to remove antibodies present in the media, primarily from the supplemented fetal bovine serum. Precleared conditioned media was incubated overnight with Protein G beads pre-bound with anti-agnoprotein antibody at 4° C. Following overnight incubation, beads were washed with lysis buffer and heated to 95° C to denature bound proteins prior to visualization with Western Blotting. Both whole cell lysate samples and conditioned media immunoprecipitation were resolved on a 15% polyacrylamide gel prior to transfer to 0.2 µm nitrocellulose membrane and incubation with anti-agnoprotein antibody. Whole cell lysate samples showed agnoprotein expression following transfection (Figure 22A, Lanes 1 and 2). After immunoprecipitation, conditioned media samples were positive for agnoprotein, suggesting that agnoprotein is released from transfected cells (Figure 22A, Lanes 3 and 4).

To quantify released agnoprotein in conditioned media, a direct ELISA was used. Conditioned media samples were coated onto a 96-well plate overnight, after which wells were blocked and incubated with anti-agnoprotein IgG antibody overnight. After primary antibody incubation, wells were incubated with anti-rabbit HRP conjugated secondary antibody and washed before treatment with TMB substrate,

which is oxidized in the presence of peroxidases to a diimine, resulting in the development of a blue color that is dependent on the amount of HRP in the well. Diimine development is stopped by treatment with 0.16 M sulfuric acid, which results in the blue color changing to a yellow color. The absorbance spectra of both CM-control and CM-agnoprotein samples were assessed at 405 nm. For quantification purposes, MBP-agnoprotein complexes were used to calculate the standard curve. An average concentration of 50 ng/mL of agnoprotein was determined for multiple CM-agno collections (Figure 22B).

To ensure that extracellular agnoprotein was not released due to cellular death, an MTT viability assay was performed assessing TC620 viability following transfection with pcGT7-agnoprotein. TC620 cells were plated in a 6-well dish and transiently transfected with pcGT7-alone or pcGT7-agnoprotein. At 48 hours, cells were incubated for 2 hours with MTT substrate at 37° C, after which media was aspirated and cells were incubated with MTT solvent (100 mL isopropanol, 0.1 % NP-40, 4 mM HCl) for 10 minutes with rocking. The MTT solvent was collected and the absorbance at 570 and 630 nm (reference read) were determined using a ThermoScientific Genesys 10S Vis Spectrophotometer. The absorbance at 630 nm was subtracted from the absorbance at 570 nm to yield experimental absorbances. Normal TC620 viability was characterized using untransfected cells. Each condition was completed in triplicate, after which average viability and standard deviations were collected. This data shows that transfection with an agnoprotein expression vector has no impact on cellular viability, suggesting that extracellular

agnoprotein is not the byproduct of cell death or lysis following transfection (Figure 22C).

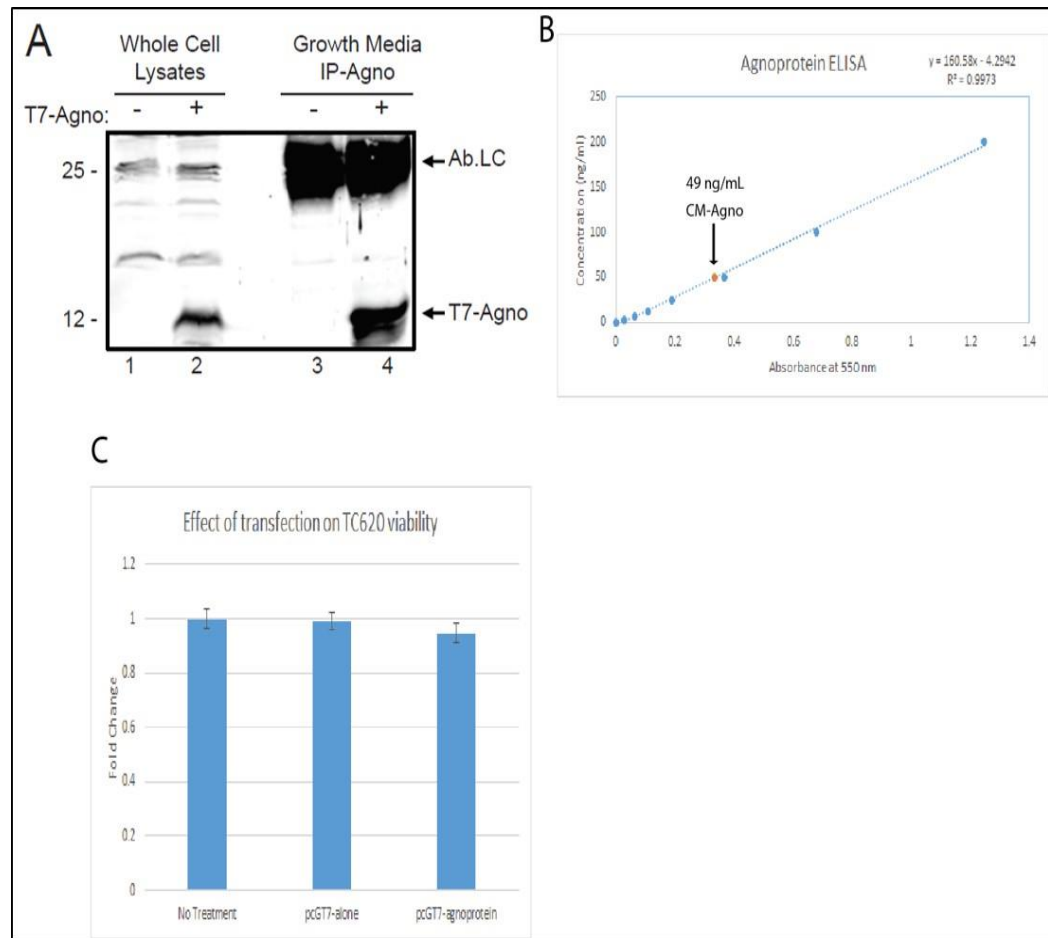


**Figure 22: Agnoprotein is released from Transfected Cells.** *A.* Western blot analysis of whole cell lysates and growth media collected from TC620 cells transfected with an agnoprotein expression. Growth media was subjected to immunoprecipitation for agnoprotein prior to western blot analysis. *B.* ELISA analysis of agnoprotein concentration within collected conditioned media. Standard values were obtained with recombinant agnoprotein. *C.* MTT viability assay of untransfected TC620 cells or TC620 cells transfected with empty vector or an agnoprotein expression vector. Reproduced with permission from Craigie et al, 2017, *Journal of Neuropharmacology*, **in press**.

#### 4.2.2. Extracellular Agnoprotein is Internalized by Glial Cells

To assess if extracellular agnoprotein is internalized by glial cells, PHFA and PHFM were treated with CM-control and CM-agnoprotein. Primary human glial cells were plated in a 6-well tissue culture dish and grown until confluent. At confluency, PHFA and PHFM were treated for 48 hours with CM-control or CM-

agnoprotein, after which whole cell lysates were collected and analyzed for agnoprotein uptake via Western blotting. Both astrocytes and microglia showed agnoprotein uptake following conditioned growth media treatment (Figure 23).

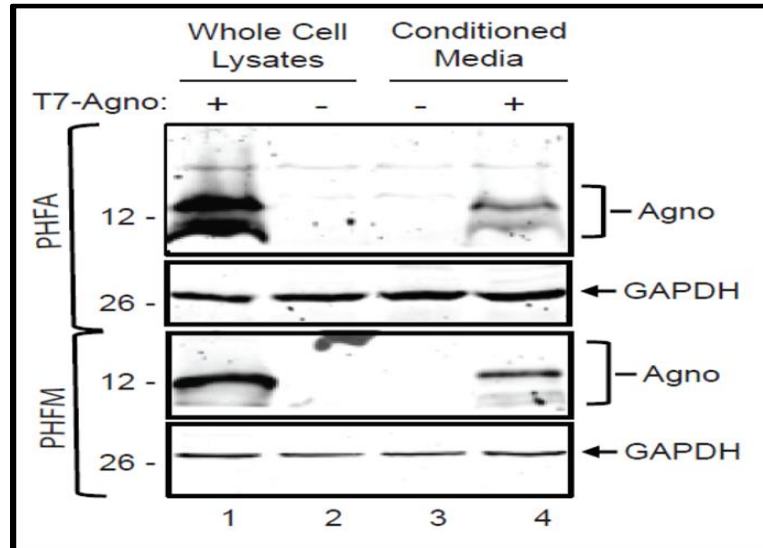


**Figure 23: Agnoprotein is internalized by Glial Cells.** Western blot analysis of PHFA and PHFM treated with CM-control or CM-agnoprotein for 48 hours to assess for agnoprotein internalization. Whole cell lysates of TC620 untransfected or agnoprotein transfected cells served as controls. Reproduced with permission from Craigie et al, 2017, *Journal of Neuropharmacology*, *in press*.

To further assess extracellular agnoprotein uptake, PHFA and PHFM were plated in 2-well chamber slides and grown until confluent. At confluency, cells were treated with CM-control or CM-agnoprotein for 48 hours. At 48 hours, cells were fixed with ice cold acetone: methanol mixture (50:50) and processed for immunocytochemistry to assess agnoprotein uptake. After fixation, cells were blocked with 5% BSA in 1X PBS for 2 hours and incubated with 1:300 anti-agnoprotein antibody overnight. Slides were washed and incubated with 1:500 anti-rabbit-FITC for PHFA or 1:500 anti-rabbit-rhodamine red for PHFM prior to staining with DAPI and mounting. After mounting, cells were visualized with a Leica Fluorescent Microscope to assess agnoprotein uptake and localization. Both

astrocytes and microglia showed robust agnoprotein uptake with perinuclear and cytoplasmic agnoprotein localization (Figure 24).

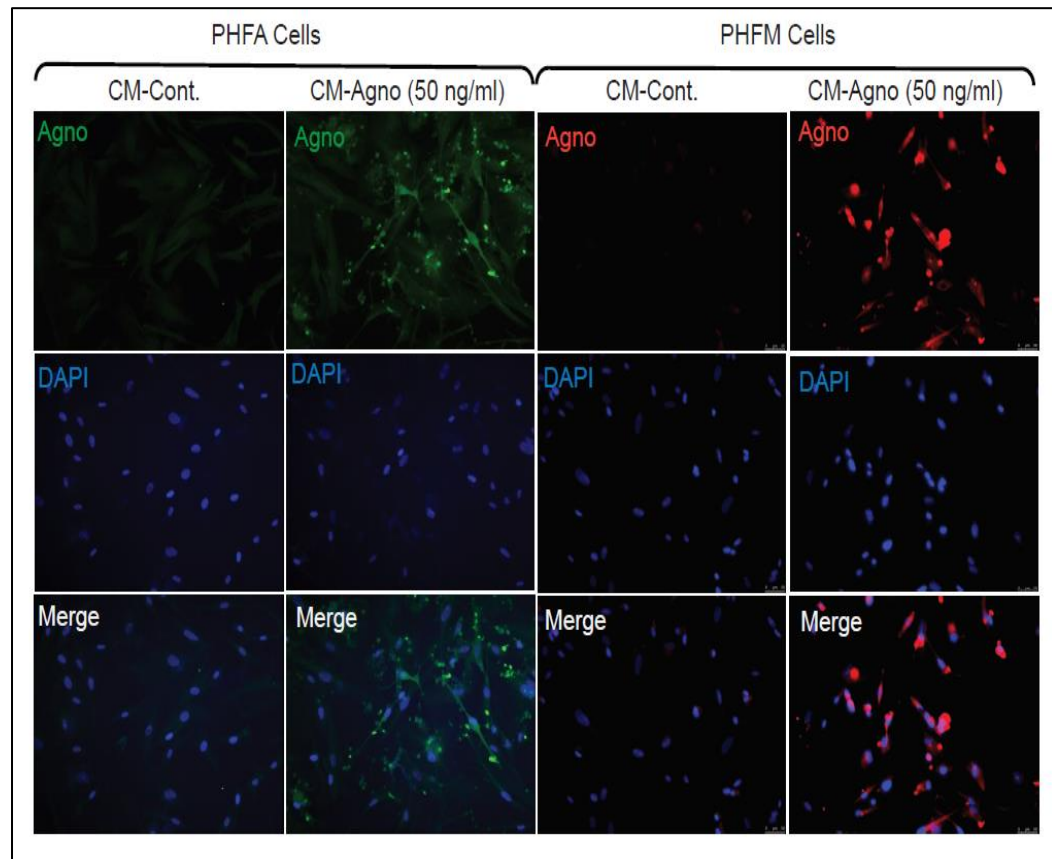


**Figure 24: Internalized Agnoprotein shows Cytoplasmic and Perinuclear Localization.** Immunocytochemistry analysis of PHFA and PHFM treated for 48 hours with CM-control or CM-agnoprotein. At 48 hours, cells were fixed and processed for immunocytochemistry to visualize extracellular agnoprotein internalization. Reproduced with permission from Craigie et al, 2017, *Journal of Neuropharmacology*, *in press*.

#### 4.2.3. Intracellular Agnoprotein Suppresses GM-CSF Release by Astrocytes

With agnoprotein being released by infected cells and subsequently internalized by primary glial cells, it was hypothesized that agnoprotein modulates the immune response to the virus through dysregulation of the cytokine profile of glial cells. The cytokine/chemokine profile of PHFA was assessed using a RayBioTech C3 cytokine array to test the media cytokine levels of 42 various cytokines. PHFA were treated with either CM-control or CM-agnoprotein for 24-hours, resulting in

agnoprotein uptake as previously shown. At 24-hours, conditioned media was removed from the cells and fresh media was added. After another 24 hours, the media was collected, and the media cytokine/chemokine profile was analyzed with the RayBioTech C3 cytokine array kit. Provided antibody coated membranes were blocked and subsequently incubated with growth media from CM-control or CM-agnoprotein treated cells. After incubation, membranes were incubated with biotinylated antibody prior to incubation with labeled streptavidin. Membranes were then developed through x-ray development and analyzed for cytokine intensities. The release of GM-CSF was significantly reduced following CM-agnoprotein treatment in contrast to CM-control treatment (Figure 25A). To quantify changes in GM-CSF release, the intensities from the cytokine array membrane were determined, revealing that CM-agnoprotein treatment resulted in a forty percent decrease of released GM-CSF. Comparison of positive control intensities and other various cytokines showed no significant differences, suggesting that reduction of GM-CSF release was specific to agnoprotein treatment and not a widespread decrease in cytokine release by treated cells or differences between membranes (Figure 25B).

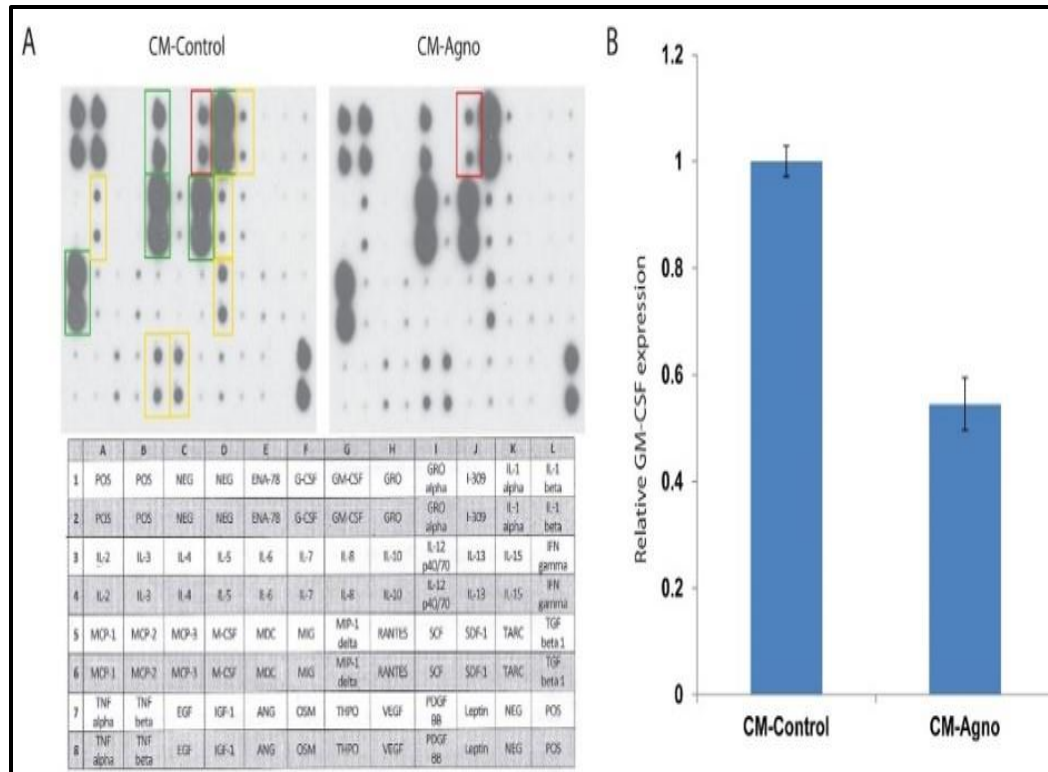


**Figure 25: GM-CSF Release is suppressed by Agnoprotein Internalization.** **A.** RayBioTech Human Cytokine Array C3 analysis of growth media of PHFA treated with CM-control or CM-agnoprotein for 24 hours. After treatments, fresh media was added and collected after 24 hours and analyzed for the concentration of 42 human cytokines within the media. Cytokine intensities were normalized to positive control signals. **B.** Quantification of relative GM-CSF expression in the media following CM-control or CM-agnoprotein treatments after intensity normalization to positive controls. Reproduced with permission from Craigie et al, 2017, *Journal of Neuropharmacology*, *in press*.

#### 4.2.4. Extracellular Agnoprotein and Recombinant Agnoprotein have no Impact on Primary Cell Viability

After determining that extracellular agnoprotein is internalized by glial cells, resulting in suppression of GM-CSF transcription and decreased GM-CSF release, the role of agnoprotein was assessed using a recombinant agnoprotein system. This system is preferential to conditioned media treatments due to the ability to assess various extracellular agnoprotein concentrations. Recombinant agnoprotein was produced using an MBP-based recombinant protein expression system. For recombinant agnoprotein, the transformed *E. coli* strain was kindly provided by Dr.

Sami Saribas and was previously published (Saribas et al, 2011). Briefly, the DH5 $\alpha$  E. coli strain was transformed with pMAL-c5x-JCV-Agno-Full Length, a plasmid containing the full length agnoprotein sequence fused with the MBP expression gene containing ampicillin resistance. The transformed E. coli strain was cultured overnight in 100 mL of Luria-Bertani (LB) media containing 100  $\mu$ g/mL ampicillin. The following day, the overnight culture was split into two fractions and diluted 1:10 with fresh LB media containing 100  $\mu$ g/mL ampicillin and 2 g/L glucose, resulting in a final volume of 500 mL for each fraction, and incubated at 37° C for 3 hours. After 3 hours, cultures were induced with 0.5 mM isopropyl  $\beta$ -D-1-thiogalactopyranoside (IPTG) treatments, which induces the expression of the MBP fusion protein, in this instance MBP-agnoprotein. Protein expression occurred for 3 hours, after which bacteria was harvested by centrifugation and the resulting bacterial pellet was resuspended and lysed with lysozyme treatment prior to further lysis via sonication. Sonicated lysates were centrifuged to remove cellular debris, and the cleared lysates were incubated overnight with amylose fast flow resin beads. These beads form a cross-linked matrix allowing for the isolation of MBP-complexes. After overnight incubation, the beads were pelleted and washed to remove unbound proteins prior to elution of the MBP-agnoprotein complex with 10 mM maltose buffer. Eluted samples were assessed through 10% polyacrylamide gel separation followed by Coomassie blue staining.

After elution, MBP-agnoprotein complexes were cleaved with Factor Xa protease, a serine endopeptidase which cleaves the fusion protein complex at the Ile-(Glu-

Asp)-Gly-Arg cleavage site present between the MBP and the fused agnoprotein protein (Eaton *et al*, 1986; Nagai *et al*, 1985; Quinlan *et al*, 1989). Following cleavage, samples were incubated overnight with amylose fast flow resin beads to bind and eliminate the residual MBP and MBP-agnoprotein complexes, leaving purified recombinant agnoprotein.

After purification, recombinant agnoprotein was assessed via Western blotting to ensure immunogenicity (Figure 26). MBP-Agno and cleaved MBP-agnoprotein were assessed, with MBP-agnoprotein showing a band at 52 kDa, corresponding to the fusion protein, with cleaved recombinant agnoprotein showing bands at 12 kDa and 8 kDa, corresponding to the dimer and monomer forms of agnoprotein, respectively (Figure 26, Lanes 4 and 5). Whole cell lysates from control or pcGT7-agnoprotein transfected TC620 cells served as controls for agnoprotein signal (Figure 26, Lanes 1 and 2). MBP alone served as a control to ensure that the MBP protein had no cross-reactivity with the agnoprotein antibody (Figure 26, Lane 3).

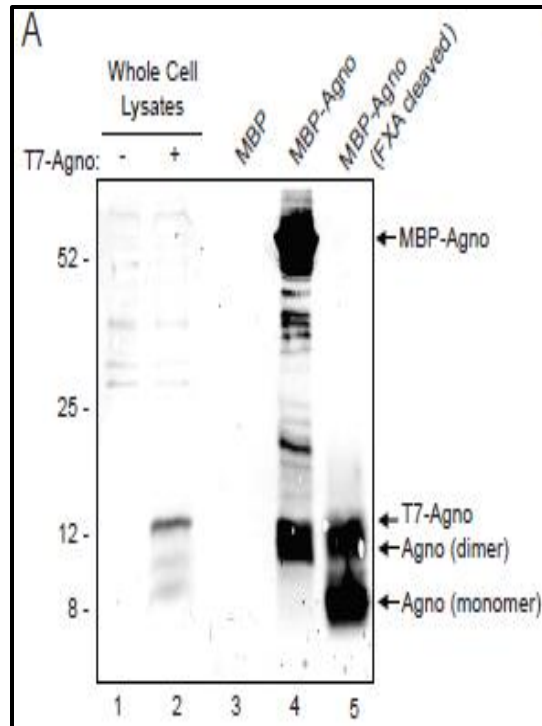


**Figure 26: Recombinant Agnoprotein from the Bacterial MBP-Expression System.** Western blot analysis of MBP, MBP-Agno, and recombinant agnoprotein (MBP-Agno Factor Xa cleaved and MBP purified). Agnoprotein dimer and monomer forms are highlighted at 12 and 8 kDa, respectively. Reproduced with permission from Craigie et al, 2017, *Journal of Neuropharmacology*, *in press*.

While agnoprotein was shown to have no impact on the viability of the oligodendroglia cell line, it was important to assess the impact of extracellular agnoprotein on primary cell types. Since cancer cell lines possess characteristics not present in primary cells, it remained a possibility that extracellular agnoprotein may impact primary cell viability. PHFA and PHFM were plated in a 6-well dish and treated with CM-control, CM-agnoprotein, MBP, or recombinant agnoprotein. At 48 hours, cells were incubated for 2 hours with MTT substrate at 37° C, after which media was aspirated and cells were incubated with MTT solvent for 10 minutes with rocking. The MTT solvent was collected and the absorbances at 570 and 630 nm (reference read) were determined using a ThermoScientific Genesys

10S Vis Spectrophotometer. The absorbance at 630 nm was subtracted from the absorbance at 570 nm to yield our experimental absorbance value. Normal PHFA and PHFM viabilities were characterized using untreated cells. Each condition was completed in triplicate, after which average viability and standard deviations were collected. This data showed that treatment with extracellular agnoprotein, either in CM-agnoprotein or recombinant agnoprotein form, had no impact on cellular viability, suggesting that extracellular agnoprotein does not impact PHFA (Figure 27A) or PHFM (Figure 27B) viability.

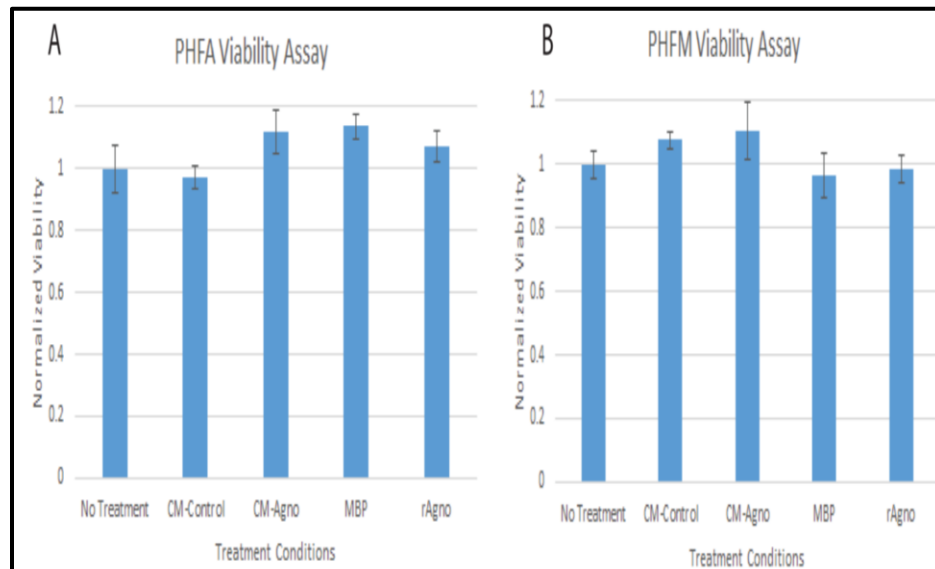


**Figure 27: GM-CSF Release is suppressed by Agnoprotein Internalization.** A. MTT cellular viability assay for the assessment of PHFA viability following treatment with CM-control, CM-agnoprotein, MBP, or recombinant agnoprotein. Cellular viabilities were normalized to untreated PHFA. B. MTT cellular viability assay for the assessment of PHFM viability following treatment with CM-control, CM-agnoprotein, MBP, or recombinant agnoprotein. Cellular viabilities were normalized to untreated PHFM. Reproduced with permission from Craigie et al, 2017, *Journal of Neuropharmacology*, *in press*.

#### 4.2.5. Agnoprotein Inhibits GM-CSF Transcription

With extracellular agnoprotein suppressing GM-CSF release from glial cells, the impact of extracellular agnoprotein on GM-CSF transcription was investigated. TC620 cells were plated in a 6-well tissue culture plate with 100,000 cells plated

per well and were grown until confluency. After becoming confluent, cells were transiently transfected in triplicate with luciferase reporter constructs containing the GM-CSF -627 to +48 base pair promoter region (pLuc.GM-CSF) and either co-transfected with the viral protein expression plasmid encoding agnoprotein (pcGT7-agnoprotein) or treated with CM-control or CM-agnoprotein. Transfections of pLuc.GM-CSF used 2 µg of plasmid DNA, while pcGT7-agnoprotein was used at 2 µg per plasmid, with pcGT7-empty vector used to normalize the total amount of transfected DNA. Conditioned media treatments consisted of 2 mL fresh DMEM supplemented with 10% FBS mixed with 2 mL conditioned media. At 48 hours post-transfection, cells were harvested with trypsin, collected, and centrifuged and the resulting cellular pellet was resuspended and lysed with Promega reporter active lysis buffer by rotation for 1 hour at 4° C. After lysis, samples were centrifuged to pellet cellular debris. After centrifugation, 20 µL of the supernatant was added to 100 µL of LAR. The luciferase activity was read using a luminometer and corrected for protein concentrations for each sample. To ensure no background luciferase activity was occurring, untransfected cell lysates served as the negative control (Figure 28A and 28B, Lane 1). The corrected luciferase activities were normalized to the basal transcriptional activity, determined by transfecting cells with pLuc.GMCSF plasmid alone (Figure 28A and 28B, Lane 2). When agnoprotein was expressed through co-transfection, GM-CSF promoter activity significantly decreased while co-transfection with the control vector had no impact on GM-CSF transcription (Figure 28A, Lane 3 and 4). Similarly, extracellular agnoprotein treatments with CM-agnoprotein significantly

suppressed GM-CSF promoter activity while CM-control treatments had no impact on GM-CSF transcription (Figure 28B, Lane 3 and 4). All conditions were completed in triplicate and the graphed values are the averages of the three replicates. These combined data suggest that agnoprotein internalization or expression is sufficient for GM-CSF transcriptional suppression.

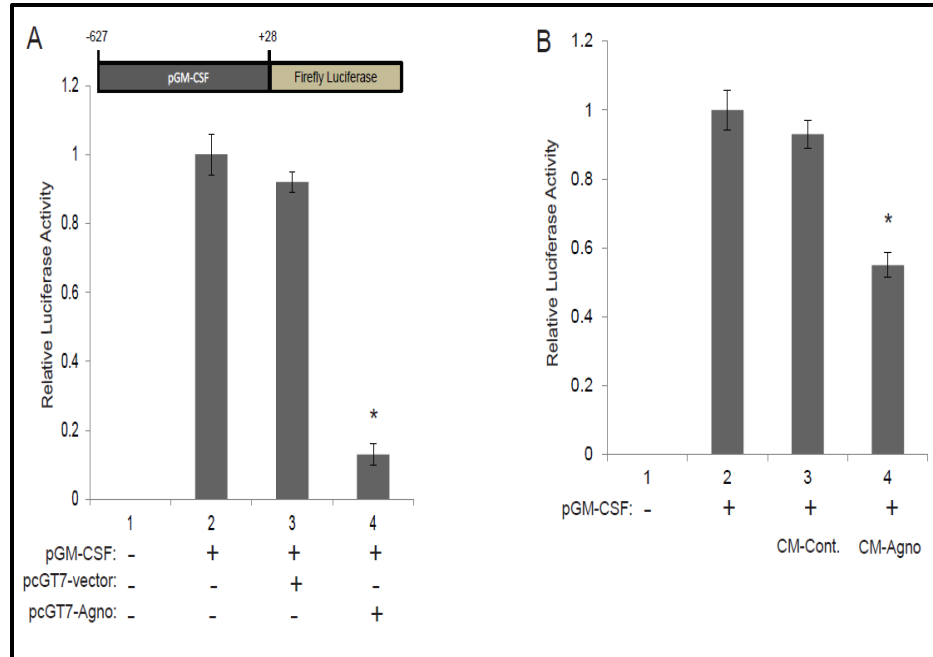


**Figure 28: Intracellular and Extracellular Agnoprotein Inhibit GM-CSF Transcription.** **A.** Luciferase assay to assess GM-CSF transcription in TC620 cells following intracellular expression of agnoprotein. Luminescence activity was assessed and corrected for protein concentration and normalized to basal GM-CSF transcriptional activity. Graphed values are the averages of three replicates with the standard deviations. **B.** Luciferase assay to assess GM-CSF transcription in TC620 cells following treatments with extracellular agnoprotein. Luminescence activity was assessed and corrected for protein concentration and normalized to basal GM-CSF transcriptional activity. Graphed values are the averages of three replicates with the standard deviations. Reproduced with permission from Craigie et al, 2017, *Journal of Neuropharmacology*, **in press**.

#### 4.2.6. GM-CSF Suppresses JCV Early and Late Gene Transcription

With agnoprotein specifically suppressing GM-CSF transcription and decreasing the GM-CSF release by glial cells, it was proposed that GM-CSF may serve an anti-viral function regarding JCV infection and PML development. The first anti-viral

function assessed was the impact of GM-CSF on JCV transcription for both early and late promoter regions. As previously described, the JCV genome contains a bi-directional NCCR with a bi-directional promoter region to induce either early or late JCV gene transcription in an orientation dependent manner. To assess GM-CSF regulation of JCV early and late gene transcription, TC620 cells were plated in a 6-well tissue culture plate with 400,000 cells plated per well and were grown until confluency. After becoming confluent, cells were transiently transfected with the JCV bi-directional luciferase-renilla dual reporter constructs containing the early and late JCV promoter regions (pbJCV) and co-transfected with the viral protein expression plasmid encoding T-antigen (pcDNA3.1-T-ag) and treated with 1 and 10  $\mu\text{g}/\text{mL}$  of recombinant GM-CSF. The pbJCV construct is designed so that renilla expression is controlled by the JCV early region promoter orientation and luciferase expression is controlled by the JCV late region promoter orientation (Figure 29A). Transfections of pb.JCV used 2  $\mu\text{g}$  of plasmid DNA, while pcDNA3.1-T-ag was used at 2  $\mu\text{g}$  per plasmid, with pcDNA3.1-empty vector used to normalize the total amount of transfected DNA.

At 48 hours post-transfection, cells were harvested with trypsin, collected, and centrifuged. The resulting cellular pellet was resuspended and lysed with Promega reporter active lysis buffer and rotated for 1 hour at 4° C. After lysis, samples were collected and centrifuged to pellet cellular debris. After centrifugation, 20  $\mu\text{L}$  of the supernatant was added to 100  $\mu\text{L}$  of LAR. The luciferase activity was read using a luminometer. After luciferase activity was determined, 100  $\mu\text{L}$  of Stop-and-Glo®

solution was added and the renilla activity was determined using the luminometer. Luciferase and renilla luminescence values were corrected for protein concentrations.

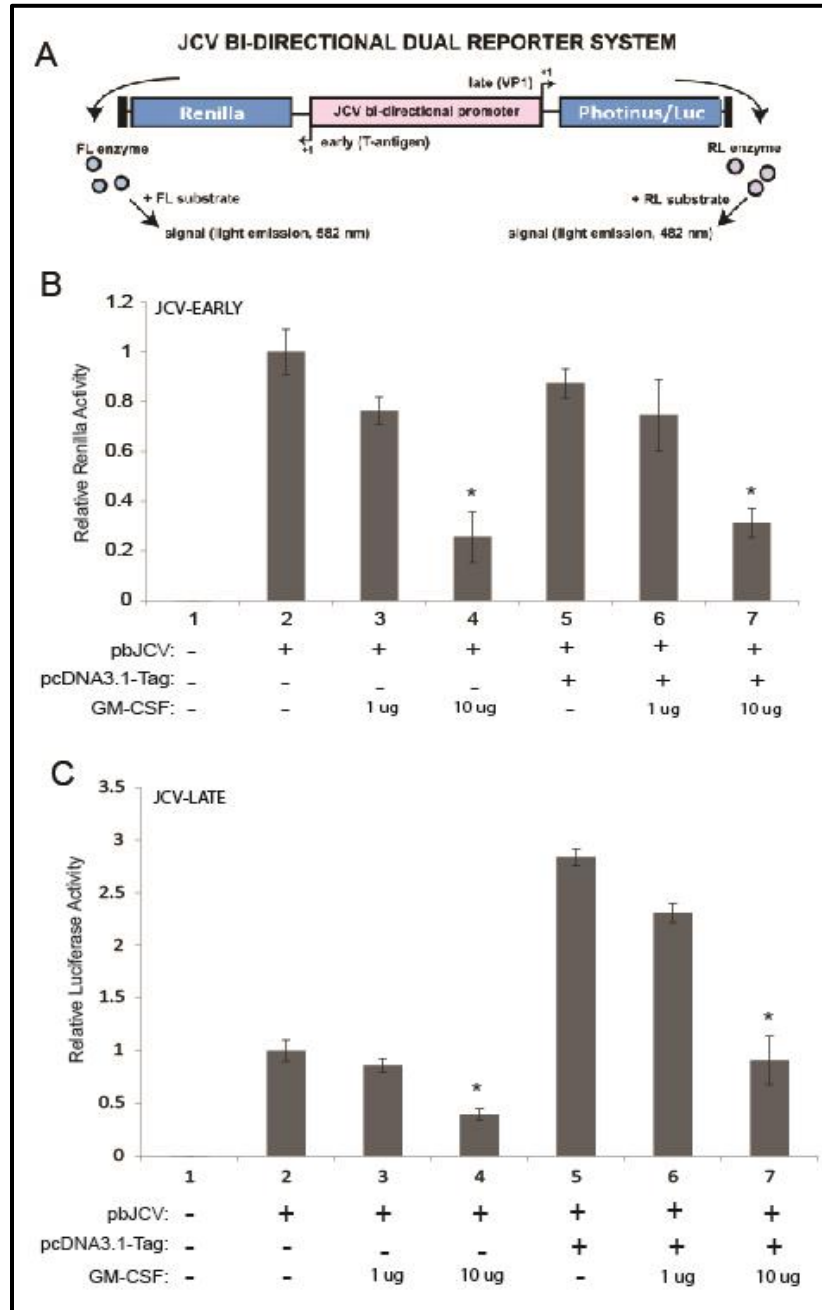


**Figure 29: GM-CSF Suppresses JCV-early and -late Gene Transcription.** *A. Schematic model of the JCV bi-directional dual reporter system used for JCV transcriptional assays. B. Dual reporter assay to assess JCV-early gene transcription in TC620 cells following GM-CSF treatments of 1 and 10  $\mu\text{g}/\text{mL}$ . Renilla luminescence activity was assessed and corrected for protein concentration and normalized to basal JCV transcriptional activity. Graphed values are the averages of three*

*replicates with the standard deviations. C. Dual reporter assay to assess JCV-late gene transcription in TC620 cells following GM-CSF treatments of 1 and 10 µg/mL. Luciferase luminescence activity was assessed and corrected for protein concentration and normalized to basal JCV transcriptional activity. Graphed values are the averages of three replicates with the standard deviations. Reproduced with permission from Craigie et al, 2017, Journal of Neuropharmacology, in press.*

To ensure no background luciferase activity, untransfected cell lysates served as the negative control (Figure 29B and 29C, Lane 1). The corrected luciferase activity was normalized to the basal transcriptional activity, determined by transfecting cells with pbJCV plasmid alone (Figure 29B and 29C, Lane 2). When pbJCV transfected cells were treated with GM-CSF, there was a dose-dependent decrease in both early and late JCV transcription (Figure 29B and 29C, Lanes 3 and 4). With 10 µg/mL treatments of GM-CSF, JCV early gene transcription was suppressed by 80% while JCV late gene transcription was suppressed by 60% (Figure 29B and 29C, Lane 4). In the model system, expression of T-antigen did not impact JCV early gene transcription and possessed no rescuing ability of JCV early gene transcription following GM-CSF treatments (Figure 29B, Lanes 5-7). Additionally, the expression of T-antigen induced JCV late gene transcription, however, GM-CSF treatments decreased this induction to basal levels at the 10 µg/mL GM-CSF dosage (Figure 29C, Lanes 5-7).

All conditions were completed in triplicate and the graphed values are the averages of the three replicates. These combined data suggest that GM-CSF possesses antiviral capacity by suppressing JCV early and late gene transcription.

#### 4.2.7. Agnoprotein Suppresses U937 Differentiation

GM-CSF is a hematopoietic growth factor which stimulates monocyte differentiation into macrophages and serves as a chemoattractant for monocytes (Burgess *et al*, 1978; Hamilton, 2002; Metcalf, 1979). Since agnoprotein suppresses GM-CSF transcription, the impact of extracellular agnoprotein on monocytes, the target of GM-CSF, was assessed. The ability of extracellular agnoprotein to suppress monocyte differentiation and attachment determined since GM-CSF induces monocyte differentiation; thus, it was hypothesized that extracellular agnoprotein may potentially disrupt this process. p

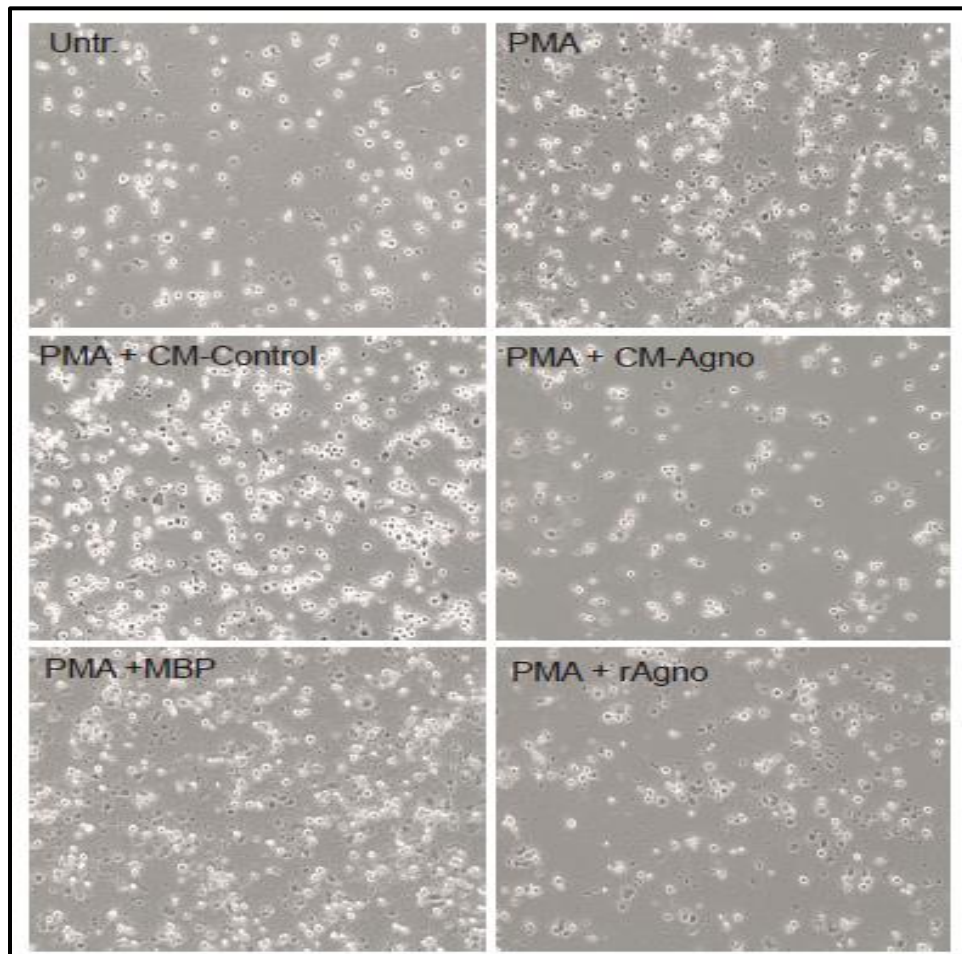


**Figure 30: Extracellular Agnoprotein Suppresses U937 Differentiation.** Phase contrast images of U937 cells pulsed with PMA to induce differentiation and subsequently treated with CM-control,

*CM-agno, MBP, or recombinant agno. Untreated U937 served as control images. Images are representative sections from the 48-hour time point. Reproduced with permission from Craigie et al, 2017, Journal of Neuropharmacology, in press.*

The human monocyte cell line, U937, were plated in a 6-well dish with 1,000,000 cells per well. After plating, cells were pulsed with 100 ng/mL PMA for 2 hours to induce differentiation from suspension-based monocytes into attached macrophage-like cells. Following the PMA pulse, cells were treated with either CM-control, CM-agnoprotein, MBP, or recombinant agnoprotein at 50 ng/mL. At 24-, 48-, and 72-hours, unattached cells were removed, and phase contrast images were taken for each condition to determine the amount of differentiated, or attached, cells. Small representative sections of these images were enlarged for visualization purposes (Figure 30).

After imaging, ten representative images of different regions were selected, and the total number of attached cells was counted and averaged to determine the average number of cells attached. To determine cellular attachment based on factors present within the media, U937 cells were plated and not treated with PML.

At 48 hours, the number of attached cells served as the background attachment level showing a low number of attached cells, with around 400 cells per image section (Figure 31, Lane 1). To determine normal differentiation rate, U937 cells were plated and pulsed with PMA with no subsequent treatment conditions. At 48 hours, the number of attached cells served as the maximum differentiation level, with attached cell counts averaging 1600 cells per image section (Figure 31, Lane 2).

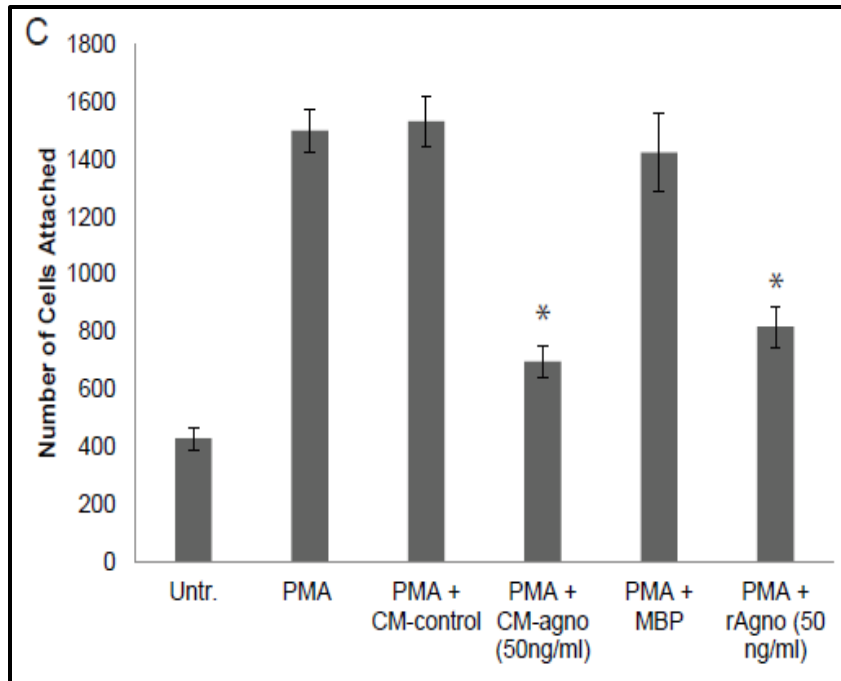


**Figure 31: Quantification of U937 Differentiation in the Presence of Agnoprotein.** U937 differentiation and attachment following PMA induction and treatments with CM-control, CM-agno, MBP, or recombinant agno was assessed through cell counting and represented as a bar graph. Reproduced with permission from Craigie et al, 2017, *Journal of Neuropharmacology*, **in press**.

Two treatment groups existed, the first group using conditioned media with the second group using either MBP or recombinant agnoprotein, with both treatment groups serving to assess the impact of extracellular agnoprotein on monocyte differentiation and attachment. U937 were plated and pulsed with PMA for two hours and subsequently treated with 50% CM-control or CM-agnoprotein. At 48 hours, CM-control treated U937 attached similarly to untreated PMA-induced cells, with attached cell counts averaging 1600 cells per image section (Figure 31, Lane 3). However, when U937 were pulsed with PMA and subsequently treated with CM-agnoprotein, there was a significant reduction in monocyte differentiation. At 48 hours, CM-agnoprotein treated U937 showed a significant suppression in cellular attachment compared to PMA-induced cells, with attached cell counts

averaging less than 800 cells per image section (Figure 31, Lane 4). Like conditioned media treated cells, the recombinant protein treatment group resulted in extracellular agnoprotein significantly suppressing U937 cellular attachment. At 48 hours, MBP treated U937 attached similarly to untreated PMA-induced cells, with attached cell counts averaging 1600 cells per image section (Figure 31, Lane 5). However, when U937 were pulsed with PMA and subsequently treated with recombinant agnoprotein, there was a significant reduction in monocyte differentiation. At 48 hours, recombinant agnoprotein treated U937 showed a significant decrease in cellular attachment compared to PMA-induced cells, with attached cell counts averaging less than 800 cells per image section (Figure 31, Lane 4).

#### **4.2.8. Extracellular Agnoprotein does not Impact U937 Cellular Viability**

As agnoprotein treatments significantly decreased U937 attachment, the question arose asking if cellular attachment was suppressed as a secondary effect of agnoprotein decreasing cellular viability, thus resulting in few cells present as opposed to specifically altering the differentiation process.

To assess U937 viability, 1,000,000 cells were plated in a 6-well dish and pulsed with 100 ng/mL PMA to induce differentiation and simultaneously treated with CM-control, CM-agnoprotein, MBP, or recombinant agnoprotein. At 48 hours, cells were incubated for 2 hours with MTT substrate at 37° C, after which media was aspirated and cells were incubated with MTT solvent for 10 minutes with

rocking. The MTT solvent was collected and the absorbance at 570 and 630 nm (reference read) were determined using a ThermoScientific Genesys 10S Vis Spectrophotometer. The absorbance at 630 nm was subtracted from the absorbance at 570 nm to yield our experimental absorbance value. Normal U937 viability was characterized using untreated PMA-induced cells. Each condition was completed in duplicate, after which average viability and standard deviations were collected.

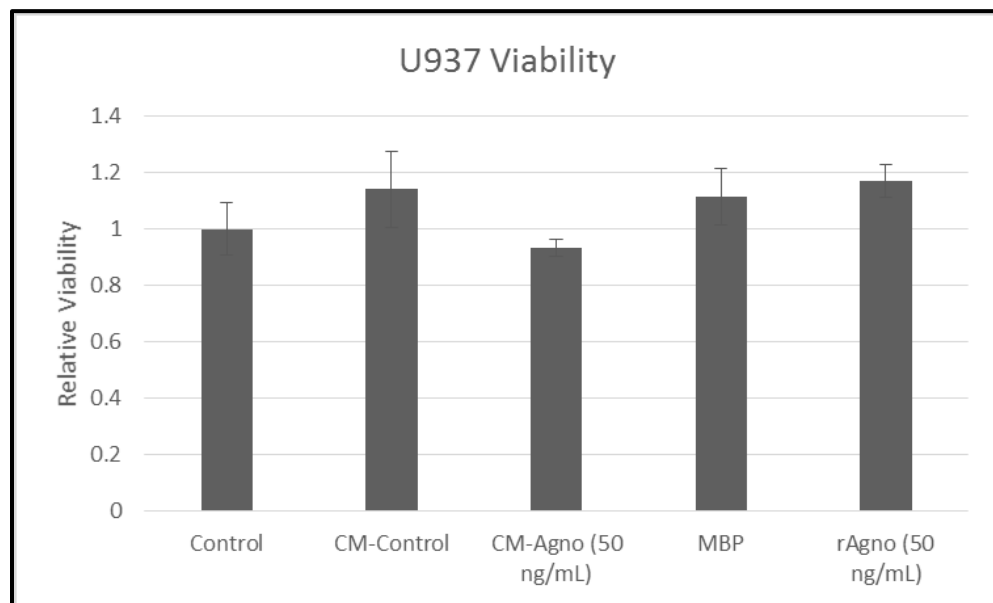


**Figure 32: Agnoprotein has no Impact on U937 Viability.** MTT cellular viability assay for the assessment of U937 viability following pulsing with PMA and subsequent treatment with CM-control, CM-agnoprotein, MBP, or recombinant agnoprotein. Cellular viabilities were normalized to untreated PMA-induced U937. Reproduced with permission from Craigie et al, 2017, *Journal of Neuropharmacology*, *in press*.

This data showed that treatment with extracellular agnoprotein, either in CM-agnoprotein or recombinant agnoprotein form, had no impact on cellular viability, suggesting that extracellular agnoprotein does not impact U937 viability and that cellular attachment differences are not an artifact of decreased viability (Figure 32).

#### **4.2.9. Agnoprotein Dysregulates U937 Surface Marker Expression**

Since agnoprotein suppresses monocyte differentiation, it was proposed that agnoprotein may also dysregulate the expression of various surface markers on the differentiated macrophages. To assess this, U937 cells were plated in a two-well chamber slide (500,000 cells per well) and pulsed with 100 ng/mL phorbol myristate acetate treatments for 2 hours to induce differentiation. At 24-hours, induced cells were treated with 50% CM-control or CM-agnoprotein in fresh RPMI 1640 media at 24- and 48-hours post-induction. At 72-hours, cells were fixed with ice-cold acetone: methanol (50:50 mixture) and subsequently washed. Slides were blocked with 10% BSA in 1X PBS for 1 hour at room temperature. Slides were incubated overnight with rocking at 4° C with primary anti-CD16, anti-CD68, or anti-CD71 antibody diluted 1:300. After overnight incubation, slides were washed and incubated with secondary antibody solution, 1:500-Rhodamine-mouse, for 2 hours at room temperature with gentle rocking. After secondary antibody, slides were washed and mounted using Vectashield mounting medium containing DAPI (Vector Laboratories).

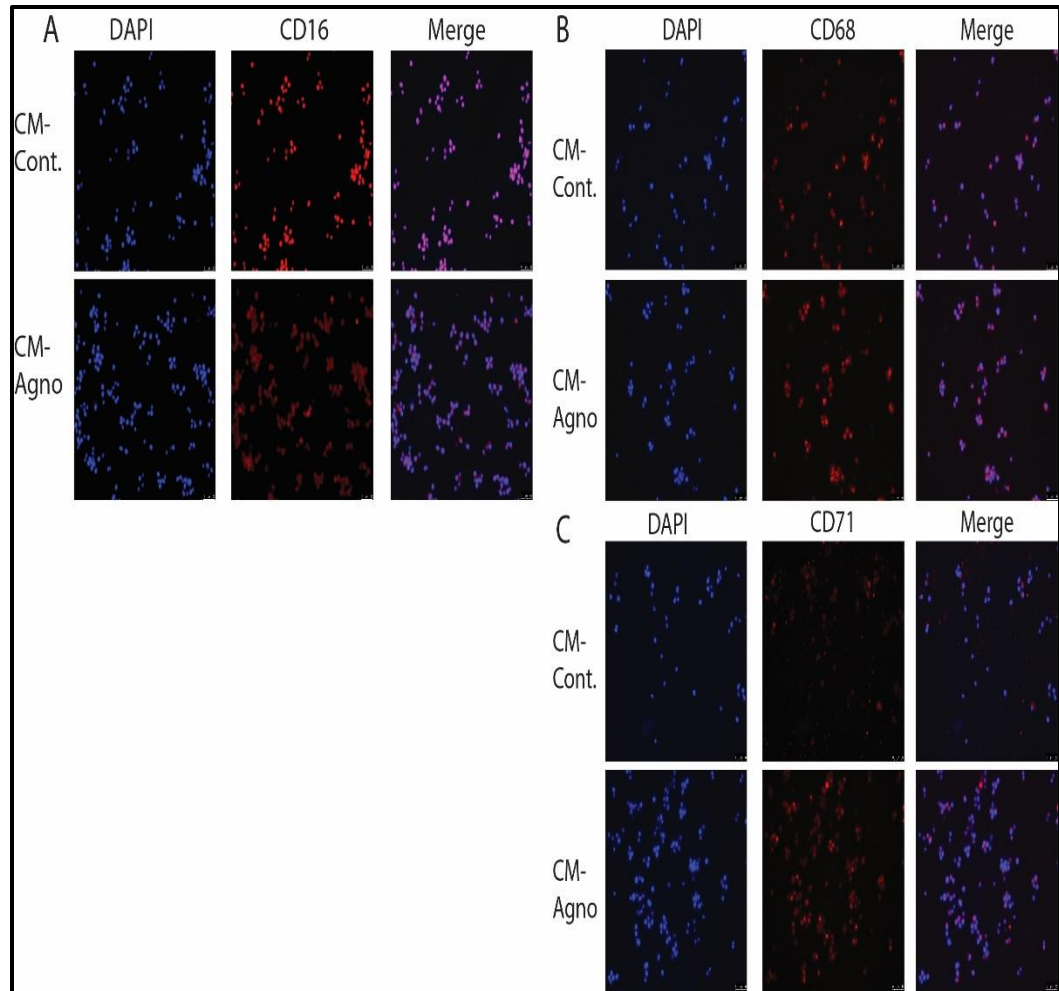


**Figure 33: Agnoprotein Dysregulates U937 Surface Marker Expression.** Immunocytochemistry analysis of U937 pulsed with PMA and treated for 48 hours with CM-control or CM-agnoprotein. At 48 hours, cells were fixed and processed for immunocytochemistry to visualize expression of CD16 (A), CD68 (B), and CD71 (C). Reproduced with permission from Craigie et al, 2017, *Journal of Neuropharmacology*, *in press*.

CM-agnoprotein treated U937 cells expressed significantly reduced CD16 than CM-control treated U937 cells, with the total number of cells being similar (Figure 33, Panel A). For CD68, there appeared to be no difference in the surface marker between CM-control and CM-agnoprotein treatments (Figure 33, Panel B). The expression of CD71 was increased on CM-agnoprotein treated cells as opposed to CM-control treated cells (Figure 33, Panel C). These data suggest that agnoprotein

dysregulates the surface marker expression of macrophages, further supporting previous data that extracellular agnoprotein impacts monocytes.

#### **4.2.10. Extracellular Agnoprotein Suppresses Phagocytosis**

With extracellular agnoprotein suppressing monocyte differentiation and attachment as well as dysregulating surface marker expression, the potential for extracellular agnoprotein to alter monocyte function was assessed. The primary function of macrophages is phagocytosis, a process that is impacted by surface marker expression, including CD14 and CD16 (Nagarajan *et al*, 1995; Schiff *et al*, 1997). To assess phagocytosis, four cell types were used, including U937 cells, U937-derived macrophages, human primary macrophages, and microglia. U937 were plated in a 96-well plate with 100,000 cells per well. After plating, cells were pulsed with 100 ng/mL PMA for 2 hours to induce differentiation from suspension-based monocytes into attached macrophage-like cells and simultaneously treated with CM-control, CM-agnoprotein, MBP, or recombinant agnoprotein for 24 hours. U937-derived macrophages were obtained by plating 100,000 U937 in a 96-well plate and pulsing with 100 ng/mL PMA for 2 hours. After 2 hours, fresh media was added, and the cells were sub-cultured for 3 days until a confluent layer of macrophages was present. After sub-culturing, cells were treated with either CM-control, CM-agnoprotein, MBP, or recombinant agnoprotein for 24 hours. U937-derived macrophages were utilized to ameliorate phagocytosis assay value differences based on a different number of attached cells between conditions. As shown in figures 29 and 30, agnoprotein reduced monocyte differentiation into macrophages, resulting in a reduction of the number of cells present at 72 hours.

To avoid this pitfall, U937 cells were differentiated into macrophages prior to agnoprotein treatments and were denoted as U937-derived macrophages. Human primary macrophages were obtained by plating 100,000 human primary monocytes in a 96-well plate and pulsing with 100 ng/mL PMA for 2 hours. After 2 hours, fresh media was added, and the cells were sub-cultured for 3 days, resulting in a population of macrophages. After sub-culturing, cells were treated with either CM-control, CM-agnoprotein, MBP, or recombinant agnoprotein for 24 hours. Primary human fetal microglia were plated in a 96-well plate with 100,000 cells per well and simultaneously treated with CM-control, CM-agnoprotein, MBP, or recombinant agnoprotein for 24 hours. At 24 hours, media was aspirated and 100  $\mu$ L of fluorescein-labeled *Escherichia coli* K-12 bioparticles was added to the cells and incubated for 2 hours, resulting in phagocytosis of the *E. coli* particles. After 2 hours, *E. coli* particles were removed, and trypan blue was added, which serves to quench extracellular fluorescence of non-phagocytized particles, for one minute. After trypan blue incubation, the fluorescence of each well was determined through 480 nm excitation and 520 nm emission spectra. Fluorescence values were corrected for background readings prior to determination of the net effect of agnoprotein on phagocytosis.

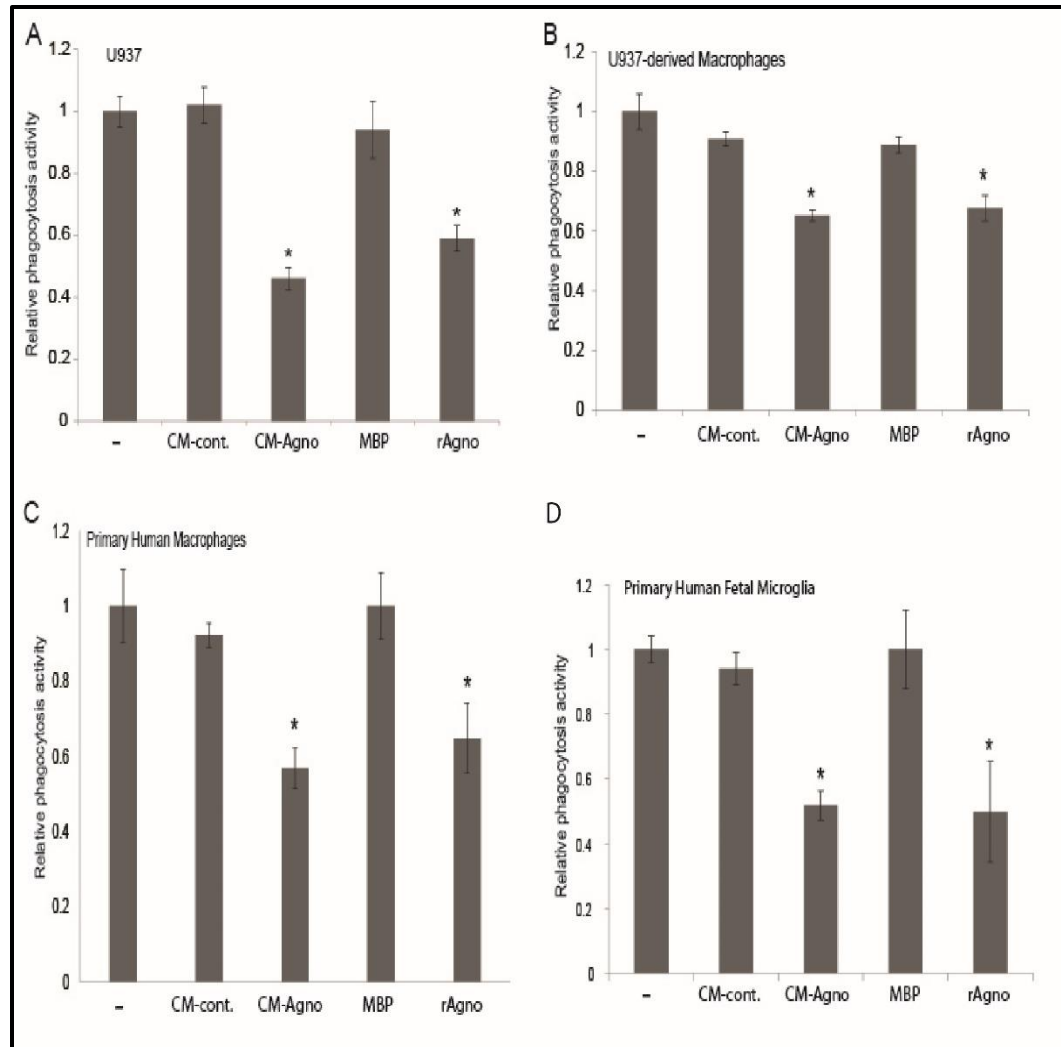


**Figure 34: Agnoprotein Inhibits Myeloid-Derived Cells Phagocytic Ability.** Phagocytosis assay using the Vybrant phagocytosis assay kit. After treatments with fluorescently labeled *E. coli* particles, the fluorescence of U937 cells (A), U937-derived macrophages (B), primary human macrophages (C), and PHFM (D) was assessed to determine the relative amount of *E. coli* particles that were phagocytosed. Fluorescence values were corrected for background fluorescence and normalized to PMA-induced conditions. Reproduced with permission from Craigie et al, 2017, *Journal of Neuropharmacology*, *in press*.

For U937 monocytes, extracellular agnoprotein treatment, through either CM-agnoprotein or recombinant agnoprotein, resulting in a significant reduction of phagocytic activity by 50% on average (Figure 34A). A similar trend was seen for macrophages; however, the suppression was not as strong although it did remain significant, with agnoprotein treatment of both U937 macrophages and human

primary macrophages suppressing phagocytic ability by 40% on average (Figure 34B, 34C). Within the CNS, the prominent macrophage-like cells are microglia. Extracellular agnoprotein treatment of primary human fetal microglia suppressed phagocytic ability by 50% on average (Figure 34D). Together, these data suggest that agnoprotein significantly suppresses the phagocytic ability of myeloid-derived cells *in vitro*.

#### **4.2.11. Extracellular Agnoprotein Decreases Monocyte Migration Across a Blood-Brain Barrier Model in Response to Astrocyte Activation**

Since the hallmark feature of PML is limited inflammation, it was hypothesized that extracellular agnoprotein may leukocyte infiltration to lesions. With previous results showing that agnoprotein suppresses monocyte differentiation, dysregulates surface marker expression, and suppresses phagocytosis, it was proposed that agnoprotein may possess other immunomodulatory functions. To assess the impact of extracellular agnoprotein on monocyte migration, a BBB model was developed. The designed BBB model (Figure 35) utilizes a Corning Transwell™ permeable support for 6-well plates with a 3.0 μm polyester membrane (Corning #3452) to mimic the permeable BBB. This membrane allows for migration of monocytes from the top chamber into the bottom chamber following either astrocyte activation.

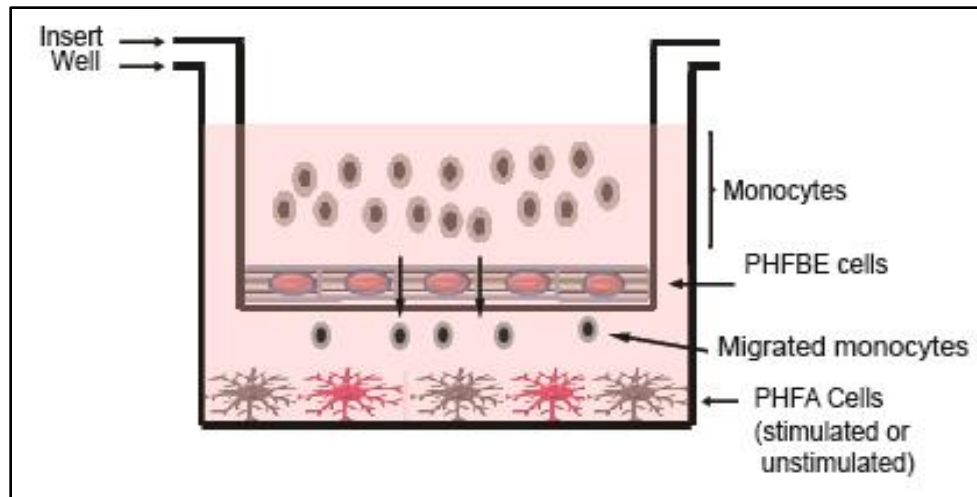


**Figure 35: Blood-Brain Barrier Model.** A schematic representation of the blood-brain barrier model used for PBMC and monocyte migration assays.

Within the BBB model, PHFA were seeded at 250,000 cells per well in a 6-well tissue culture dish and cultured for 48 hours. Simultaneously, 250,000 PHFBE were seeded onto Transwell permeable supports in a separate 6-well tissue culture dish and grown for 48 hours until developing a confluent layer mimicking the BBB. The first requirement was to determine background leukocytic migration through the model. As serum in the media can activate astrocytes at low levels to induce monocyte migration, differences in migration were assessed between normal (10%) and low (3%) serum medias. After 48 hours, the PHFA media was replaced with either normal serum media or low serum media and the permeable supports were added into the PHFA-seeded wells, resulting in co-cultured wells containing astrocytes and brain endothelial cells. Simultaneously, two wells containing normal medium were treated with CM-control or CM-agnoprotein to assess migration in the presence of agnoprotein. After treatments, 1,000,000 PBMCs were added into

the top portion of model system and migration was assessed at 6, 24, and 48 hours through cell counting.

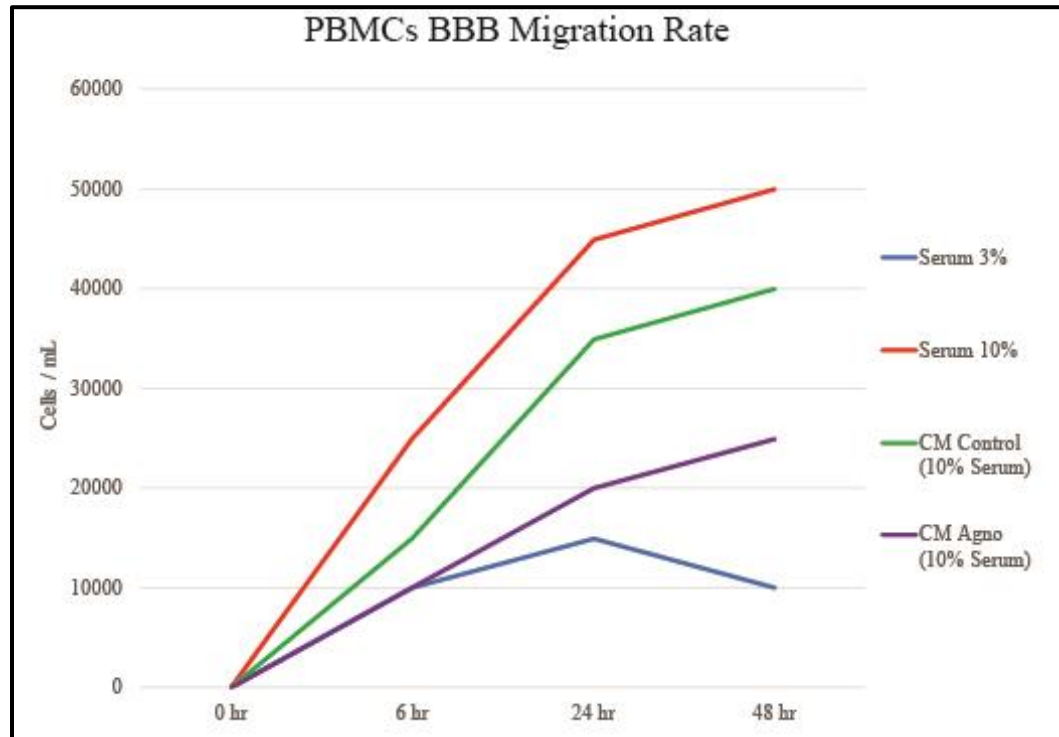


**Figure 36: Serum Induces PBMC Migration across the BBB Model.** PBMC migration assay using the pre-described BBB-model. Differences in PBMC migration between 10% serum (red), 10% serum with CM-control (green), 10% serum with CM-agnoprotein (purple), and 3% serum (blue) treatments were assessed at 6, 24, and 48 hours and graphed. Reproduced with permission from Craigie et al, 2017, *Journal of Neuropharmacology*, *in press*.

The model system containing only normal serum media yielded the highest rates of migration, with upwards of 50,000 cells per mL migrating at the 48-hour time point.

The model system containing low serum media yielded the lowest rates of migration, with only 10,000 cells per mL migrating at the 48-hour time point. When comparing CM-control and CM-agnoprotein treated wells, the CM-control well had migration rates similar to the normal serum media, with an average of 45,000 cells per mL having migrated by the 48-hour time point. Interestingly, CM-agnoprotein treatment suppressed PBMC migration in response to low level astrocyte

activation, with an average of 25,000 cells per mL migrating (Figure 36). These data suggest that the serum concentration within the media impacts migration rates, resulting in the use of 3% serum media for other iterations of the BBB-model.

After determination that agnoprotein impacts PBMC migration, the focus was shifted towards monocyte migration following the activation of astrocytes based on previous data suggesting that agnoprotein impacts GM-CSF, thus leading to the hypothesis that monocytes are the primary PBMC cell type impacted by extracellular agnoprotein. During PML, there is widespread tissue damage which would, in theory, activate astrocytes, resulting in the release of pro-inflammatory cytokines and leukocyte infiltration. In PML, leukocyte infiltration is not generally observed, leading to the hypothesis that extracellular agnoprotein impacts astrocyte activation or cytokine release, resulting in the suppression of infiltration. To assess this, the BBB-model was used as described above. Within this migration assay, human monocytes purified from whole blood was used in place of the entire leukocyte fraction of whole blood. To induce monocyte migration, primary human fetal astrocytes were activated with LPS as previously described (Gorina *et al*, 2011; Li *et al*, 2016; Tarassishin *et al*, 2014). Since monocytes are non-adherent cells, migrated monocytes remained in suspension, allowing for counting migrated cells in the media. However, the process of monocyte migration and astrocyte activation both serve to induce monocyte differentiation into adherent macrophages, thus phase contrast images furthered the assessment of the total number of migrated cells.

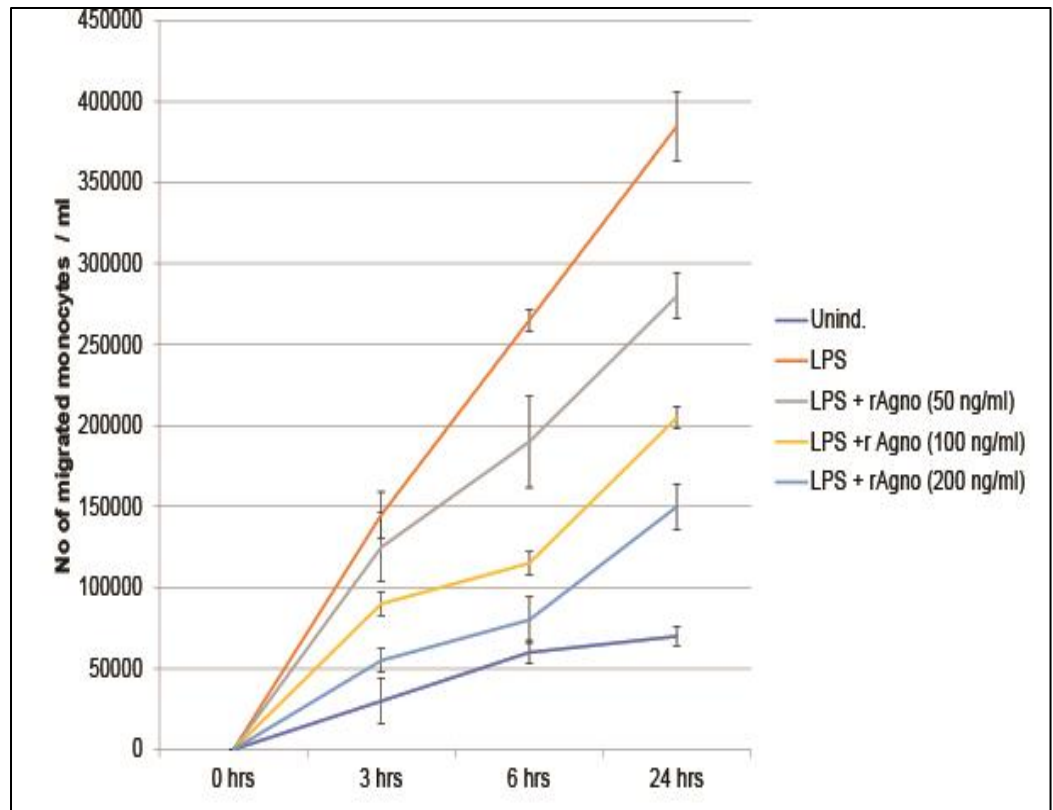


**Figure 37: Agnoprotein Decreases Monocyte Migration across the BBB Model.** Monocyte migration assay using the pre-described BBB-model. Differences in monocyte migration following LPS-activation of PHFA and LPS-activated PHFA treated with recombinant agnoprotein were assessed by cell counting at 3, 6, and 24 hours. The experiment was completed in triplicate and averages and standard deviations were calculated and graphed. Reproduced with permission from Craigie et al, 2017, *Journal of Neuropharmacology*, *in press*.

Without LPS activation, there was a minimal level of background monocyte migration through the transwell support. At 24 hours, the background count for migration was 50,000 cells per mL. When astrocytes were activated with LPS treatments, monocyte migration was significantly increased, with an average of 400,000 cells per mL migrating during the 24-hour time course. These data demonstrated that astrocyte activation induces monocyte migration through the designed BBB-model. When LPS-activated astrocytes were treated with recombinant agnoprotein there was a dose-dependent decrease in monocyte

migration. At the lowest concentration of agnoprotein, 50 ng/mL, monocyte migration was reduced to less than 300,000 cells per mL, representing a 25% decrease in cellular migration. With 100 ng/mL of agnoprotein, monocyte migration was 200,000 cells per mL, representing a 50% decrease in cellular migration from the LPS only condition. With the highest concentration of extracellular agnoprotein, 200 ng/mL, monocyte migration was reduced to 150,000 cells per mL, representing a 66% decrease in cellular migration (Figure 37). Experiments were completed in triplicate and the average monocyte migration was calculated. Taken together, these results suggest that extracellular agnoprotein functions decreases monocyte migration in response to astrocytic activation.

#### **4.2.12. Immunohistochemical Analysis of PML Lesions for Agnoprotein, VP-1, and GM-CSF**

The presented *in vitro* data suggests that agnoprotein is released from oligodendrocytes and internalized by astrocytes and microglia, resulting in the suppression of GM-CSF transcription and expression. Additionally, agnoprotein decreased monocyte migration in response to a model of neuroinflammation. To validate this data *in vivo*, immunohistochemical analysis of PML lesion sites kindly provided by the Manhattan HIV Brain Bank headed by Susan Morgello, M.D., and normal brain frontal cortex tissue samples were kindly provided by the Comprehensive NeuroAIDS Core Facility at the Lewis Katz School of Medicine of Temple University headed by Kamel Khalili, Ph.D. were completed.

Tissue samples from 3 AIDS+PML+ patients were provided, denoted MHBB #547, MHBB #624, and MHBB #010084. The provided tissue samples were paraffin embedded and subsequently sectioned at 5.0  $\mu\text{m}$  and mounted prior to immunohistochemical staining.

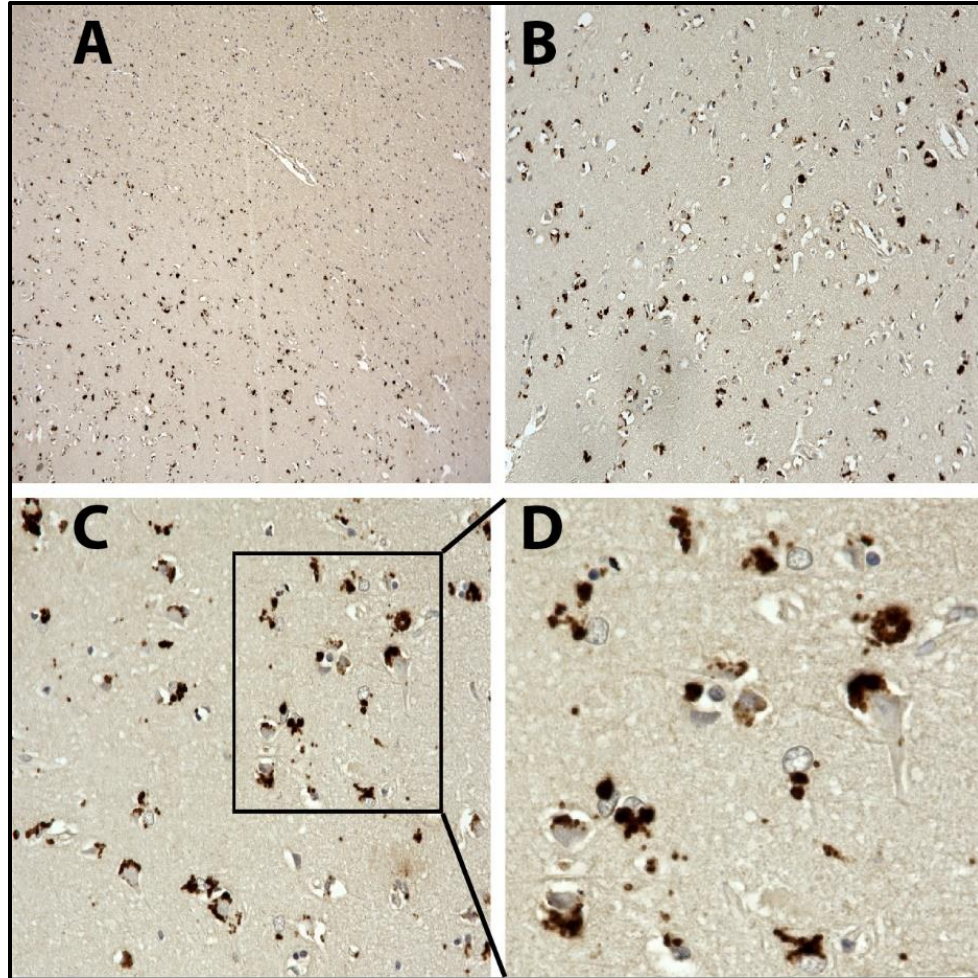


**Figure 38: GM-CSF Histology in Normal Frontal Cortex.** Normal brain frontal cortex sections were prepared and immunohistochemically analyzed for GM-CSF expression. Magnifications are 10x (**Panel A**), 20x (**Panel B**), and 40x (**Panel C**). Panel D is an increased zoom of the section denoted by the rectangle in Panel C.

To confirm the *in vitro* data that agnoprotein was released from infected cells, lesion sites were stained for the JCV viral capsid protein VP1, agnoprotein, and

GM-CSF in addition to hematoxylin and eosin staining. Since VP1 is only present within JCV infected cells, this staining pattern allows for the identification of cells surrounding lesion sites that are actively infected with JCV. Additionally, GM-CSF levels were analyzed to determine if cells around PML lesions expressed reduced GM-CSF as the *in vitro* data suggests.

Initially, normal frontal cortex sections were processed to assess basal GM-CSF staining within the brain. The sections were de-paraffinized and stained with anti-GM-CSF primary antibody and developed using the DAB chromogen system, producing a vibrant brown signal. GM-CSF staining was characterized as associated with cell bodies throughout the cortex (Figure 38). At 40x magnification, GM-CSF staining shows a punctate pattern and limited background staining (Figure 38C and 38D).

When analyzing the lesion sites within the donated PML-positive tissue sections, donor MHBB #547 had the most defined lesion sites, presenting with two large lesions, denoted lesion site A and lesion site B, with significant agnoprotein and VP1 staining (Figure 39). Lesion site A was observable macroscopically through the wide-spread cell loss, observable at both 2x magnification (Figure 39, panels A-D). When assessing agnoprotein, a strong signal is observed surrounding the lesion site, with significant cellular-association in addition to a dispersed staining pattern, possibly corresponding to extracellular agnoprotein (Figure 40, 10x and 40x magnification, panel A). For GM-CSF levels for lesion site A, imaging shows

limited staining surrounding the lesion site, suggesting that although cells are infected with JCV and there is significant cell death at the lesion, there is limited expression of GM-CSF, especially compared to the control normal frontal cortex GM-CSF staining pattern (Figure 40, 10x and 40x magnification, panel B). While agnoprotein staining is robust around the lesion site, there are significantly less VP-1 positive cells surrounding the lesion (Figure 40, 10x and 40x magnification, panel C). As previously mentioned, VP-1 positive cells correspond to productively infected cells, primarily oligodendrocytes, allowing for quantification of the number of JCV infected cells at the lesion site.

For lesion site A, there were 60 cells characterized as agnoprotein positive compared to 25 cells characterized as VP-1 positive (Figure 40, 10x magnification, panel A and C). As shown *in vitro* (Figures 22-24), these results suggest that agnoprotein may be released from infected cells and internalized by uninfected VP-1 negative cells. The hematoxylin and eosin staining for lesion site A shows marked cellular decrease within the lesion in addition to potential leukocytic infiltration in the center of the demyelinated lesion (Figure 40, 10x and 40x magnification, panel D).

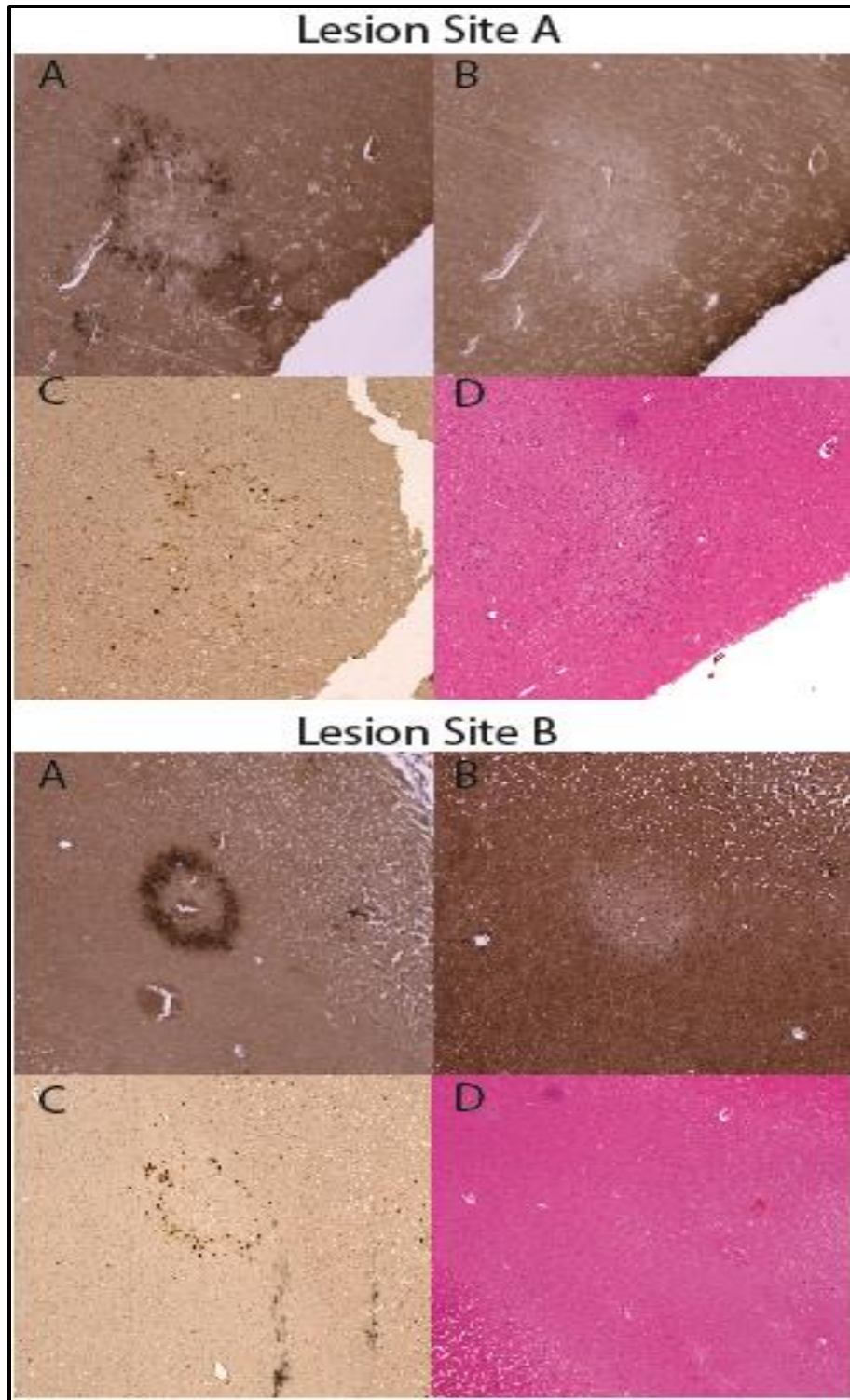


**Figure 39: Agnoprotein, GM-CSF, VP-1, and H&E Histology for PML Brain MHBB #547 Lesion Sites A and B.** Lesion site A in MHBB #547 was identified and assessed for expression of viral proteins agnoprotein (**Panel A**), GM-CSF (**Panel B**), VP-1 (**Panel C**), and stained for H&E analysis (**Panel D**). Lesion site B in MHBB #547 was identified and assessed for expression of viral proteins agnoprotein (**Panel E**), GM-CSF (**Panel F**), VP-1 (**Panel G**), and stained for H&E analysis (**Panel H**).

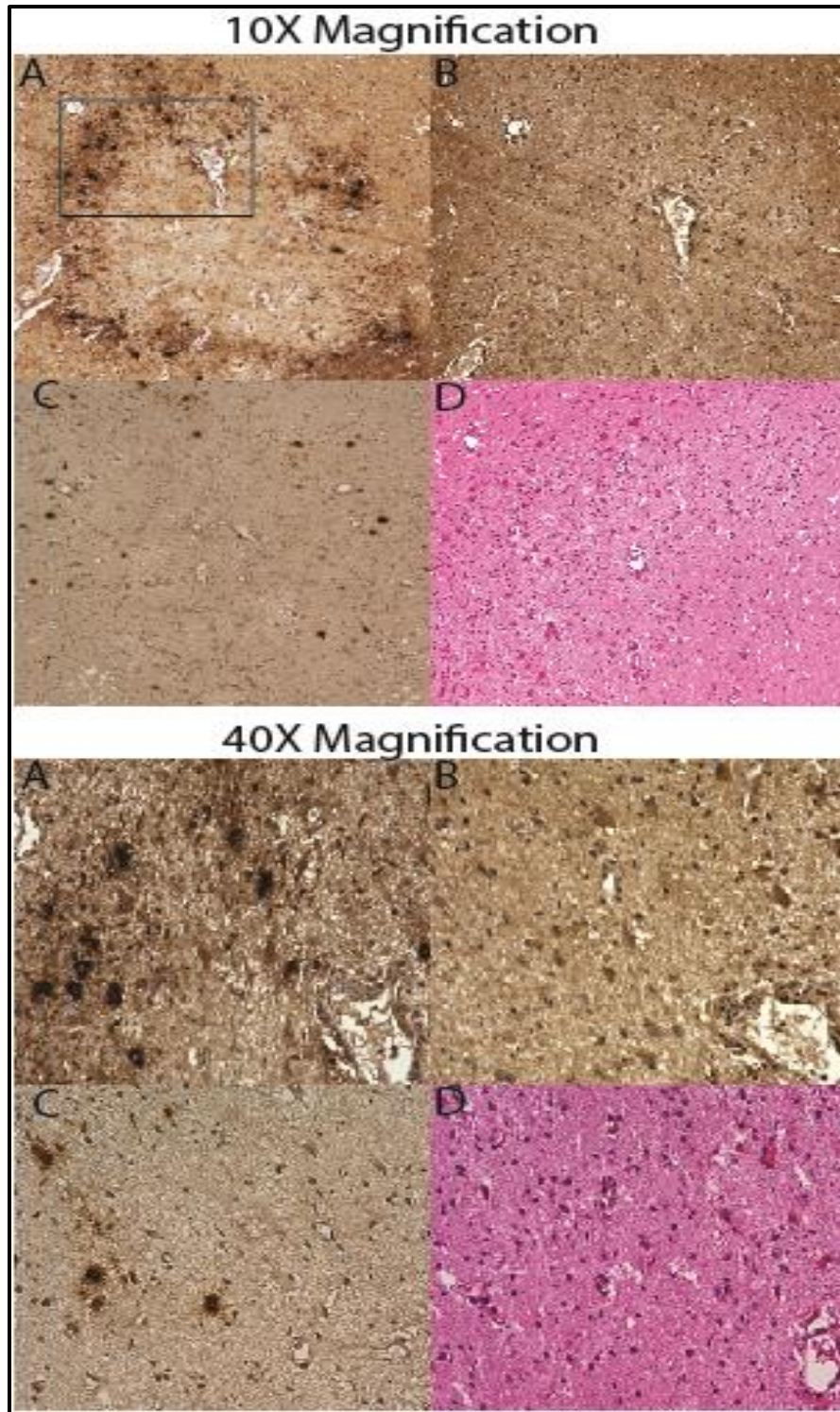


**Figure 40: Agnoprotein, GM-CSF, VP-1, and H&E Histology for PML Brain MHBB #547 Lesion Site A.** Lesion site A in MHBB #547 was identified and assessed for expression of viral proteins agnoprotein (10x and 40x magnification, Panel A), VP-1 (10x and 40x magnification, Panel C), GM-CSF (10x and 40x magnification, Panel B), and stained for H&E analysis (10x and 40x magnification, Panel D). The black rectangle denotes the area corresponding to the 40x magnification images for all sections.

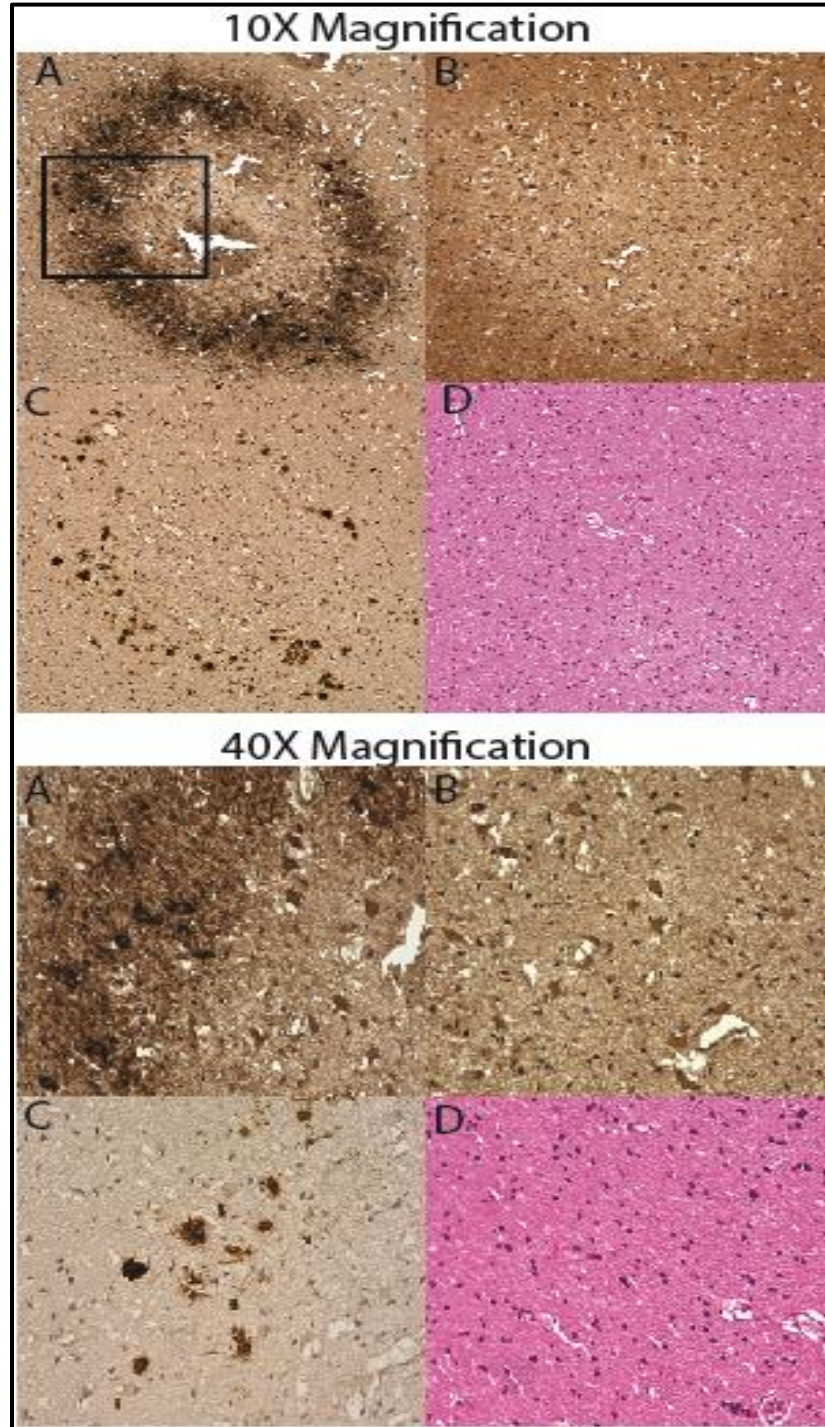


**Figure 41: Agnoprotein, GM-CSF, VP-1, and H&E Histology for PML Brain MHBB #547 Lesion Site B.** Lesion site A in MHBB #547 was identified and assessed for expression of viral proteins agnoprotein (10x and 40x magnification, **Panel A**), VP-1 (10x and 40x magnification, **Panel C**), GM-CSF (10x and 40x magnification, **Panel B**), and stained for H&E analysis (10x and 40x magnification, **Panel D**). The black rectangle denotes the area corresponding to the 40x magnification images for all sections.

Lesion site B presented overall with a similar staining pattern to lesion site A (Figure 39, panels E-H). Overall, there was a significant loss of cells within the lesion site with agnoprotein forming a border around the lesion, with both cell-localized and non-cell localized staining patterns (Figure 41, 10x and 40x magnification, panel A). For GM-CSF levels for lesion site B, imaging shows limited staining surrounding the lesion site, suggesting that although cells are infected with JCV and there is significant cell death at the lesion, there is limited expression of GM-CSF (Figure 41, 10x and 40x magnification, panel B). Likewise, VP1-positive cells were fewer than agnoprotein positive cells, once again suggesting that agnoprotein may be released from infected cells and internalized by uninfected cells (Figure 41, 10x and 40x magnification, panel A and C). The hematoxylin and eosin staining for lesion site B shows potential leukocytic infiltration in the center of the demyelinated lesion, with the potential infiltrating leukocytes being GM-CSF positive (Figure 41, 10x and 40x magnification, panel B and D). In combination, these *in vivo* data support the *in vitro* conclusions that were made, primarily that agnoprotein is released from infected cells and internalized by uninfected cells and that agnoprotein suppresses GM-CSF release and expression around lesion sites.

### **4.3. Discussion**

The human immune system possesses two primary response pathways for eliminating pathogens from the body, cell-mediated immune responses or humoral-mediated immune pathways. Cell-mediated immunity is driven by the activation of phagocytes, such as monocytes and neutrophils, the function of T-lymphocytes,

primarily CD8+ cytotoxic T-cells, and cytokine release in response to the presence of the pathogen. Humoral immunity is driven by B cells, but in general refers to immune control of pathogens through antibodies or complement proteins.

In regard to JC virus, cellular immunity pathways are the primary regulators of viral reactivation in a majority of the population (Koralnik, 2002). Both JCV reactivation and PML development generally presents within immunosuppressed patients, either with co-morbidities depleting T-cell function or pharmacological interventions targeting leukocyte migration into the CNS to prevent immune function, although PML development can occur within patients with immune recovery and function (Crossley *et al*, 2016; Koralnik, 2002; Sethi *et al*, 2012; Weber F. *et al*, 2001; Weber T. *et al*, 2001). The most prevalent example of cellular immune suppression leading to JCV reactivation and PML development can be found in AIDS patients, in which the virus targets CD4+ T-cells and macrophages, resulting in large scale cell loss (Berger *et al*, 2001).

As previously mentioned, one of the histological hallmarks of PML is limited leukocyte infiltration to lesions and the overall lack of inflammation, contrasting what is expected with multifocal demyelination and the resulting tissue damage from a lytic infection (Cinque *et al*, 2009; Koralnik, 2002; Santa Cruz *et al*, 2016; Richardson *et al*, 1961; von Einsiedel *et al*, 1993). However, JCV is also the etiologic agent of other diseases, including the inflammatory JC virus encephalopathy (Dang *et al*, 2012; Wüthrich *et al*, 2009). JCVE results from the productive infection of cortical pyramidal neurons, resulting in necrosis at the gray

matter-white matter junction and inflammation. The JCV strain isolated from a JCVE patient revealed a 143 base pair deletion in the agnoprotein gene, resulting in the production of a truncated peptide. While no published data has assessed the functional domain of agnoprotein required for the immunomodulatory effect described herein this thesis, we hypothesize that the deletion in the agnoprotein gene of the JCVE isolate results in disruption of the functional domain. If the hypothesis that agnoprotein suppresses inflammation during PML is valid, then the inflammation seen within JCVE may be partly explained by the mutant agnoprotein peptide. Further studies are required to completely identify functional domains within the agnoprotein protein, especially regarding its immunomodulatory function. Our data suggests that the truncated peptide found in JCVE isolate strains lacks the domains required for immunomodulation, however, studies must be completed to validate that hypothesis.

Viral proteins serving an immunomodulatory role can be found throughout literature, with the neurotropic rabies virus serving as an example. Similar to JCV, rabies virus is neurotropic and preferentially infects the CNS, although rabies infects neurons as opposed to oligodendrocytes for JCV. After the initial viral entry into the body, rabies infects muscular tissue and initiates low levels of viral replication due to muscle tissue not being a productive infection site. The virus eventually reaches muscle-associated motor endplates through binding with acetylcholine receptors, resulting in viral entry into the peripheral nervous system and trafficking to the CNS via motor neurons (Gluska *et al*, 2014; Hemachudha *et*

*al*, 2013). Within the CNS, the virus replicates within neurons, leading to the production and release of the rabies virus phosphoprotein. Neighboring cells internalize the phosphoprotein where it suppresses the transcription of many antiviral genes, including the interferons ( $\alpha$ ,  $\beta$ ,  $\gamma$ ) and myxovirus resistance protein 1, within both infected and uninfected cells (Scott *et al*, 2016; Srithayakumar *et al*, 2014).

Rabies virus release of phosphoprotein appears analogous to JC virus release of agnoprotein in terms of modulating the immune response to the infectious cycle. Our data revealed that agnoprotein is released from cells in a process not mediated by cell death and internalized by non-infected glial cells, serving to decrease the transcription and expression of GM-CSF, a cytokine with antiviral functions against JCV infection. Our data also reveals that agnoprotein treatments suppress the function of myeloid-derived cells, particularly through inhibiting monocyte differentiation, phagocytosis, and decreasing migration in response to activated glial cells. Through the presented data, a model was developed in which extracellular agnoprotein-mediated suppression of GM-CSF serves to induce evasion of the immune response through reduction in peripheral monocyte infiltration to PML lesions (Figure 42).

The neuroinflammatory process is the host response to a myriad of CNS insults, including infectious pathogens, such as measles, herpes, and HIV, through autoimmune diseases of the CNS, such as MS, or through traumatic brain injury

(Gendelman 2002). However, as the CNS requires a precisely tuned microenvironment as to not permanently damage long-living cell types, such as neurons, there is a fine balance in the neuroinflammatory response, with high levels of activation resulting in widespread tissue damage and destruction, such as the case of meningitis, and with too low levels of activation not clearing the inflammation-inducing agent. The immune system has many mechanisms to induce neuroinflammation, with one primary mechanism being the release of CCL2/MCP-1 within the CNS (Conductier *et al*, 2010). During neurodegenerative diseases and neuroinflammation, monocytes are primarily recruited into the CNS to sites of tissue damage, with monocyte recruitment mediated by monocyte chemoattractant proteins, primarily CCL2/MCP-1 (Conductier *et al*, 2010).

An example of a CCL2/MCP-1 driven disease state is HIV-associated dementia (HAD). During primary HIV infection, viral particles enter the brain through either migration within infected lymphocytes or monocytes across the BBB or through free viral particle entry into the cerebral spinal fluid (CSF) and eventual migration into the brain (Booss *et al*, 1987; Eggers *et al*, 2017). With CNS entry, a potential complication is the development of HAD, an inflammatory condition characterized by HIV encephalitis (HIVE) and astrogliosis (Price *et al*, 1988; Price and Brew, 1988). For clinical prognosis, the severity of HAD/HIVE is correlated monocyte infiltration into the CNS, where the migrated monocytes produce neurotoxic agents including pro-inflammatory cytokines, free radicals, and nitric oxide (Glass *et al*, 1995; Kaul *et al*, 2001). It was shown that HIV TAT protein upregulates

CCL2/MCP-1 production, resulting in the increased monocyte migration observed during HAD/HIVE (Cinque *et al*, 1998; Conant *et al*, 1998). Notably, PHFA are the primary cell type in HAD/HIVE that express increased CCL2/MCP-1 production (Conant *et al*, 1998; Lehmann *et al*, 2006). Since PML occurs primarily in AIDS patients, CCL2/MCP-1 was also assessed as a potential cytokine target of extracellular agnoprotein, especially since CCL2/MCP-1 induces monocyte migration into the CNS. Our results show that extracellular agnoprotein does not suppress CCL2/MCP-1 release, yet whether it has any impact on CCL2/MCP-1 mediated pro-inflammatory signaling remains to be determined.

These results demonstrated a novel immunomodulatory function of extracellular agnoprotein within the CNS to limit monocyte migration through the BBB.

## CHAPTER 5

### CONCLUSIONS AND FUTURE DIRECTIONS

#### 5.1. Conclusions

To summarize, the first part of this thesis focused on viral protein interactions with host factors, primarily SRSF1. Our results have elucidated a novel role of T-antigen in rescuing SRSF1-mediated suppression of JCV gene expression within glial cells (Figure 42). Initially, JCV enters the body and infects permissive cells, characterized by the presence of sialic acid-associated receptors or serotonin receptors, allowing for VP1 binding to the receptor and endocytosis of the viral particle. After the virus is endocytosed, it is transported through the cell, resulting in viral genome nuclear transport. Within the nucleus, without any negative cellular regulation, viral genes are transcribed and subsequently spliced and translated into the viral proteins. However, viral transcription and splicing is negatively regulated by the host cellular splicing factor SRSF1 (Sariyer and Khalili, 2011; Sariyer IK *et al*, 2016; Sariyer R *et al*, 2016; Uleri *et al*, 2011; Uleri *et al*, 2013). Immune system functional changes can alter SRSF1 expression within the cells, serving as a mechanism for viral transcription and replication to occur, even in the presence of SRSF1, albeit at low levels. Our data suggests that once T-antigen is expressed, it rescues SRSF1-mediated suppression of both viral early and late gene transcription. As the model suggests, T-antigen is expressed and then functions to inhibit the anti-viral effects of SRSF1, including negative regulation of viral transcription and splicing. Our data suggests that T-antigen interacts with the SRSF1 promoter to suppresses SRSF1 transcription, ultimately reducing SRSF1 protein expression

within infected cells. This suppression allows JCV transcription, splicing, and translation to occur without inhibition, resulting in eventual cellular inundation with viral particles, leading to cellular lysis and the focal lesions observed in PML.

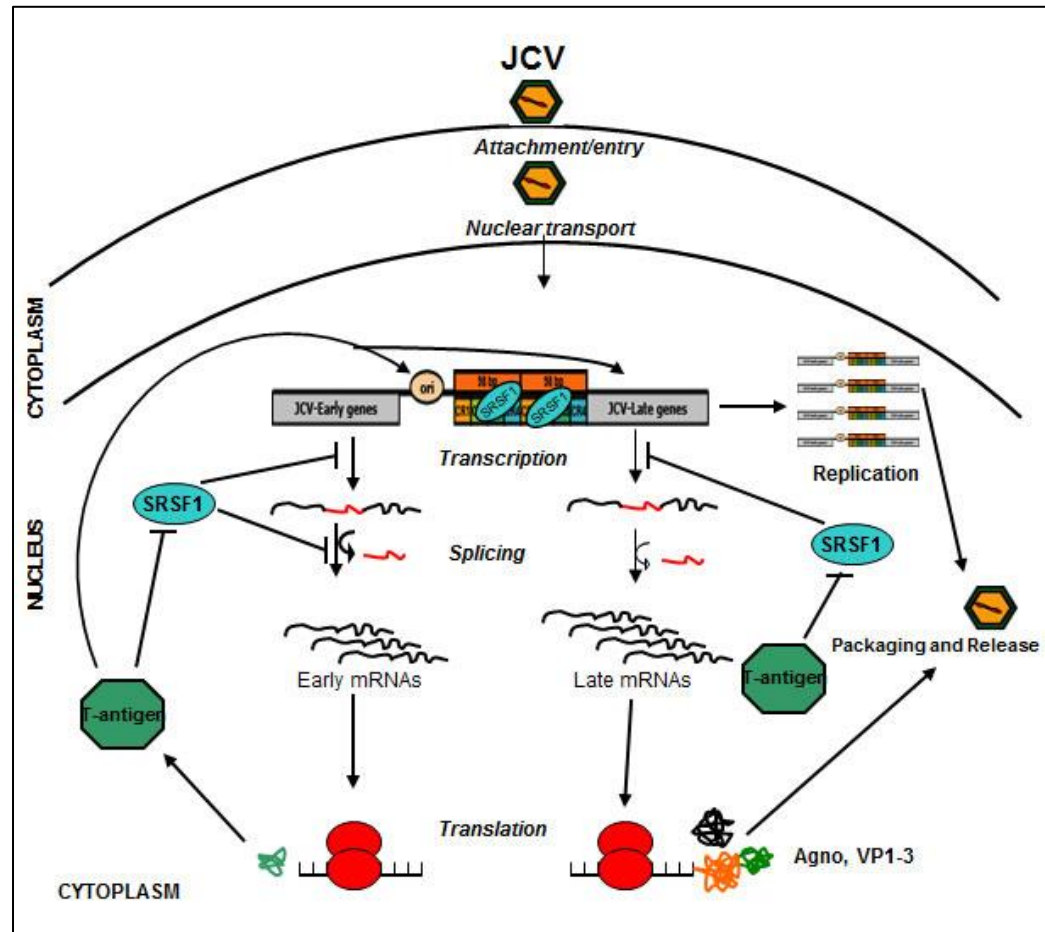


**Figure 42: Molecular Interplay between T-antigen and SRSF1 in Regulation of JCV Transcription and Gene Splicing.** Schematic representation of the interactions between SRSF1 and T-antigen in regulation of JCV transcription and early gene splicing.

The second part of this thesis focused on viral protein interactions with the immune system, primarily via agnoprotein release by infected glial cells. Our results elucidated a novel immunomodulatory role of extracellular agnoprotein during JCV infection within the CNS (Figure 43). After initial infection, JCV remains latent within the body at peripheral sites as well as potentially within the brain (Degener

*et al*, 1997; Tan *et al*, 2010). In the healthy population, the immune system controls viral reactivation through prototypical anti-viral functions, including potent suppression of viral replication by interferon gamma (De Simone *et al*, 2015). Within this thesis, we propose that T-antigen expression drives viral transcription and downstream viral protein expression through inhibition of the anti-viral functions of SRSF1. After agnoprotein is expressed in infected cells, it is released into the extracellular space, resulting in uptake by uninfected glial cells (Otlu *et al*, 2014). Since the hallmark pathological feature of PML is characterized as the focal destruction of myelin due to lysis of infected oligodendrocytes, we hypothesize that the widespread tissue damage should activate astrocytes, resulting in proinflammatory signaling, including the release of GM-CSF to induce monocyte migration to sites of tissue damage. We propose that the uptake of extracellular agnoprotein by uninfected cells results in suppression of GM-CSF release, thus decreasing monocyte chemoattraction to sites of tissue damage within PML lesions. Additional functional assays revealed that agnoprotein suppresses many functions of monocytes, including monocyte differentiation into macrophages, phagocytosis of myeloid-derived cells, including microglia, and surface marker expression, leading to a dysregulated macrophage phenotype. Taken together, these data elucidate a novel mechanism of agnoprotein during JCV infection and potentially reveal a major mechanism explaining the limited leukocyte infiltration and inflammation observed in a majority of PML patients.

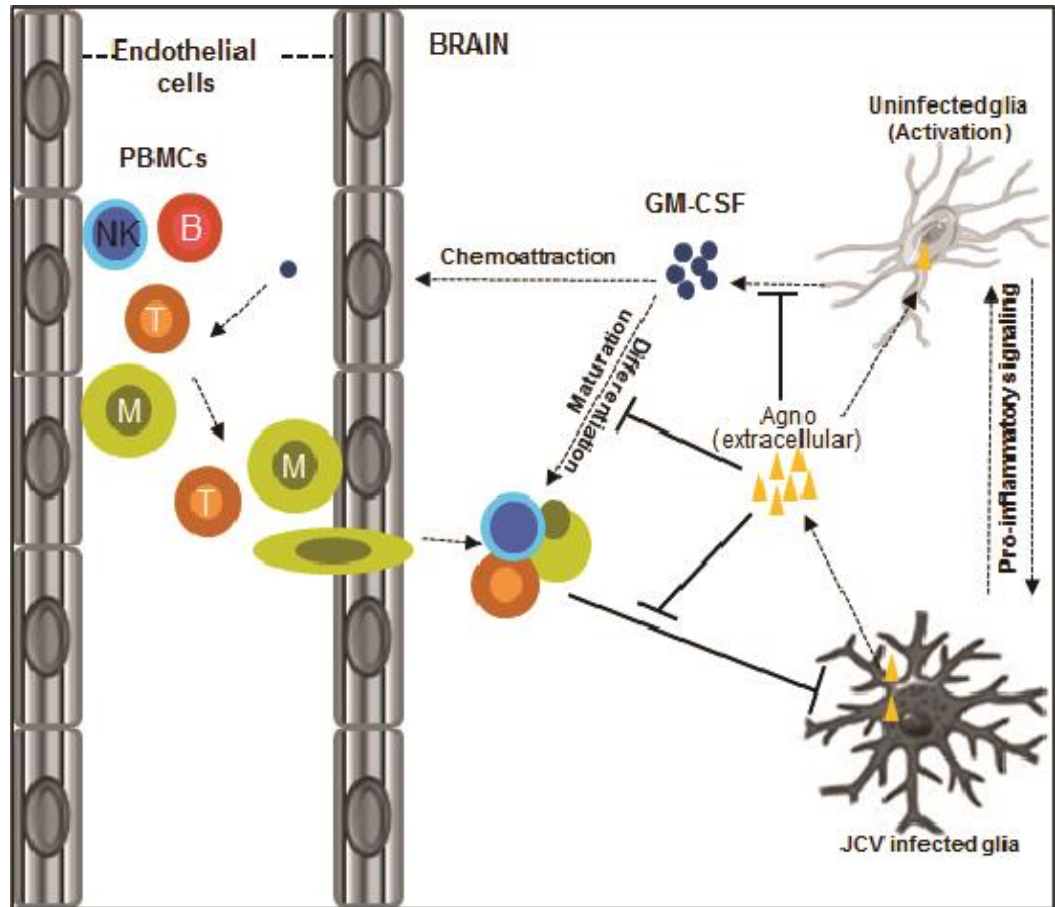


**Figure 43: Role of Extracellular and Intracellular Agnoprotein in the Neuroimmune Response to JC Virus.** Schematic representation of the interactions between extracellular agnoprotein and GM-CSF in regulation of leukocyte infiltration and monocyte maturation within the CNS in response to JCV infection.

## 5.2. Future Directions

When assessing JCV reactivation, the major unknown is the exact process of viral reactivation. The question “what is required to induce or inhibit viral reactivation?” remains at the forefront of JCV research. From a general perspective, one would propose that normal immune function inhibits viral reactivation, yet it is inevitably more complicated than solely immune system control. Analyzing cases of PML underlies this statement, in which it is possible to broadly look at the risk factors for PML development, such as AIDS or those on monoclonal antibody therapies.

For example, AIDS patients are the primary population in which PML development occurs, however it is not yet possible to predict which HIV patients will develop PML and why. One could hypothesize that immune cell counts, primarily the CD4+ T-cell count, would be correlated with PML risk, yet no data supports this conclusion (Crossley *et al*, 2016). Since JCV infection is in such a high percentage of PML high risk populations, the major question becomes why does patient A develop PML while patient B, with the same underlying conditions and the same JCV infection, not develop PML. The prevailing hypothesis is that the immune system is not the only regulatory of JCV, with a wide variety of other “non-immunological” factors affecting viral reactivation.

To further elucidate the mechanisms of JCV reactivation, we propose a wide variety of exploratory experiments designed to further isolate the exact controllers of viral reactivation. The first proposed experimental plan focuses on potential genetic predispositions to JCV, which could serve to additionally identify potential negative regulators of the virus. As previously mentioned, between 3-5% of the HIV/AIDS positive population develops PML. Presently, the genetic differences between the population that develops PML and the population that does not develop PML are not understood. There potentially exists differences between these populations, with mutations within discovered or potential negative regulators of JCV, thus ameliorating their suppressive functions, could be assessed through a genome-wide association study. Briefly, we could compare the genomes of PML patients to non-PML patients with the same underlying conditions, whether it be

AIDS or multiple sclerosis, as well as PML patients with differing underlying conditions, to determine mutations or expression profiles that are significantly correlated with the development of PML. This data may potentially elucidate novel proteins or signaling pathways that control JCV reactivation.

Likewise, it would be pertinent to further analyze agnoprotein modulation of the GM-CSF signaling pathway. The data presented herein demonstrates that extracellular agnoprotein significantly modulates GM-CSF production, thereby potentially regulating or impacting the GM-CSF signaling pathway. A novel analysis of the GM-CSF signaling pathway via digital droplet PCR (ddPCR) would elucidate any alterations within this signaling pathway. Additionally, ddPCR could be used to assess colony stimulating factor 1 (CSF1), also called macrophage colony stimulating factor (M-CSF), promoted macrophage differentiation as a potential target of extracellular agnoprotein. While extracellular agnoprotein did not significantly alter CSF-1 levels in the cytokine array, our data suggests that agnoprotein does significantly modulate monocyte to macrophage differentiation. When regarding monocyte to macrophage differentiation and macrophage function, a prevalent hypothesis that exists is the existence of two primary macrophage subpopulations, denoted M1-like macrophages and M2-like macrophages (Hamilton 2008) (Figure 44). During normal homeostatic conditions within tissues, macrophages tend to exist in the M2-like phenotype, which is regulated by M-CSF signaling (Hamilton 2008). M2-like macrophages typically function in tissue repair and scavenging and are anti-inflammatory (Stanley *et al*, 1997). However, when

homeostasis is interrupted, as is the case during viral infections and inflammation, the M2-like macrophages are exposed to pro-inflammatory cytokines, and the switch to the M1-like phenotype is driven by GM-CSF in addition to interferon gamma and LPS. The M1-like macrophages continue to drive the inflammatory state through expression of proinflammatory cytokines, such as tumor necrosis factor alpha (TNF- $\alpha$ ), IL23, and IL12 (Fleetwood *et al*, 2007; McKenzie *et al*, 2006).

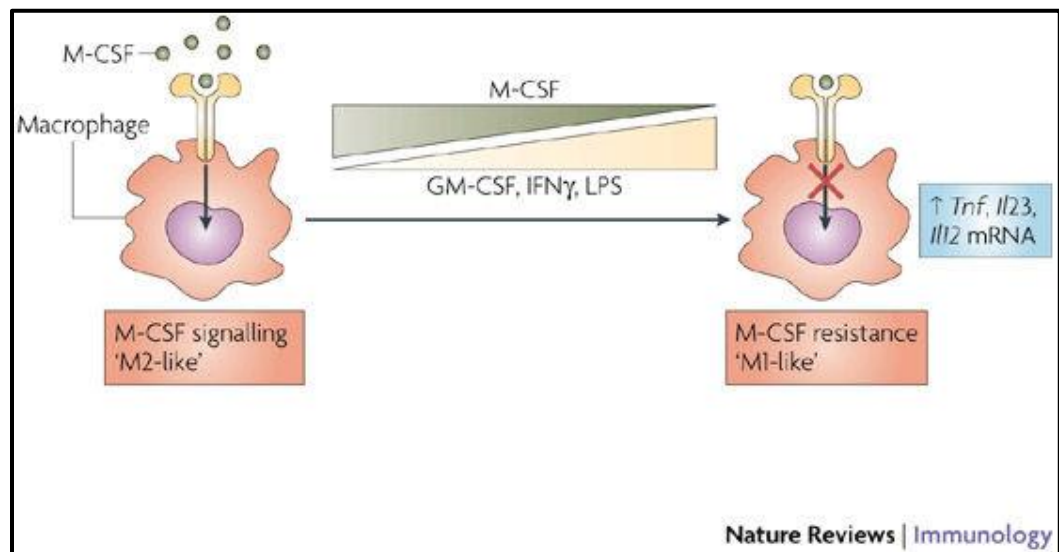


**Figure 44: Impact of M-CSF and GM-CSF on Macrophage Phenotypes.** Under normal conditions, macrophages are typically exposed to M-CSF, resulting in an M2-like phenotype, which can be described as “anti-inflammatory” or “repair” oriented. However, during inflammatory conditions, GM-CSF release polarizes macrophages to an M1-like phenotype, resulting in the expression of pro-inflammatory cytokines. (Reproduced with permission from Hamilton 2008 and Nature Publishing Group).

Our hypothesis is that agnoprotein decreases GM-CSF expression, shifting macrophages towards an M-CSF regulated, or an M-2 like, phenotype. Since CSF-1 promoted macrophage differentiation acts through the M-CSF receptor, we propose that differences would exist within the CSF1-promoted macrophage

differentiation pathway between agnoprotein treated macrophages and non-treated macrophages (Kharbanda *et al*, 1995; Rohrschneider *et al*, 1997). This data may potentially elucidate novel cellular factors impacted by extracellular agnoprotein and may reveal the mechanism of agnoprotein-mediated suppression of monocyte differentiation and function.

The final proposed future direction is to assess the immunomodulatory role of agnoprotein in an animal model. The data presented within this thesis proposes that extracellular agnoprotein suppresses PBMC and monocyte migration across a blood-brain barrier model, yet, if this phenomenon occurs outside of the model system has not been assessed. Idealistically, an animal model for JCV would exist, in which the animals would be infected with a wild-type strain of productive neurotropic JC virus and an agnoprotein-mutant of the same strain. In this system, immunohistochemistry of CNS sections would assess leukocyte infiltration to determine differences in the number of infiltrating cells with and without agnoprotein during the course of infection. However, a JCV animal model still does not exist, despite the efforts of multiple labs (White *et al*, 2015). As a JCV animal model does not exist, a secondary option would be to use an animal model of leukocyte infiltration into the brain, with a strain of mice susceptible to experimental autoimmune encephalopathy, an animal model for multiple sclerosis, being a potential candidate (Terry *et al*, 2016). One potential mouse strain is the C57BL/6 mouse, in which experimental autoimmune encephalopathy (EAE) can be induced with immunization of myelin oligodendrocyte glycoprotein (MOG) 35-

55 peptide (Kuerten *et al*, 2007). With leukocyte infiltration being a hallmark of this model, it provides *in vivo* conditions to test the ability of agnoprotein to suppress migration through the blood-brain barrier. Experimental animals would be immunized with MOG to induce EAE and monocyte migration into the brain. After immunization, animals would be treated with recombinant agnoprotein or vehicle and monocyte migration and EAE progression would be assessed to determine if agnoprotein treatment suppress monocyte migration *in vivo* and to elucidate a potential therapeutic use of agnoprotein.

## CHAPTER 6

### SCIENTIFIC PRODUCTS AND AWARDS

#### *Published full-length papers (\*peer-reviewed)*

- \*1. De-Simone, F.I., Sariyer, R., Otolora, Y.L., Yarandi, S., **Craigie, M.**, Gordon, J., Sariyer, I.K. (2015) Interferon-Gamma inhibits JC virus replication in glial cells by suppressing T-antigen expression. *PLoS One*, **10**(6):e0129694. PMID: PMC4465661.
- \*2. **Craigie, M.**, Regan, P., Otolora, Y.L., Sariyer, I.K. (2015) Molecular interplay between T-antigen and splicing factor, arginine/serine-rich 1 (SRSF1) controls JC virus gene expression in glial cells. *Virology Journal*, **12**: 196. PMID: PMC4657255.
- \*3. **Craigie, M.**, Cicalese, S., Sariyer, I.K. (2017) Neuroimmune regulation of JC virus by intracellular and extracellular agnoprotein. *Journal of Neuroimmune Pharmacology*, <https://doi.org/10.1007/s11481-017-9770-5>.

#### *Manuscript(s) in preparation*

- \*4. **Craigie, M.**, Sariyer, I.K. (2017) Host factor and immune regulation of JC virus gene expression. Review Article. Manuscript in preparation.

#### *Abstracts, Posters, Scientific Meetings*

1. De Simone, F.I., Otolora, Y., Yarandi, S., **Craigie, M.**, Sariyer, I.K. Translation of Large T antigen is suppressed by soluble immune mediators: implications for JC virus reactivation in immunocompromised individuals. 13<sup>th</sup> Annual Dawn B. Marks Research Conference, Temple University, Philadelphia, PA, USA, June 12, 2014.
2. **Craigie, M.**, De Simone, F.I., Yarandi, S., Sariyer, I.K. Interplay between Large T antigen and SF2/ASF in controlling JC virus gene expression in glial cells. 3<sup>rd</sup> Annual Temple University Translational Science Symposium, Temple University, Philadelphia, PA, USA, September 19, 2014.

3. De Simone, F.I., Sariyer, R., Otalora, Y., Yarandi, S., **Craigie, M.**, Gordon, J., Sariyer, I.K. Interferon gamma inhibits JC virus replication in glial cells by suppressing T-antigen expression. 13<sup>th</sup> International Symposium on Neurovirology. The Westin San Diego Gaslamp Quarter, San Diego, California, USA, June 2-6, 2015.
4. **Craigie, M.**, De Simone, F.I., Yarandi, S., Sariyer, I.K. Molecular interplay between Large T antigen and SRSF1 in controlling JC virus gene expression in glial cells. 14<sup>th</sup> Annual Dawn B. Marks Research Conference, Temple University, Philadelphia, PA, USA, June 4, 2015.
5. **Craigie, M.**, Cicalese, S., Donadoni, M., Sariyer, I.K. Neuroimmune regulation of JC virus by host and viral factors. 15<sup>th</sup> Annual Dawn B. Marks Research Conference, Temple University, Philadelphia, PA, USA, June 8, 2016.
6. **Craigie, M.**, Cicalese, S., Donadoni, M., Sariyer, I.K. Agnoprotein interferes with the neuroimmune response to JC virus. 14<sup>th</sup> International Symposium on Neurovirology, Omni King Edward Hotel, Toronto, Ontario, Canada, USA, October 25-28, 2016.
7. **Craigie, M.**, Cicalese, S., Sariyer, I.K. Neuroimmune Regulation of JC virus by intracellular and extracellular agnoprotein. Drexel University College of Medicine Discovery Day 2017, Philadelphia Convention Center, Philadelphia, Pennsylvania, USA, October 12, 2017.
8. **Craigie, M.**, Cicalese, S., Sariyer, I.K. Neuroimmune Regulation of JC virus by intracellular and extracellular agnoprotein. 2017 International Symposium on Molecular Medicine and Infectious Disease, Drexel University College of Medicine, Philadelphia, Pennsylvania, USA, November 16, 2017.

## ***HONORS AND AWARDS***

### **1. Lewis Katz School of Medicine at Temple University Biomedical Sciences Travel**

**Award.** Temple University School of Medicine, Philadelphia, Pennsylvania, USA.

October 25<sup>th</sup>, 2016.

## REFERENCES

1. Ahuja, D. Sáenz-Robles, M.T., Pipas, J.M. (2005) SV40 large T antigen targets multiple cellular pathways to elicit cellular transformation. *Oncogene*. **24**: 7729-7745.
2. Al-Barazi, H.O., Colberg-Poley, A.M. (1996) The human cytomegalovirus UL37 immediate-early regulatory protein is an integral membrane N-glycoprotein which traffics through the endoplasmic reticulum and Golgi apparatus. *J Virol*. **70**: 7198-7208.
3. Al-Tawfiq, J.A., Banda, R.W., Daabil, R.A., Dawamneh, M.F. (2015) Progressive multifocal leukoencephalopathy in a patient with lymphoma treated with rituximab: A case report and literature review. *J Infec and Public Health*. **8**: 493-497.
4. Amemiya, K., Traub, R., Durham, L., Major, E.O. (1992) Adjacent nuclear factor-1 and activator protein binding sites in the enhancer of the neurotropic JC virus. A common characteristic of many brain specific genes. *J Biol Chem*. **267**: 14204-14211.
5. Amirhaeiri, S., Wohlrab, F., Major, E.O., Wells, R.D. (1988) Unusual DNA structure in the regulatory region of the human papovirus JC virus. *J Virol*. **62**: 922-931.
6. Anczukow, O., Akerman, M., Clery, A., Wu, J., Shen, C., Shirole, N.H., Raimer, A., Sun, S., Jensen, M.A., Hua, Y., Allain, F.H.T., Krainer, A. (2015) SRSF1-regulated alternative splicing in breast cancer. *Molecular Cell*. **60**: 105-117.

7. Astrom, K.E., Mancall, E.L., Richardson Jr, E.P. (1958) Progressive multifocal leuko-encephalopathy; a hitherto unrecognized complication of chronic lymphatic leukaemia and Hodgkin's disease. *Brain*. **81**: 93-111.
8. Atwood, W.J., Amemiya, K., Traub, R., Harms, J., Major, E.O. (1992) Interaction of the human polyomavirus, JCV, with human B-lymphocytes. *Virology*. **190**: 716-723.
9. Ault, G.S. (1997) Activity of JC virus archetype and PML-type regulatory regions in glial cells. *J Gen Virol*. **78**: 163-169.
10. Bateman, O.J., Squires, G., Thannhauser, S.J. (1945) Hodgkin's disease associated with Schilder's disease. *Ann Intern Med*. **22**: 426-431.
11. Baum, S., Ashok, A., Gee, G., Dimitrova, G., Querbes, W., Jordan, J., Atwood, W.J. (2003) Early events in the life cycle of JC virus as potential therapeutic targets for the treatment of progressive multifocal leukoencephalopathy. *J Neurovirol*. **9**: 32-37.
12. Behzad-Behbahani, A., Klapper, P.E., Vallely, P.J., Cleator, G.M., Bonington, A. (2004) BKV-DNA and JCV-DNA in CSF of patients with suspected meningitis or encephalitis. *Infection*. **31**: 374-378.
13. Berger, J.R., Chauhan, A., Galey, D., Nath, A. (2001) Epidemiological evidence and molecular basis of interactions between HIV and JC virus. *J Neurovirol*. **7**: 329-338.
14. Berger, J.R., Miller, C.S., Mootoor, Y., Avdiushko, S.A., Kryscio, R.J., Zhu, H. (2006) JC virus detection in bodily fluids: clues to transmission. *Clin Infect Dis*. **43**: e9-12.

15. Berger, J.R., Houff, S.A., Gurwell, J., Vega, N., Miller, C.S., Danaher, R.J. (2013a) JC virus antibody status underestimates infection rates. *Ann Neurol.* **74**: 84-90.
16. Berger, J.R., Aksamit, A.J., Clifford, D.B., Davis, L., Koranik, I.J., Sejvar, J.J., Bartt, R., Major, E.O., Nath, A. (2013b) PML diagnostic criteria: consensus statement from the AAN Neuroinfectious Disease Section. *Neurology.* **80**: 1430-1438.
17. Bezrodnik, L., Samara, R., Krasovec, S., Garcia-Erro, M., Sevlever, G. (1998) Progressive multifocal leukoencephalopathy in a patient with hypogammaglobulinemia. *Clin Infect Dis.* **27**: 181-184.
18. Bienaime, A., Colson, P., Moreau, J. (2006) Progressive multifocal leukoencephalopathy in HIV-2-infected patient. *AIDS.* **20**: 1342-1343.
19. Bofill-Mas, S., Pina, S., Girones, R. (2000) Documenting the epidemiologic patterns of polyomaviruses in human populations by studying their presence in urban sewage. *Appl Environ Microbiol.* **66**: 238-245.
20. Bollag, B., Prins, C., Snyder, E.L., Frisque, R.J. (2000) Purified JC virus T and T' proteins differentially interact with the retinoblastoma family of tumor suppressor proteins. *Virology.* **274**: 165-178.
21. Booss, J., Harris, S.A. (1987) Neurology of AIDS virus infection: a clinical classification. *Yale J Biol Med.* **60**: 537-543.
22. Brew, B.J., Davies, N.W.S., Cinque, P., Clifford, D.B., Nath, A. (2010) Progressive multifocal leukoencephalopathy and other forms of JC virus disease. *Nat Rev Neurol.* **6**: 667-679.

23. Brooks, B.R., Walker, D.L. (1984) Progressive multifocal leukoencephalopathy. *Neurol Clin.* **2**: 299-313.
24. Bullock, P.A., Seo, Y.S., Hurwitz, J. (1991) Initiation of simian virus 40 DNA synthesis in vitro. *Mol Cell Biol.* **11**: 2350-2361.
25. Burgess, A.W., Metcalf, D., Watt, S.M. (1978) Regulation of hematopoietic cell differentiation and proliferation. *J Supramol Struct.* **8**: 489-500.
26. Cáceres, J.F., Misteli, T., Sreaton, G.R., Spector, D.L., Krainer, A.R. (1997) Role of the modular domains of SR proteins in subnuclear localization and alternative splicing specificity. *J Cell Biol.* **138**: 225-238.
27. Calabrese, L.H., Molloy, E., Berger, J. (2015) Sorting out the risks in progressive multifocal leukoencephalopathy. *Nat Rev Rheumatology.* **11**: 119-123.
28. Campisi, J. (2003) Cancer and ageing: rival demons? *Nat Rev Cancer.* **3**: 339-349.
29. Carter, C.C., Onafuwa-Nuga, A., McNamara, L.A., Riddell IV, J., Bixby, D., Savona, M.R., Collins, K.L. (2010) HIV-1 infects multipotent progenitor cells causing cell death and establishing latent cellular reservoirs. *Nature Med.* **16**: 446-451.
30. Casado, J.L., Corral, I., Garcia, J., Martinez-San Millan, J., Navas, E., Moreno, A., Moreno, S. (2014) Continued declining incidence and improved survival of progressive multifocal leukoencephalopathy in HIV/AIDS patients in the current era. *Eur J Clin Microbiol Infect Dis.* **33**: 179-187.
31. Cavanaugh, J.B., Greenbaum, D., Marchall, A., Rubinstein, L. (1959) Cerebral demyelination associated with disorder of the reticuloendothelial system. *Lancet.* **II**: 524-529.

32. Chen, N.N., Khalili, K. (1995) Transcriptional regulation of human JC polyomavirus promoters by cellular proteins YB-1 and p300 in glial cells. *J Virol.* **69**: 5843-5848.
33. Chen, N.N., Kerr, D., Chang, C.F., Honjo, T., Khalili, K. (1997) Evidence for regulation of transcription and replication of the human neurotropic virus JCV genome by the human S(mu)bp-2 protein in glial cells. *Gene.* **185**: 55-62.
34. Chen, B.J., Atwood, W.J. (2002) Construction of a novel JCV/SV40 hybrid virus (JCSV) reveals a role for the JCV capsid in viral tropism. *Virology.* **300**: 282-290.
35. Chin, K.C., Cresswell, P. (2001) Viperin (cig5), an IFN-inducible antiviral protein directly induced by human cytomegalovirus. *Proc Natl Acad Sci USA.* **99**: 2460.
36. Chowdhury, M., Taylor, J.P., Tada, H., Rappaport, J., Wong-Stall, F., Amini, S., Khalili, K. (1990) Regulation of the human neurotropic virus promoter by JCV-T antigen and HIV-1 tat protein. *Oncogene.* **5**: 1737-1742.
37. Chowdhury, M., Taylor, J.P., Chang, C.F., Rappaport, J., Khalili, K. (1992) Evidence that a sequence similar to TAR is important for induction of the JC virus late promoter by human immunodeficiency virus type 1 Tat. *J Virol.* **66**: 7355-7361.
38. Chowdhury, M., Kundu, M., Khalili, K. (1993) GA/GC-rich sequence confers Tat responsiveness to human neurotropic virus promoter, JCVL, in cells derived from central nervous system. *Oncogene.* **8**: 887-892.
39. Christensen, E., Fog, M. (1955) A case of Schilder's disease in an adult with remarks to etiology and pathogenesis. *ACTA Psychiatr Neurol Scand.* **30**: 141-154.

40. Cinque, P., Vago, L., Mengozzi, M., Torri, V., Ceresa, D., Vicenzi, E., Transidico, P., Vagani, A., Sozzani, S., Mantovani, A., Lazzarin, A., Poli, G. (1998) Elevated cerebrospinal fluid levels of monocyte chemotactic protein-1 correlate with HIV-1 encephalitis and local viral replication. *AIDS*. **12**: 1327-1332.
41. Cinque, P., Koralnik, I.J., Gerevini, S., Miro, J.M., Price, R.W. (2009) Progressive multifocal leukoencephalopathy in HIV-1 infection. *Lancet Infect Dis*. **9**: 625-636.
42. Cobrinik, D. (2005) Pocket proteins and cell cycle control. *Oncogene*. **24**: 2796-2809.
43. Cockerill, P.N., Bert, A.G., Roberts, D., Vadas, M.A. (1999) The human granulocyte-macrophage colony-stimulating factor gene is autonomously regulated in vivo by an inducible tissue-specific enhancer. *Proc Natl Acad Sci USA*. **96**: 15097-15102.
44. Colberg-Poley, A.M., Patel, M.B., Erez, D.P., Slater, J.E. (2000) Human cytomegalovirus UL37 immediate-early regulatory proteins traffic through the secretory apparatus and to the mitochondria. *J Gen Virol*. **81**: 1779-1789.
45. Conant, K., Garzino-Demo, A., Nath, A., McArthur, J.C., Halliday, W., Power, C., Gallo, R.C., Major, E.O. (1998) Induction of monocyte chemoattractant protein-1 in HIV-1 Tat-stimulated astrocytes and elevation in AIDS dementia. *Proc Natl Acad Sci USA*. **95**: 3117-3121.
46. Conductier, G., Blondeau, N., Guyon, A., Nahon, J.L., Rovere, C. (2010) The role of monocyte chemoattractant protein MCP1/CCL2 in neuroinflammatory diseases. *J Neuroimmunol*. **224**: 93-100.

47. Craigie, M., Regan, P., Otalora, Y.L., Sariyer, I.K. (2015) Molecular interplay between T-antigen and splicing factor, arginine/serine-rich 1 (SRSF1) controls JC virus gene expression in glial cells. *Virol J.* **12**: 196.
48. Crossley, K.M., Agnihotri, S., Chaganti, J., Rodriguez, M.L., McNally, L.P., Venna, N., Turbett, S.E., Gutman, M., Morey, A., Koralnik, I.J., Brew, B.J. (2016) Recurrence of progressive multifocal leukoencephalopathy despite immune recovery in two HIV seropositive individuals. *J Neurovirol.* **22**: 541-545.
49. Dang, X., Wuthrich, C., Gordon, J., Sawa, H., Koralnik, I.J. (2012) JC virus encephalopathy is associated with a novel agnoprotein-deletion JCV variant. *PLoS One.* **7**:e35793.
50. Daniel, D.C., Kinoshita, Y., Khan, M.A., Del Valle, L., Khalili, K., Rappaport, J., Johnson, E.M. (2004) Internalization of exogenous human immunodeficiency virus-1 protein, Tat, by KG-1 oligodendrogloma cells followed by stimulation of DNA replication initiated at the JC virus origin. *DNA Cell Biol.* **23**: 858-867.
51. Darbinyan, A., Siddiqui, K.M., Slonina, D., Darbinyan, N., Amini, S., White, M.K., Khalili, K. (2004) Role of JC virus agnoprotein in DNA repair. *J Virol.* **78**: 8593-8600.
52. Das, S., Krainer, A.R. (2014) Emerging functions of SRSF1, splicing factor and oncoprotein, in RNA metabolism and cancer. *Mol Cancer Res.* **12**: 1195-1204.
53. De Simone, F.I., Sariyer, R., Otalora, Y.L., Yarandi, S., Craigie, M., Gordon, J., Sariyer, I.K. (2015) Interferon-gamma inhibits JC virus replication in glial cells by suppressing T-antigen expression. *PLoS One.* **10**: e0129694.

54. Degener, A.M., Pietropaolo, V., Di Taranto, C., Rizzuti, V., Ameglio, F., Cordiali Fei, P., Caprilli, F., Capitano, B., Sinibaldi, L., Orsi, N. (1997) Detection of JC and BK viral genome in specimens of HIV-1 infected subjects. *New Microbiol.* **20**: 115-122.
55. Del Valle, L., Baehring, J., Lorenzana, C., Giordano, A., Khalili, K., Croul, S. (2001) Expression of a human polyomavirus oncoprotein and tumor suppressor proteins in medulloblastomas. *Mol Pathol.* **54**: 331-337.
56. Del Valle, L., Gordon, J., Enam, S., Delbue, S., Croul, S., Abraham, S., Radhakrishnan, S., Assimatkopoulou, M., Katsetos, C.D., Khalili, K. (2002) Expression of human neurotropic polyomavirus JCV late gene product agnoprotein in human medulloblastoma. *J Natl Cancer Instit.* **94**: 267-273.
57. Dubbs, D.R., Trkula, D., Kit, S. (1978) T antigen and initiation of cell DNA synthesis in a temperature-sensitive mouse line transformed by an SV40tsA mutant and in heterokaryons of the transformed cells and chick erythrocytes. *Somatic Cell Genet.* **4**: 95-110.
58. Dubois, V., Dutronc, H., Lafon, M.E., Poinso, V., Pellegrin, J.L., Ragnaud, J.M., Ferrer, A.M., Fleury, H.J. (1997) Latency and reactivation of JC virus in peripheral blood of human immunodeficiency virus type-1 infected patients. *J Clin Microbiol.* **35**: 2288-2292.
59. Dugan, A.S., Gasparovic, M.L., Atwood, W.J. (2008) Direct correlation between sialic acid binding and infection of cells by two human polyomaviruses (JC virus and BK virus). *J Virol.* **82**: 2560-2564.

60. Duschene, K.S., Broderick, J.B. (2010) The antiviral protein viperin is a radical SAM enzyme. *FEBS Lett.* **584**: 1263-1267.
61. Eaton, D., Rodrigues, H., Vehar, G.A. (1986) Proteolytic processing of human factor VIII. Correlation of specific cleavages by thrombin, factor Xa, and activated protein C with activation and inactivation of factor VIII coagulant activity. *Biochemistry.* **25**: 505-512.
62. Eddy, B.E., Borman, G.S., Grubbs, G.E., Young, R.D. (1962) Identification of the oncogenic substance in rhesus monkey kidney cell cultures as simian virus 40. *Virology.* **17**: 65-75.
63. Eggers, C., Arendt, G., Hahn, K., Husstedt, I.W., Mashchke, M., Neuen-Jacob, E., Obermann, M., Rosenkranz, T., Schielke, E., Straube, E. (2017) HIV-1-associated neurocognitive disorder: epidemiology, pathogenesis, diagnosis, and treatment. *J Neurol.* doi: 10.1007/s00415-017-8503-2.
64. Elphick, G.F., Querbes, W., Jordan, J.A., Gee, G.V., Eash, S., Manley, K., Dugan, A., Stanifer, M., Bhatnagar, A., Kroeze, W.K., Roth, B.L., Atwood, W.J. (2004) The human polyomavirus, JCV, uses serotonin receptors to infect cells. *Science.* **19**: 1380-1383.
65. Enam, S., Sweet, T.M., Amini, S., Khalili, K., Del Valle, L. (2004) Evidence for involvement of transforming growth factor beta 1 signaling pathway in activation of JC virus in human immunodeficiency virus 1-associated progressive multifocal leukoencephalopathy. *Arch Pathol Lab Med.* **128**: 282-291.

66. Engel, S., Heger, T., Mancini, R., Herzog, F., Kartenbeck, J., Hayer, A., Helenius, A. (2011) Role of endosomes in simian virus 40 entry and infection. *J Virol.* **85**: 4198-4211.
67. Engelhardt, B. (2008) The blood-central nervous system barrier actively control immune cell entry into the central nervous system. *Curr Pharm Des.* **14**: 1555-1565.
68. Engelhardt, B., Kappos, L. (2008) Natalizumab: targeting alpha4-integrins in multiple sclerosis. *Neurodegener Dis.* **5**: 16-22.
69. Ensoli, B., Buonaguro, L., Barillari, G., Fiorelli, V., Gendelman, R., Morgan, R.A., Wingfield, P., Gallo, R.C. (1993) Release, uptake, and effects of extracellular human immunodeficiency virus type 1 Tat protein on cell growth and transactivation. *J Virol.* **67**: 277-287.
70. Fairman, M.P., Stillman, B. (1988) Cellular factors required for multiple stages of SV40 DNA replication in vitro. *EMBO.* **7**: 1211-1218.
71. Feigenbaum, L., Khalili, K., Major, E.O., Khoury, G. (1987) Regulation of the host range of human polyomaviruses. *Proc Natl Acad Sci USA.* **84**: 3695-3698.
72. Feigenbaum, L., Hinrichs, S.H., Jay, G. (1992) JC virus and simian virus 40 enhancers and transforming proteins: role in determining tissue specificity and pathogenicity in transgenic mice. *J Virol.* **66**: 1176-1182.
73. Ferenczy, M.W., Marshall, L.J., Nelson, C.D., Atwood, W.J., Nath, A., Khalili, K., Major, E.O. (2012) Molecular biology, epidemiology, and pathogenesis of progressive multifocal leukoencephalopathy, the JC virus-induced demyelinating disease of the human brain. *Clin Microbiol Rev.* **25**: 471-506.

74. Fleetwood, A.J., Lawrence, T., Hamilton, J.A., Cook A.D. (2007) Granulocyte-macrophage colony stimulating factor (CSF) and macrophage CSF-dependent macrophage phenotypes display differences in cytokine profiles and transcription factor activities: implications for CSF blockade in inflammation. *J Immunol.* **178**: 5245-5252.
75. Focosi, D., Marco, T., Kast, R.E., Maggi, F., Ceccherini-Nelli, L., Petrini, M. (2010) Progressive multifocal leukoencephalopathy: what's new? *Neuroscientist.* **16**: 308-323.
76. Frisque, R.J. (1983) Regulatory sequences and viral cell interaction of JC virus. *Prog Clin Biol Res.* **105**: 41-59.
77. Frisque, R.J., Bream, G.L., Cannella, M.T. (1984) Human polyomavirus JC virus genome. *J Virol.* **51**: 458-469.
78. Gasparovic, M.L., Maginnis, M.S., O'Hara, B.A., Dugan, A.S., Atwood, W.J. (2009) Modulation of PML protein expression regulates JCV infection. *Virology.* **390**: 279-288.
79. Ge, H., Manley, J.L. (1990) A protein factor, ASF, controls cell-specific alternative splicing of SV40 early pre-mRNA in vitro. *Cell.* **13**: 25-34.
80. Gendelman, H. (2002) Neural immunity: Friend or foe? *Journal of Neurovirology.* **8**: 474-479.
81. Gheuens, S., Pierone, G., Peeters, P., Koralnik, I.J. (2010) Progressive multifocal leukoencephalopathy in individuals with minimal or occult immunosuppression. *J Neurol Neurosurg Psychiatry.* **81**: 247-254.

82. Glass, J.D., Fedor, H., Wesselingh, S.L., McArthur, J.C. (1995) Immunocytochemical quantification of human immunodeficiency virus in the brain: correlations with dementia. *Ann Neurol.* **38**: 755-762.
83. Gluska, S., Zahavi, E.E., Chein, M., Gradus, T., Bauer, A., Finke, S., Perlson, E. (2014) Rabies virus hijacks and accelerates the p75NTR retrograde axonal transport machinery. *PLoS Pathogens.* **10**: e1004348.
84. Goldmacher, V.S., Bartle, L.M., Skaletskaya, A., Dionne, C.A., Kedersha, N.L., Vater, C.A., Han, J.W., Lutz, R.J., Watanabe, S., Cahir McFarland, E.D., Kieff, E.D., Mocarski, E.S., Chittenden, T. (1999) A cytomegalovirus-encoded mitochondria-localized inhibitor of apoptosis structurally unrelated to Bcl-2. *Proc Natl Acad Sci USA.* **96**: 12536-12541.
85. Goldmacher, V.S. (2002) vMIA, a viral inhibitor of apoptosis targeting mitochondria. *Biochimie.* **84**: 177-185.
86. Gorelik, L., Lerner, M., Bixler, S., Crossman, M., Schlain, B., Simon, K., Pace, A., Cheung, A., Chen, L.L., Berman, M., Zein, F., Wilson, E., Yednock, T., Sandrock, A., Goelz, S.E., Subramanyam, M. (2010) Anti-JC virus antibodies: implications for PML risk stratification. *Ann Neurol.* **68**: 295-303.
87. Gorina, R., Font-Nieves, M., Marquez-Kisinousky, L., Santalucia, T., Planas, A.M. (2011) Astrocyte TLR4 activation induces a proinflammatory environment through the interplay between MyD88-dependent NFkB signaling, MAPK, and JAK1/Stat1 pathways. *Glia.* **59**: 242-255.
88. Gosert, R., Kardas, P., Major, E.O., Hirsch, H.H. (2010) Rearranged JC virus noncoding control regions found in progressive multifocal leukoencephalopathy

- patient samples increase viral early gene expression and replication rate. *J Virol.* 84: 10448-10456.
89. Gross, L. (1953) A filterable agent, recovered from Ak leukemic extracts, causes salivary gland carcinomas in C3H mice. *Proc Soc Exp Biol Med.* 83: 414-421.
90. Haider, S., Nafziger, D., Gutierrez, J.A., Brar, I., Mateo, N., Fogle, J. (2000) Progressive multifocal leukoencephalopathy and idiopathic CD4+ lymphocytopenia; a case report and review of reported cases. *Clin Infect Dis.* **31**: E20-22.
91. Haley, S.A., O'Hara, B.A., Nelson, C.D.S., Brittingham, F.L.P., Henriksen, K.J., Stopa, E.G., Atwood, W.J. (2015) Human polyomavirus receptor distribution in brain parenchyma contrasts with receptor distribution in kidney and choroid plexus. *Am J Pathol.* **185**: 2246-2258.
92. Hallervorden, J. (1930) Eigennartige und nicht rubizierbare prozesse. p 1063-1107. *Bumke O (ed).* Handbuch der Geisteskrankheiten Springer, Berlin, Germany.
93. Hamilton, J.A. (2002) GM-CSF in inflammation and autoimmunity. *Trends Immunol.* **23**: 403-408.
94. Hamilton, J.A. (2008) Colony-stimulating factors in inflammation and autoimmunity. *Nat Rev Immunol.* **8**: 533-544.
95. Hemachundha, T., Ugolini, G., Wacharapluesadee, S., Sungkarat, W., Shuangshoti, S., Laothamatas, J. (2013) Human rabies: neuropathogenesis, diagnosis, and management. *Lancet Neurology.* **12**: 498-513.

96. Henson, J., Saffer, J., Furneaux, H. (1992) The transcription factor Sp1 binds to the JC virus promoter and is selectively expressed in glial cells in human brain. *Ann Neurol.* **32**: 72-77.
97. Houff, S.A., Major, E.O., Katz, D.A., Kufta, C.V., Sever, J.L., Pittaluga, S., Roberts, J.R., Gitt, J., Saini, N., Lux, W. (1988) Involvement of JC virus-infected mononuclear cells from the bone marrow and spleen in the pathogenesis of progressive multifocal leukoencephalopathy. *N Engl J Med.* **318**: 301-305.
98. Houff, S.A., Berger, J.R. (2008) The bone marrow, B cells, and JC virus. *J Neurovirol.* **14**: 341-343.
99. Ishii, N., Minami, N., Chen, E.Y., Medina, A.L., Chico, M.M., Kasamatsu, H. (1996) Analysis of a nuclear localization signal of simian virus 40 major capsid protein Vp1. *J Virol.* **70**: 1317-1322.
100. Jing, D., Oelschlaegel, U., Ordemann, R., Holig, K., Ehniger, G., Reichmann, H., Zeimssen, T., Bornhauser, M. (2010) CD49b blockade by natalizumab in patients with multiple sclerosis affects steady-state hematopoiesis and mobilizes progenitors with a distinct phenotype and function. *Bone Marrow Transplant.* **45**: 1489-1496.
101. Kasamatsu, H., Nakanishi, A. (1998) How do animal DNA viruses get to the nuclear? *Ann Rev Microbiol.* **52**: 627-686.
102. Kaul, M., Garden, G.A., Lipson, S.A. (2001) Pathways to neuronal injury and apoptosis in HIV-associated dementia. *Nature.* **410**: 988-994.
103. Kean, J.M., Rao, S., Wang, M., Garcea, R.L. (2009) Seroepidemiology of human polyomaviruses. *PLoS Pathog.* **5**: e1000363.

104. Kenney, S., Natarajan, V., Strike, D., Khoury, G., Salzman, N.P. (1984) JC virus enhancer-promoter active in human brain cells. *Science*. **226**: 1337-1339.
105. Kepes, J.J., Chou, S.M., Price Jr, L.W. (1975) Progressive multifocal leukoencephalopathy with 10-year survival in a patient with nontropical sprue. Report of a case with unusual light and electron microscopic features. *Neurology*. **25**: 1006-1012.
106. Kerr, D., Chang, C.F., Chen, N., Gallia, G., Raj, G., Schwartz, B., Khalili, K. (1994) Transcription of a human neurotropic virus promoter in glial cells: effect of YB-1 on expression of the JC virus late gene. *J Virol*. **68**: 7637-7643.
107. Khalili, K., Feigenbaum, L., Khoury, G. (1987) Evidence for a shift in 5-termini of early viral RNA during they lytic cycle of JC virus. *Virology*. **158**: 469-472.
108. Khalili, K., Rappaport, J., Khoury, G. (1988) Nuclear factors in human brain cells bind specifically to the JCV regulatory region. *EMBO J*. **7**: 1205-1210.
109. Khalili, K., White, M.K., Sawa, H., Nagashima, K., Safak, M. (2005) The agnoprotein of polyomaviruses: a multifunctional auxiliary protein. *J Cell Physiol*. **204**: 1-7.
110. Khanna, N., Wolbers, M., Mueller, N.J., Garzoni, C., Du Pasquier, R.A., Fux, C.A., Vernazza, P., Bernasconi, E., Viscidi, R., Battegay, M., Hirsch, H.H., Swiss HIV Cohort Study (2009a) JC virus-specific immune responses in human immunodeficiency virus type 1 patients with progressive multifocal leukoencephalopathy. *J Virol*. **83**: 4404-4411.
111. Khanna, N., Elzi, L., Mueller, N.J., Garzoni, C., Cavassini, M., Fux, C.A., Vernazza, P., Bernasconi, E., Battegay, M., Hirschi, H.H., Swiss HIV Cohort

- Study. (2009b) Incidence and outcome of progressive multifocal leukoencephalopathy over 20 years of the Swiss HIV cohort study. *Clin Infect Dis.* **15:** 1459-1466.
112. Kharbanda, S., Saleem, A., Yuan, Z., Emoto, Y., Prasad, K.V., Kufe, D. (1995) Stimulation of human monocytes with macrophage colony-stimulating factor induces a Grb2-mediated association of the focal adhesion kinase pp125FAK and dynamin. *Proc Natl Acad Sci USA.* **92:** 6132-6136.
113. Kim, J., Woolridge, S., Biffi, R., Borghi, E., Lassak, A., Ferrante, P., Amini, S., Khalili, K., Safak, M. (2003) Members of the AP-1 family, c-Jun and c-Fos, functionally interact with JC virus early regulatory protein large T antigen. *J Virol.* **77:** 5241-5252.
114. Knowles, W.A., Pipkin, P., Andrews, N., Vyse, A., Minor, P., Brown, D.W., Miller, E. (2003) Population-based study of antibody to the human polyomavirus BKV and JCV and the simian polyomavirus SV40. *J Med Virol.* **71:** 115-123.
115. Kondo, Y., Windrem, M.S., Zou, L., Chandler-Militello, D., Schanz, S.J., Auvergne, R.M., Betstadt, S.J., Harrington, A.R., Johnson, M., Kazarov, A., Gorelik, L., Goldman, S.A. (2014) Human glial chimeric mice reveal astrocytic dependence of JC virus infection. *J Clin Invest.* **124:** 5323-5336.
116. Koralnik, I.J. (2002) Overview of the cellular immunity against JC virus in progressive multifocal leukoencephalopathy. *J Neurovirol.* **8:** 59-65.
117. Koralnik, I.J., Du Pasquier, R.A., Kuroda, M.J. (2002) Response specific for a commonly recognized JC virus. *J Immunol.* **168:** 499-504.

118. Korálnik, I.J., Wuthrich, C., Dang, X., Rottnek, M., Gurtman, A., Simpson, D., Morgello, S. (2005) JC virus granule cell Neuronopathy: A novel clinical syndrome distinct from progressive multifocal leukoencephalopathy. *Annals Neurol.* **57**: 576-580.
119. Krumbholz, A., Bininda-Emonds, O.R., Wutzler, P., Zell, R. (2009) Phylogenetics, evolution, and medical importance of polyomaviruses. *Infect Genet Evol.* **9**: 784-799.
120. Krumbholz, M., Meinl, I., Kumpfel, T., Hohlfeld, R., Meinl, E. (2008) Natalizumab disproportionately increases circulating pre-B and B cells in multiple sclerosis. *Neurology.* **71**: 1350-1354.
121. Kuerten, S., Kostova-Bales, D.A., Frenzel, L.P., Tigno, J.T., Tary-Lehmann, M., Angelov, D.N., Lehmann, P.V. (2007) MP4- and MOG:35-55-induced EAE in C57BL/6 mice differentially targets brain, spinal cord, and cerebellum. *J Neuroimmunol.* **189**: 31-40.
122. Lebwohl, M., Tying, S.K., Hamilton, T.K., Toth, D., Glazer, S., Tawfik, N.H., Walicke, P., Dummer, W., Wang, X., Garovoy, M.R., Pariser, D., Efalizumab Study Group (2003) A novel targeted T-cell modulator, efalizumab, for plaque psoriasis. *N Engl J Med.* **349**: 2004-2013.
123. Lee, S.H., Hurwitz, J. (1990) Mechanism of elongation of primed DNA by DNA polymerase delta, proliferating cell nuclear antigen, and activator 1. *Proc Natl Acad Sci USA.* **87**: 5672-5676.
124. Lee, P., Plavina, T., Castro, A., Berman, M., Jaiswal, D., Rivas, S., Schlain, B., Subramanyam, M. (2013) A second-generation ELISA (STRATIFY JCV<sub>TM</sub>

- DxSelect™) for detection of JC virus antibodies in human serum and plasma to support progressive multifocal leukoencephalopathy risk stratification. *J Clin Virol.* **57**: 141-146.
125. Lehmann, M.H., Masanetz, S., Kramer, S., Erfle, V. (2006) HIV-1 Nef upregulates CCL2/MCP-1 expression in astrocytes in a myristoylation- and calmodulin-dependent manner. *J Cell Sci.* **119**: 4520-4530.
126. Li, N., Zhang, X., Dong, H., Zhang, S., Sun, J., Qian, Y. (2016) Lithium ameliorates LPS-induced astrocytes activation partly via inhibition of toll-like receptor 4 expression. *Cell Physiol Biochem.* **38**: 714-725
127. Lindberg, R.L., Achtnichts, L., Hoffmann, F., Kuhle, J., Kappos, L. (2008) Natalizumab alters transcriptional expression profiles of blood cell subpopulations of multiple sclerosis patients. *J Neuroimmunol.* **194**: 153-164.
128. Liu, C.K., Wei, G., Atwood, W.J. (1998) Infection of glial cells by the human polyomavirus JC is mediated by N-linked glycoprotein containing terminal alpha (2,6)-linked sialic acids. *J Virol.* **72**: 4643-4649.
129. Liu, Y., Peterson, D.A., Kimura, H., Schubert, D. (1997) Mechanism of cellular 3-(4,5-dimethylthiazol-2-yl)-2,5-diphenyltetrazolium bromide (MTT) reduction. *J Neurochem.* **69**: 581-593.
130. Lynch, K.J., Frisque, R.J. (1991) Factors contributing to the restricted DNA replicating activity of JC virus. *Virology.* **180**: 306-317.
131. Maginnis, M.S., Haley, S.A., Gee, G.V., Atwood, W.J. (2010) Role of N-linked glycosylation of the 5-HT<sub>2A</sub> receptor in JC virus infection. *J Virol.* **84**: 9677-9684.

132. Major, E.O., Miller, A.E., Mourrain, P., Traub, R.G., de Widt, E., Sever, J. (1985) Establishment of a line of human fetal glial cells that supports JC virus multiplication. *Proc Natl Acad Sci USA*. **82**: 1257-1261.
133. Major, E.O., Amemiya, K., Elder, G., Houff, S.A. (1990) Glial cells of the human developing brain and B cells of the immune system share a common DNA binding factor for recognition of the regulatory sequences of the human polyomavirus, JCV. *J Neurosci Res*. **27**: 461-471.
134. Major, E.O., Amemiya, K., Elder, G., Tornatore, C.S., Houff, S.A., Berger, J.R. (1992) Pathogenesis and molecular biology of progressive multifocal leukoencephalopathy, the JC virus induced demyelinating disease of the human brain. *Clin Microbiol Rev*. **5**: 49-73.
135. Major, E.O., Neel, J.V. (1998) The JC and BK human polyoma viruses appear to be recent introductions to some South American Indian tribes: There is no serological evidence of cross-reactivity with the simian polyoma virus SV40. *Proc Natl Acad Sci USA*. **95**: 15525-15530.
136. Major, E.O. (2010) Progressive multifocal leukoencephalopathy in patients on immunomodulatory therapies. *Annu Rev Med*. **61**: 35-47.
137. Marshall, L.J., Dunham, L., Major, E.O. (2010) Transcription factor Spi-B binds unique sequences present in the tandem repeat promoter/enhancer of JC virus and supports viral activity. *J Gen Virol*. **91**: 3042-3052.
138. Marshall, L.J., Moore, L.D., Mirsky, M.M., Major, E.O. (2012) JC virus promoter/enhancers contain TATA box-associated Spi-B-binding sites that support early viral gene expression in primary astrocytes. *J Gen Virol*. **93**: 651-661.

139. Martin, J.D., King, D.M., Slauch, J.M., Frisque, R.J. (1985) Differences in regulatory sequences of naturally occurring JC virus variants. *J Virol.* **53**: 306-311.
140. Martin, J.D., Li, P. (1991) Enhancer/promoter activities of regulatory regions of representative JC virus isolates. *Arch Virol.* **120**: 305-311.
141. Marzocchetti, A., Wüthrich, C., Tan, C.S., Tompkins, T., Bernal-Cano, F., Bhargava, P., Ropper, A.H., Koralnik, I.J. (2008) Rearrangement of the JC virus regulatory region sequence in the bone marrow of a patient with rheumatoid arthritis and progressive multifocal leukoencephalopathy. *J Neurovirol.* **14**: 455-458.
142. McKenzie, B.S., Kastelein, R.A., Cua, D.J. (2006) Understanding the IL-23-IL-17 immune pathway. *Trends Immunol.* **27**: 17-23.
143. McLaughlin, P., Grillo-Lopez, A.J., Link, B.K., Levy, R., Czuczman, M.S., Williams, M.E., Heyman, M.R., Bence-Bruckler, I., White, C.A., Cabanillas, F., Jain, V., Ho, A.D., Lister, J., Wey, K., Shen, D., Dallaire, B.K. (1998) Rituximab chimeric anti-CD20 monoclonal antibody therapy for relapsed indolent lymphoma: half of patients respond to a four-dose treatment program. *J Clin Oncol.* **16**: 2825-2833.
144. Metcalf, D. (1979) Clonal analysis of the action of GM-CSF on the proliferation and differentiation of myelomonocytic leukemia cells. *Int J Cancer.* **24**: 616-623.
145. Monaco, M.C., Atwood, W.J., Gravell, M., Tornatore, C.S., Major, E.O. (1996) JC virus infection of hematopoietic progenitor cells, primary B lymphocytes, and tonsillar stromal cells: implications for viral latency. *J Virol.* **70**: 7004-7012.

146. Monaco, M.C., Jensen, P.N., Hou, J., Durham, L.C., Major, E.O. (1998) Detection of JC virus DNA in human tonsil tissue: evidence for site of initial viral infection. *J Virol.* **72**: 9918-9923.
147. Monaco, M.C., Sabath, B.F., Durham, L.C., Major, E.O. (2001) JC virus multiplication in human hematopoietic progenitor cells requires NF-1 class D transcription factor. *J Virol.* 9687-9695.
148. Mosmann, T. (1983) Rapid colorimetric assay for cellular growth and survival: application to proliferation and cytotoxicity assays. *J Immunol Methods.* 65: 55-63
149. Nagai, K., Perutz, M.F., Poyart, C. (1985) Oxygen binding properties of human mutant hemoglobins synthesized in *Escherichia coli*. *Proc Natl Acad Sci USA.* **82**: 7252-7255.
150. Nagarajan, S., Chesla, S., Cobern, L., Anderson, P., Zhu, C., Selvaraj, P. (1995) Ligand binding and phagocytosis by CD16 (Fc gamma receptor III) isoforms. Phagocytic signaling by associated zeta and gamma subunits in Chinese hamster ovary cells. *J Biol Chem.* **270**: 25762-25770.
151. Nakanishi, A., Clever, J., Yamada, M., Li, P.P. Kasamatsu, H. (1996) Association with capsid proteins promotes nuclear targeting of simian virus 40 DNA. *Proc Natl Acad Sci USA.* **93**: 96-100.
152. Nakshatri, H., Pater, A., Pater, M.M. (1990) Activity and enhancer binding factors for JC virus regulatory elements in differentiating embryonal carcinoma cells. *Virology.* **177**: 784-789.

153. Negerov, D., Maul, G.G. (2001) Cellular proteins localized at and interacting within ND10/PML nuclear bodies/PODs suggest functions of a nuclear depot. *Oncogene*. **20**: 7234-7242.
154. Nesper, J., Smith, R.W., Kautz, A.R., Sock, E., Wegner, M., Grummt, F., Nasheuer, H.P. (1997) A cell-free system replication system for human polyomavirus JC DNA. *J Virol*. **71**: 7421-7428.
155. Nukuzuma, S., Nakamichi, K., Kameoka, M., Sugiura, S., Nikuzuma, C., Miyoshi, I., Takegami, T. (2010) Efficient propagation of progressive multifocal leukoencephalopathy-type JC virus in COS-7-derived cell lines stably expressing Tat protein of human immunodeficiency virus type 1. *Microbiol Immunol*. **54**: 758-762.
156. Okada, Y., Endo, S., Takahashi, H., Sawa, H., Umemura, T., Nagashima, K. (2001) Distribution and function of JCV agnoprotein. *J Neurovirol*. **7**: 302-306.
157. Okada, Y., Sawa, H., Endo, S., Orba, Y., Umemura, T., Nishihara, H., Stan, A.C., Tanaka, S., Takahashi, H., Nagashima, K. (2002) Expression of JC virus agnoprotein in progressive multifocal leukoencephalopathy brain. *Acta Neuropathol*. **104**: 130-136.
158. Orba, Y., Suzuki, T., Makino, Y., Kubota, K., Tanaka, S., Kimura, T., Sawa, H. (2009) Large T antigen promotes JC virus replication in G2-arrested cells by inducing ATM- and ATR-mediated G2 checkpoint signaling. *J Biol Chem*. **285**: 1544-1554.

159. Otlu, O., De Simone, F.I., Otalora, Y.L., Khalili, K., Sariyer, I.K. (2014) The agnoprotein of polyomavirus JC is released by infected cells: evidence for its cellular uptake by uninfected neighboring cells. *Virology*. **468-470**: 88-95.
160. Padgett, B.L., Walker, D.L. (1973) Prevalence of antibodies in human sera against JC virus, an isolate from a case of progressive multifocal leukoencephalopathy. *J Infect Dis*. **127**: 467-470.
161. Petito, C.K., Cash, K.S. (1992) Blood-brain barrier abnormalities in the acquired immunodeficiency syndrome: immunohistochemical localization of serum proteins in postmortem brain. *Ann Neurol*. **32**: 658-666.
162. Pho, M.T., Ashok, A., Atwood, W.J. (2000) JC virus enters human glial cells by clathrin-dependent receptor-mediated endocytosis. *J Virol*. **74**: 2288-2292.
163. Piña-Oviedo, S., Urbanska, K., Radhakrishnan, S., Sweet, T., Reiss, K., Khalili, K., Del Valle, L. (2007) Effects of JC virus infection on anti-apoptotic protein survivin in progressive multifocal leukoencephalopathy. *Am J Pathol*. **170**: 1291-1304.
164. Plavina, T., Subramanyam, M., Bloomgren, G., Richman, S., Pace, A., Lee, S., Schlain, B., Campagnolo, D., Belachew, S., Ticho, B. (2014) Anti-JC virus antibody levels in serum or plasma further define risk of natalizumab-associated progressive multifocal leukoencephalopathy. *Ann Neurol*. **76**: 802-812.
165. Polyomaviridae Study Group of the International Committee on Taxonomy of Viruses, Calvignac-Spencer, S., Feltkamp, M.C., Daugherty, M.D., Moens, U., Ramqvist, T., Johne, R., Ehlers, B. (2016) A taxonomy update for the family Polyomaviridae. *Arch Virol*. **161**: 1739-1750.

166. Price, R.W., Brew, B., Sidtis, J., Rosenblum, M., Scheck, A.C., Cleary, P. (1988) The brain in AIDS: central nervous system HIV-1 infection and AIDS dementia complex. *Science*. **239**: 586-592.
167. Price, R.W., Brew, B. (1988) Infection of the central nervous system by human immunodeficiency virus. Role of the immune system in pathogenesis. *Ann N Y Acad Sci*. **540**: 162-175.
168. Puri, V., Chaudhry, N., Gulati, P., Patel, N., Tatke, M., Sinha, S. (2010) Progressive multifocal leukoencephalopathy in a patient with idiopathic CD4+ T lymphocytopenia. *Neurol India*. **58**: 118-121.
169. Querbes, W., Benmerah, A., Tosoni, D., Di Fiore, P.P., Atwood, W.J. (2004) A JC virus-induced signal is required for infection of glial cells by a clathrin- and eps15-dependent pathway. *J Virol*. **78**: 250-256.
170. Querbes, W., O'Hara, B.A., Williams, G., Atwood, W.J. (2006) Invasion of host cells by JC virus identifies a novel role for caveolae in endosomal sorting of noncaveolar ligands. *J Virol*. **80**: 9402-9413.
171. Quinlan, R.A., Moir, R.D., Stewart, M. (1989) Expression in *Escherichia coli* of fragments of glial fibrillary acidic protein: characterization, assembly properties and paracrystal formation. *J Cell Sci*. **93**: 71-83.
172. Raj, G.V., Khalili, K. (1995) Transcriptional regulation: lessons from the human neurotropic polyomavirus, JCV. *Virology*. **213**: 283-291.
173. Ravichandran, V., Sabath, B.F., Jensen, P.N., Houff, S.A., Major, E.O. (2006) Interactions between c-Jun, nuclear factor 1, and JC virus promoter sequences: implications for viral tropism. *J Virol*. **80**: 10506-10513.

174. Ray, U., Cinque, P., Gerevini, S., Longo, V., Lazzarin, A., Schippling, S., Martin, R., Buck, C.B., Pastrana, D.V. (2015) JC polyomavirus mutants escape antibody-mediated neutralization. *Sci Transl Med.* **7**: 306ra151.
175. Reff, M.E., Carner, K., Chambers, K.S., Chinn, P.C., Leonard, J.E., Raab, R., Newman, R.A., Hanna, N., Anderson, D.R. (1994) Depletion of B cells in vivo by a chimeric mouse human monoclonal antibody to CD20. *Blood.* **83**: 435-445.
176. Reuwer, A.Q., Heron, M., van der Dussen, D., Schneider-Hohendorf, T., Murk, J.L. (2017) The clinical utility of JC virus antibody index measurements in the context of progressive multifocal leukoencephalopathy. *Acta Neurol Scand.* **136**: 37-44.
177. Rice, G.P., Hartung, H.P., Calabresi, P.A. (2005) Anti-alpha4 integrin therapy for multiple sclerosis: mechanisms and rationale. *Neurology.* **64**: 1336-1342.
178. Richardson Jr, E.P. (1961) Progressive multifocal leukoencephalopathy. *N Engl J Med.* **265**: 815-823.
179. Richardson Jr, E.P., Webster, H.D. (1983) Progressive multifocal leukoencephalopathy: its pathological features. *Prog Clin Biol Res.* **105**: 191-203.
180. Richardson-Burns, S.M., Kleinschmidt-DeMasters, B.K., DeBiasi, R.L., Tyler, K.L. (2002) Progressive multifocal leukoencephalopathy and apoptosis of infected oligodendrocytes in the central nervous system of patients with and without AIDS. *Arch Neurol.* **59**: 1930-1936.
181. Rohrschneider, L.R., Bourette, R.P., Lioubin, M.N., Algate, P.A., Myles, G.M., Carlberg, K. (1997) Growth and differentiation signals regulated by the M-CSF receptor. *Mol Reprod and Devel.* **46**: 96-103.

182. Roux, D., Bouldouyre, M.A., Mercier-Delarue, S., Seilhean, D., Zagdanski, A.M., Delaugerre, C., Simon, F., Molina, J.M., Legoff, J. (2011) JC virus variant associated with cerebellar atrophy in a patient with AIDS. *J Clin Microb.* **49**: 2196-2199.
183. Rudnicka, D., Oszmiana, A., Finch, D.K., Strickland, I., Schofield, D.J., Lowe, D.C., Sleeman, M.A., Davis, D.M. (2013) Rituximab causes a polarization of B cells that augments its therapeutic function in NK-cell-mediated antibody-dependent cellular toxicity. *Blood.* **121**: 4694-4702.
184. Safak, M., Gallia, G.L., Ansari, S.A., Khalili, K. (1999) Physical and functional interaction between the Y-box binding protein YB-1 and human polyomavirus JC virus large T antigen. *J Virol.* **73**: 10146-10157.
185. Safak, M., Gallia, G.L., Khalili, K. (1999) Reciprocal interaction between two cellular proteins, p<sub>ur</sub>-alpha and YB-1, modulates transcriptional activity of JCVCY in glial cells. *Mol Cell Biol.* **19**: 2712-2723.
186. Safak, M., Khalili, K. (2001) Physical and functional interaction between viral and cellular proteins modulates JCV gene transcription. *J Neurovirol.* **7**: 288-292.
187. Santa Cruz, K.S., Roy, G., Spigel, J., Bearer, E.L. (2016) Neuropathology of JC virus infection in progressive multifocal leukoencephalopathy in remission. *World J Virol.* **5**: 31-37.
188. Saribas, A.S., Arachea, B.T., White, M.K., Viola, R.E., Safak, M. (2011) Human polyomavirus JC small regulatory agnoprotein forms highly stable dimers and oligomers: implications for their roles in agnoprotein function. *Virology.* **420**: 51-65.

189. Sariyer, I.K., Khalili, K. (2011a) Regulation of human neurotropic JC virus replication by alternative splicing factor SF2/ASF in glial cells. *PLoS One*. **6**: e14630.
190. Sariyer, I.K., Saribas, A.S., White, M.K., Safak, M. (2011) Infection by agnoprotein-negative mutants of polyomavirus JC and SV40 results in the release of virions that are mostly deficient in DNA content. *Virology*. **8**: 255.
191. Sariyer, I.K., Sariyer, R., Otte, J., Gordon, J. (2016) Pur-alpha induces JCV gene expression and viral replication by suppressing SRSF1 in glial cells. *PLoS One*. **11**:e0156819.
192. Sariyer, R., De Simone, F.I., Gordon, J., Sariyer, I.K. (2016) Immune suppression of JC virus gene expression is mediated by SRSF1. *J Neurovirology*. **22**: 597-606.
193. Schelhaas, M., Malstrom, J., Pelkmans, L., Haugstetter, J., Ellgaard, L., Grunewald, K., Helenius, A. (2007) Simian virus 40 depends on ER protein folding and quality control factors for entry into host cells. *Cell*. **131**: 516-529.
194. Schiff, D.E., Kline, L., Soldau, K., Lee, J.D., Pugin, J., Tobias, P.S., Ulevitch, R.J. (1997) Phagocytosis of gram-negative bacteria by a unique CD14-dependent mechanism. *J Leukoc Biol*. **62**: 786-794.
195. Schreiner, S., Martinez, R., Groitl, P., Rayne, F., Vaillant, R., Wimer, P., Bossis, G., Sternsdorf, T., Marcinowski, L., Ruzsics, Z., Dobner, T., Wodrich, H. (2012) Transcriptional activation of adenoviral genome is mediated by capsid protein VI. *PLoS Pathog*. **8**: e1002549.
196. Scott, T.P., Nel, L.H. (2016) Subversion of the immune response by rabies virus. *Viruses*. **8**: doi:10.3390/v8080231.

197. Sethi, N.K., Torgovnick, J., McArthur, J.C., Tan, I.L., Koralnik, I.J. (2012) Progressive multifocal leukoencephalopathy in a patient without immunodeficiency. *Neurology*. **78**: 73-74.
198. Seo, J.Y., Yaneva, R., Cresswell, P. (2011) Viperin: a multifunctional, interferon-inducible protein that regulates virus replication. *Cell Host Microbe*. **10**: 534-539.
199. Shaveta, G., Shi, J., Chow, V.T., Song, J. (2010) Structural characterization reveals that viperin is a radical S-adenosyl-L-methionine (SAM) enzyme. *Biochem Biophys Res Commun*. **391**: 1390-1395.
200. Sherr, C.J., McCormick, F. (2002) The RB and p53 pathways in cancer. *Cancer Cell*. **2**: 103-112.
201. Shishido-Hara, Y., Higuchi, K., O'Hara, S., Duyckaerts, C., Hauw, J.J., Uchihara, T. (2008) Promyelocytic leukemia nuclear bodies provide a scaffold for human polyomavirus JC replication and are disrupted after development of viral inclusions in progressive multifocal leukoencephalopathy. *J Neuropathol Exp Neurol*. **67**: 299-308.
202. Shishido-Hara, Y. (2010) Progressive multifocal leukoencephalopathy and promyelocytic leukemia nuclear bodies: a review of clinical, neuropathological, and virological aspects of JC virus-induced demyelinating disease. *Acta Neuropathol*. **120**: 403-417.
203. Shivakumar, C.V., Das, G.C. (1994) Biochemical and mutational analysis of the polyomavirus core promoter: involvement of nuclear factor-1 in early promoter function. *J Gen Virol*. **75**: 1281-1290.

204. Srithayakumar, V., Sribalachandran, H., Rosatte, R., Nadin-Davis, S.A., Kyle, C.J. (2014) Innate immune responses in raccoons after raccoon rabies virus infection. *J Gen Virol.* **95**: 16-25.
205. Stanley, E.R., Berg, K.L., Einstein, D.B., Lee, P.S., Pixley, F.J., Wang, Y., Yeung, Y.G. (1997) Biology and action of colony-stimulating factor-1. *Mol Reprod Dev.* **46**: 4-10.
206. Stettner, M.R., Nance, J.A., Wright, C.A., Kinoshita, Y., Kim, W-K., Morgello, S., Rappaport, J., Khalili, K., Gordon, J., Johnson, M. (2009) SMAD proteins of oligodendroglial cells regulate transcription of JC virus early and late genes coordinately with the Tat protein of human immunodeficiency virus type 1. *J Gen Virol.* **90**: 2005-2014.
207. Stewart, S.E., Eddy, B.E., Borgese, N. (1958) Neoplasms in mice inoculated with a tumor agent carried in tissue culture. *J Natl Cancer Instit.* 20: 1223-1236.
208. Stolt, A., Sasnaukas, K., Koskela, P., Lehtinen, M., Dillner, J. (2003) Seroepidemiology of the human polyomaviruses. *J Gen Virol.* **84**: 1499-1504.
209. Sumner, C., Shinohara, T., Durham, L., Traub, R., Major, E.O., Amemiya, K. (1996) Expression of multiple classes of the nuclear factor-1 family in the developing brain: Differential expression of two classes of NF-1 genes. *J Neurovirol.* **2**: 87-100.
210. Suzuki, S., Sawa, H., Komagome, R., Orba, Y., Yamada, M., Okada, Y., Ishida, Y., Nishihara, H., Tanaka, S., Nagashima, K. (2001) Broad distribution of the JC virus receptor contrasts with a marked cellular restriction of virus replication. *Virology.* **286**: 100-112.

211. Suzuki, T., Orba, Y., Okada, Y., Sunden, Y., Kimura, T., Tanaka, S., Nagashima, K., Hall, W.W., Sawa, H. (2010) The human polyoma JC virus agnoprotein acts as a viroporin. *PLoS Pathog.* **6**: e1000801.
212. Sweet, B.H., Hilleman, M.R. (1960) The vacuolating virus, S.V.40. *Proc Soc Exp Biol Med.* 105: 420-427.
213. Sweet, T.M., Del Valle, L., Khalili, K. (2002) Molecular biology and immunoregulation of human neurotropic JC virus in CNS. *J Cell Physio.* **191**: 249-256.
214. Tada, H., Lashgari, M., Rappaport, J., Khalili, K. (1989) Cell type-specific expression of JC virus early promoter is determined by positive and negative regulation. *J Virol.* **63**: 463-466.
215. Tada, H., Rappaport, J., Lashgari, M., Amini, S., Wong-Stall, F., Khalili, K. (1990) Trans-activation of the JC virus late promoter by the tat protein of type 1 human immunodeficiency virus in glial cells. *Proc Natl Acad Sci USA.* **87**: 3479-3483.
216. Tada, H., Khalili, K. (1992) A novel sequence-specific DNA-binding protein, LCP-1, interacts with single-stranded DNA and differentially regulates early gene expression of the human neurotropic JC virus. *J Virol.* **66**: 6885-6892.
217. Tamura, T., Inoue, T., Nagata, K., Mikoshiba, K. (1988) Enhancer of human polyoma JC virus contains nuclear factor 1-binding sequences: analysis using mouse brain nuclear extracts. *Biochem Biophys Res Commun.* **157**: 419-425.
218. Tan, C.S., Dezube, B.J., Bhargava, P., Autissier, P., Wüthrich, C., Miller, J., Koralknik, I.J. (2009) Detection of JC virus DNA and proteins in the bone marrow

- of HIV-positive and HIV-negative patients: implications for viral latency and neurotropic transformation. *J Infect Dis.* **199**: 881-888.
219. Tan, C.S., Ellis, L.C., Wüthrich, C., Ngo, L., Broge, Jr., T.A., Saint-Aubyn, J., Miller, J.S., Koranik, I.J. (2010) JC virus latency in the brain and extraneural organs of patients with and without progressive multifocal leukoencephalopathy. *J Virol.* **84**: 9200-9209.
220. Taoufik, Y., Gasnault, J., Karaterki, A., Pierre Ferey, M., Marchandier, E., Goujard, C. (1998) Prognostic value of JC virus load in cerebrospinal fluid of patients with progressive multifocal leukoencephalopathy. *J Infect Dis.* **178**: 1816-1820.
221. Tarassishin, L., Suh, H.S., Lee, S.C. (2014) LPS and Il-1 differentially activate mouse and human astrocytes: role of CD14. *Glia.* **62**: 999-1013.
222. Tasca, G., Iorio, R., Basile, U., Lauriola, L., Tartaglione, R., Mirabella, M., Ricci, E., Sabatelli, M. (2009) Progressive multifocal leukoencephalopathy in a patient with Franklin disease and hypogammaglobulinemia. *J Neurol Sci.* **284**: 203-204.
223. Tavis, J.E., Trowbridge, P.W., Frisque, R.J. (1994) Converting the JCV T-antigen RB binding domain to that of SV40 does not alter JCV's limited transforming activity but does eliminate viral viability. *Virology.* **199**: 384-392.
224. Taylor, J.P., Cupp, C., Diaz, A., Chowdhury, M., Khalili, K., Jimenez, S.A., Amini, S. (1992) Activation of expression of genes coding for extracellular matrix genes in Tat-producing glioblastoma cells. *Proc Natl Acad Sci USA.* **89**: 9617-9621.
225. Teramoto, T., Kaneko, H., Funato, M., Sawa, H., Nagashima, K., Hirose, Y., Kondo, N. (2003) Progressive multifocal leukoencephalopathy in a patient with X-linked agammaglobulinemia. *Scand J Infect Dis.* **35**: 909-910.

226. Terry, R.L., Ifergan, I., Miller, S.D. (2016) Experimental autoimmune encephalomyelitis in mice. *Methods Mol Biol.* **1304**: 145-160.
227. Tornatore, C., Berger, J.R., Houff, S.A., Curfman, B., Meyers, K., Winfield, D., Major, E.O. (1992) Detection of JC virus DNA in peripheral lymphocytes from patients with and without progressive multifocal leukoencephalopathy. *Ann Neurol.* **31**: 454-462.
228. Tsurimoto, T., Melendy, T., Stillman, B. (1990) Sequential initiation of lagging and leading strand synthesis by two different polymerase complexes at SV40DNA replication origin. *Nature.* **346**: 534-539.
229. Tyagarajan, S.K., Frisque, R.J. (2006) Stability and function of JC virus large T antigen and T' proteins are altered by mutation of their phosphorylated threonine 125 residues. *J Virol.* **80**: 2083-2091.
230. Uleri, E., Beltrami, S., Gordon, J., Dolei, A., Sariyer, I.K. (2011) Extinction of tumor antigen expression by SF2/ASF in JCV-transformed cells. *Genes Cancer.* **2**: 728-736.
231. Uleri, E., Regan, P., Dolei, A., Sariyer, I.K. (2013) SF2/ASF binding region within JC virus NCCR limits early gene transcription in glial cells. *Viol J.* **10**: 147.
232. Verma, A. (2004) Neurological manifestations of human immunodeficiency virus infection in adults. *Neurol Clin Prac.* **2**: 1581-1602.
233. Viillard, J.F., Ellie, E., Lazaro, E., Lafon, M.E., Pellegrin, J.L. (2005) JC virus meningitis in a patient with systemic lupus erythematosus. *Lupus.* **14**: 964-966.
234. von Einsiedel, R.W., Fife, T.D., Aksamit, A.J., Cornford, M.E., Secor, D.L., Tomiyasu, U., Itabashi, H.H., Vinters, H.V. (1993) Progressive multifocal

- leukoencephalopathy in AIDS: a clinicopathologic study and review of the literature. *J Neurol.* **240**: 391-406.
235. Weber, F., Goldmann, C., Kramer, M., Kaup, F.J., Pickhardt, M., Young, P., Petry, H., Weber, T., Luke, W. (2001) Cellular and humoral immune response in progressive multifocal leukoencephalopathy. *Ann Neurol.* **49**: 636-642.
236. Weber, T., Weber, F., Petry, H., Luke, W. (2001) Immune response in progressive multifocal leukoencephalopathy: an overview. *J Neurovirol.* **7**: 311-317.
237. Wegner, M., Drolet, D.W., Rosenfeld, M.G. (1993) Regulation of JC virus by the POU-domain transcription factor Tst-1: Implications for progressive multifocal leukoencephalopathy. *Proc Natl Acad Sci USA.* **90**: 4742-4747.
238. Wei, G., Liu, C.K., Atwood, W.J. (2000) JC virus binds to primary human glial cells, tonsillar stromal cells, and B-lymphocytes, but not to T lymphocytes. *J Neurovirol.* **6**: 127-136.
239. Weinberg, D.H., Collins, K.L., Simancek, P., Russo, A., Wold, M.S., Virshup, D.M., Kelly, T.J. (1990) Reconstitution of simian virus 40 DNA replication with purified proteins. *Proc Natl Acad Sci USA.* **90**: 8692-8696.
240. Weiss, J.M., Nath, A., Major, E.O., Berman, J.W. (1999) HIV-1 Tat induces monocyte chemoattractant protein-1 mediated monocyte transmigration across a model of the human blood-brain barrier and upregulates CCR5 expression on human monocytes. *J Immunol.* **163**: 2954-2959.
241. Westra, E.R., Swarts, D.C., Staals, R.H., Jore, M.M., Brouns, S.J., van der Oost, J. (2012) The CRISPRs, they are a-changin': How prokaryotes generate adaptive immunity. *Annu Rev Genet.* **46**: 311-339.

242. White, M.K., Khalili, K. (2006) Interaction of retinoblastoma protein family members with large T-antigen of primate polyomaviruses. *Oncogene*. **25**: 5286-5293.
243. White, M.K., Gordon, J., Berger, J.R., Khalili, K. (2015) Animal models for progressive multifocal leukoencephalopathy. *J Cell Physiol*. **230**: 2869-2874.
244. Winkleman, N.W., Moore, M.T. (1941) Lymphogranulomatosis (Hodgkin's disease) of the nervous system. *Arch Neurol Psychol*. **45**: 304-318.
245. Wollebo, H.S., Safak, M., Del Valle, L., Khalili, K., White, M.K. (2011) Role for tumor necrosis factor alpha in JC virus reactivation and progressive multifocal leukoencephalopathy. *J Neuroimmunol*. **233**: 46-53.
246. Wüthrich, C., Cheng, Y.M., Joseph, J.T., Kesari, S., Beckwith, C., Stopa, E., Bell, J.E., Koralnik, I.J. (2009a) Frequent infection of cerebellar granule cell neurons by polyomavirus JC in progressive multifocal leukoencephalopathy. *J Neuropathol Exp Neurol*. **68**: 15-25.
247. Wüthrich, C., Dang, X., Westmoreland, S., McKay, J., Maheshwari, A., Anderson, M.P., Ropper, A.H., Viscidi, R.P., Koralnik, I.J. (2009b) Fulminant JC virus encephalopathy with productive infection of cortical pyramidal neurons. *Ann Neurol*. **65**: 742-748.
248. Yamada, M., Kasamatsu, H. (1993) Role of nuclear pore complex in simian virus 40 nuclear targeting. *J Virol*. **67**: 119-130.
249. Zheng, H.C., Yan, L., Cui, L., Guan, Y.F., Takano, Y. (2009) Mapping the history and current situation of research on John Cunningham virus – a bibliometric analysis. *BMC Infect Dis*. **9**: 28.